DEVELOPMENT OF AN INJECTABLE SLOW RELEASE SYSTEM FOR BONE MORPHOGENETIC PROTEIN-2

Zahide Didem Mumcuoglu Guvenc

**DEVELOPMENT OF AN INJECTABLE SLOW RELEASE SYSTEM
FOR BONE MORPHOGENETIC PROTEIN-2**

Proefschrift

ter verkrijging van de graad van doctor aan de
Erasmus Universiteit Rotterdam
op gezag van de
rector magnificus

Prof.dr. H.A.P. Pols

en volgens besluit van het College voor Promoties.
De openbare verdediging zal plaatsvinden op

9 Mei 2018 13.30 uur

Zahide Didem Mumcuoglu Guvenc
geboren te Izmir
(Turkije)

Erasmus University Rotterdam

Promotiecommissie:

Promotor(en): Prof. dr. G.J.V.M. van Osch

Overige leden: Prof. dr. E.B. Wolvius
Prof. dr. F.C. Oner
Dr. S.C.G. Leeuwenburgh

Copromotor(en): Dr. S.G.J.M. Kluijtmans

TABLE OF CONTENTS

CHAPTER 1

INTRODUCTION

Biomaterials

Biomaterials have been investigated and used in many areas of medicine [1]. Biomaterials are defined by the American National Institute of Health as "'any substance or combination of substances, other than drugs, synthetic or natural in origin, which can be used for any period of time, which augments or replaces partially or totally any tissue, organ or function of the body, in order to maintain or improve the quality of life of the individual" [2]. Biomaterials are commonly used in tissue engineering and regenerative medicine [3]. The general aim of tissue engineering and regenerative medicine is to regenerate damaged organs or tissues by using suitable biomaterials and combination of biomaterials with cells and therapeutics [4]. The field of tissue engineering/regenerative medicine is growing and there are numerous applications in cartilage, bone, kidney, pancreas, skin, heart, muscle, tendon [5, 6].

Biomaterials are designed as scaffolds and as drug delivery systems in tissue engineering. These scaffolds and drug carriers can be in a form of hydrogel, particle, membrane, nanofiber, 3-D printed material or a porous scaffold mimicking the architecture of the organs [3, 7, 8]. The common properties to characterize a biomaterial are biocompatibility, biodegradability, mechanical property and scaffold architecture [9]. There is a variety of biomaterials exploited in the field of regenerative medicine. Depending on the type or origin of the material, biomaterials can be grouped as: inorganic materials, synthetic polymers and natural polymers [10]. Ceramics or hydroxyapatite as a bone substitute are examples of inorganic materials [11]. Most commonly used synthetic polymers are biodegradable polyester family members, which includes polycaprolactone (PCL), polyglycolides, polylactides such as poly(lactic acid) (PLA), poly(lactic-co-glycolic acid) (PLGA) [12]. These synthetic polymers are degraded in the body; however, some of the acidic monomers can decrease the pH of the surrounding tissue [13, 14]. Synthetic polymers are sometimes functionalized to mimic native tissue more closely [15]. On the other hand, natural polymers such as alginate, hyaluronic acid, chitosan are derived from biological organisms therefore resemble more to natural tissue in terms of composition and degradation time [16]. Hyaluronic acid and other sulphated or non-sulfated glycosaminoglycans (GAGs) are commonly used because they are the components of human extracellular matrix (ECM). Besides GAGs, protein derived materials are widely explored. Collagen as the main component of the ECM as well as other components such as elastins and fibrins are mainly investigated [17]. They are not only biocompatible and biodegradable but also resemble the native ECM.

 Smart materials

The above mentioned materials are engineered for practical handling and application or to better mimic the ECM and increase the regenerative capacity of the materials. Among them several smart materials have been developed. For example, materials that change

properties via an external stimulus such as temperature, pH or stress [18]. In situ gelling hydrogels are well known examples of smart materials. These materials are injectable and form a hydrogel network structure controlled by an external stimulus For example poly(N-isopropylacrylamide) (PNIPAM) modified hyaluronic acid [19] forms a hydrogel above 32 °C. Alginate forming a network in the presence of calcium ions is another example of an in-situ gelling hydrogel [20]. There are also examples of shear thinning materials that disassemble their network under shear stress and reassemble (recover) when stress is removed [21]. Hydrogels based on poly (lactic-co-glycolic acid) (PLGA) [22], sugar and oxaborole [23], hyaluronic acid [24] and alginate [25] were engineered to have such shear thinning behaviour.

Role of delivery systems in tissue engineering and regenerative medicine

Delivery systems are designed to deliver a certain drug or therapeutic agent (e.g. protein, small drug, interfering RNA) to the site of action [26]. The functionality and the structure of the delivery system are designed for a specific application. For example, in cancer treatment, the aim of the delivery system is to target only cancer cells to increase the effectiveness of drug and to reduce adverse events on healthy cells [27, 28].

In tissue engineering and regenerative medicine, delivery systems are generally used to deliver soluble factors to promote tissue regeneration, anti-inflammatory drugs to suppress inflammation or anti-microbial drugs to prevent implant infections [29, 30]. For protein/peptide based drugs such as growth factors, the challenge is to maintain stability of the protein and provide a sustained release of the protein over certain period of time that is required for the regeneration of the tissue [31].

The choice of a delivery system depends on the application. Since the release profile of a protein is very important for the protein to be effective over long time, the choice of a delivery system is important [32]. Different ways to deliver drugs using biomaterials are illustrated in Figure 1. A drug can be encapsulated in a scaffold or a sphere, or it can be adsorbed to a delivery system or covalently linked.

Bone tissue engineering and bone healing

In trauma or disease related bone defects, bone grafts are used when the natural bone formation process is insufficient (due to age or disease or size of the trauma). It is estimated that more than 2.2 million bone grafting procedures are annually performed to repair bone defects in orthopaedics, neurosurgery and dentistry worldwide [34]. The common practice is using autograft which is collected from the patient.
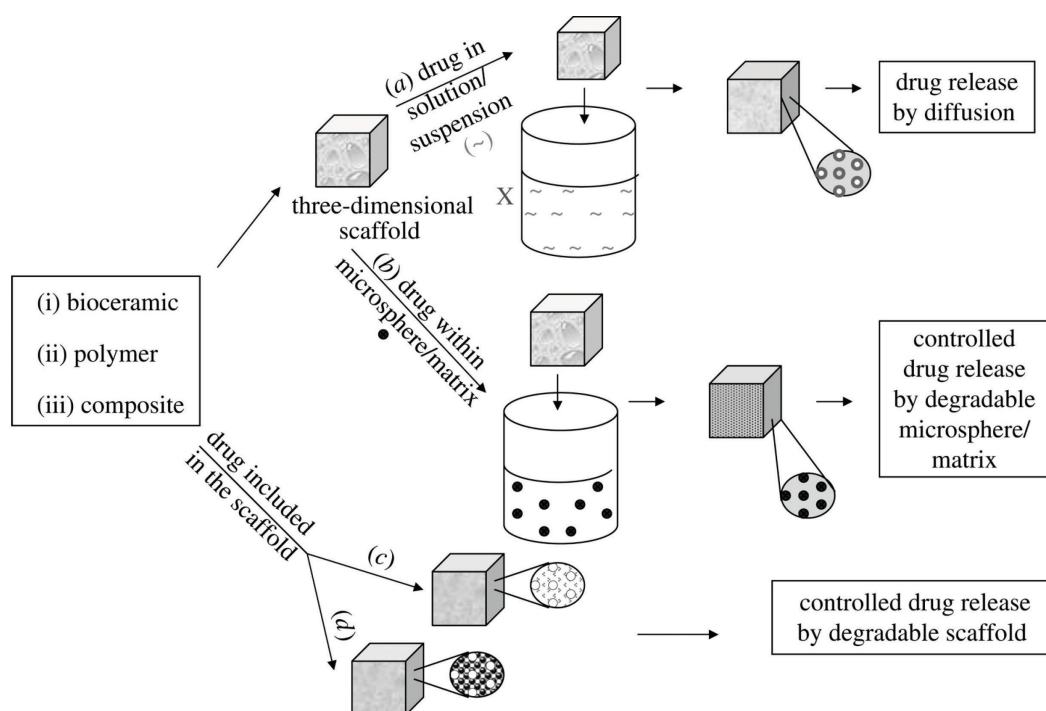
Figure 1. "Schematic representation of the most common strategies to deliver drugs from three-dimensional scaffolds in bone TE. Drugs may be adsorbed onto the pore surface of the scaffolds in either their unprotected (a) or their protected (microsphere/matrix) (b) forms. Alternatively, drugs may be entrapped in the scaffold structure in either their unprotected (c) or their protected (microsphere/matrix) (d) forms." (Reproduced with permission from Mourino *et al*. [33])

Bone tissue engineering aims to replace the use of autografts where possible. It is a developing field aiming to regenerate bone by the use of biomaterials, drugs and cells [35]. The biomaterial should serve as a scaffold for the regenerating bone and as a delivery system for the loaded drugs and cells. Bone tissue engineering can in principle be applied to any bone defect for orthotopic bone formation, and can be used in maxillofacial surgery, spinal fusion and even any soft tissue for de novo bone formation.

Bone extracellular matrix is composed of both inorganic matrix mainly hydroxyapatite, and organic matrix mainly collagen I. Hydroxyapatite crystals are deposited on the collagen fibers [36]. This extracellular matrix plays a role in the repair of the tissue by maintaining the soluble factors, hosting cells and allowing the nutrition transport. The biomaterial used for the regeneration therefore should support the regenerating extracellular matrix to maintain these roles.

Fracture healing represents a good example to understand the natural healing process (Figure 2). In fracture healing, four main bone repair processes occur: (i) inflammation (haematoma formation), (ii) soft callus formation, (iii) hard callus formation and (iv) bone remodelling [37] (Figure 2). Each stage is characterized by a specific set of cellular and molecular events. At cellular level, inflammatory cells, vascular cells, osteochondral

progenitors and osteoclasts act as key regulators in wound healing, whereas at molecular level, repair is driven by pro-inflammatory cytokines and pro-osteogenic and angiogenic factors [37, 38].

The initial stage is inflammation and inflammatory cytokines secreted in this stage are critical for the inflammatory response that triggers osteogenesis [39]. Directly after trauma, a haematoma is formed from blood, bone marrow and immune cells. Platelets, macrophages and other inflammatory cells infiltrate the haematoma and form a fibrin network (clot) that facilitates cellular migration. Within the clot, platelets degranulate, thereby releasing chemotactic signalling molecules that stimulate undifferentiated MSCs and enhance proliferation of MSCs, chondrocytes and osteoblasts. Progenitor cells of chondrocytes and osteoblasts arise from MSCs mainly in the bone marrow [40]. Over the course of time, the clot remodels into granulation tissue [41]. The next stage is cartilage formation that is driven by chondrocytes and fibroblasts, which are stimulated by cytokines and growth factors. These specific cells produce a soft (fibrocartilaginous) callus, that provides mechanical support and serves as a template [42]. In the generation of hard callus, soft callus is gradually removed and revascularization occurs. This phase is dominated by osteoblasts and characterized by active periods of osteogenesis. During the final stage, bone is remodelled, by the osteoclasts and osteoblasts and involves two main steps; bone resorption of primary bone and production of new (secondary) bone [43]. All of these steps are important for bone to regenerate and heal completely. If this regeneration fails due to a disease or a size of the defect, grafting is necessary.

Bone tissue engineering materials

Autologous bone grafting is the gold standard in clinics. However, limited source of autograft and donor site morbidity [45] has diverted the field to seek for alternatives. Several bone substitutes have been approved by the Food and Drug Administration (FDA) for clinical use. The majority of clinically used products are based on inorganic materials such as calcium phosphate ceramics, calcium phosphate cements and bioglass [46, 47]. Synthetic polymers such as methylmethacrylate polymer and porous polyethylene polymer are less commonly used as bone substitutes [48]. A limited number of natural polymers are used as bone substitutes. Collagen is the most commonly used one; it is used as a composite or as a carrier for growth factors. Hyaluronic acid is used as a carrier for demineralised bone matrix [49]. These FDA approved bone substitutes are in many cases not as effective as autologous bone. Therefore autologous bone grafting remains the gold standard. This shows that there is still room for improvement by means of bone tissue engineering and by improving biomaterials to better mimic the bone tissue. Besides, using implants such as titanium can lead to resorption of the healthy bone as it is in the case of femoral implants [50]. This means that implants should be designed to interact and integrate better with the native bone tissue along with providing mechanical strength. There are several potential pre-clinical biomaterials that can perform better than clinical products. Natural biopolymers

such as alginate, chitosan and other ECM materials such as proteoglycans, hyaluronic acid, proteins such as collagen, fibrin and the composites of these materials are examples of materials in pre-clinical development [51].
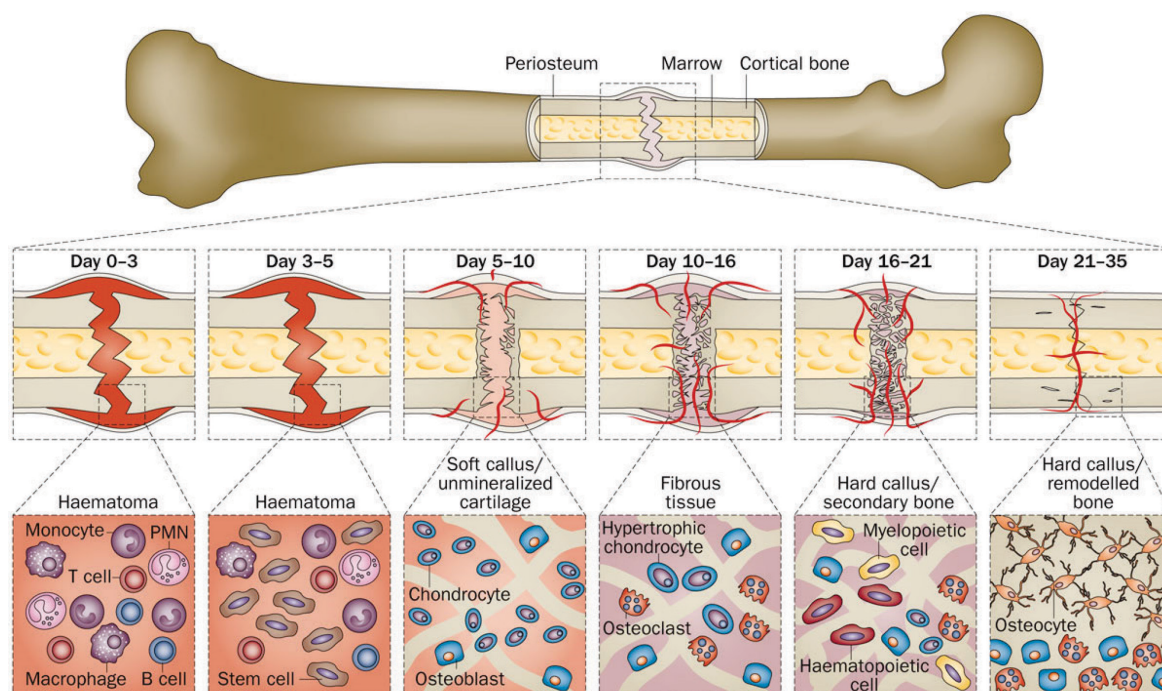
Figure 2. Bone fracture repair process. The primary cell types that are found at each stage are demonstrated (PMN: polymorphonuclear leukocyte). Time span is representative for mouse femur fracture healing. (Reproduced with permission from Einhorn et al. [44])

Bone morphogenetic protein-2 and its use in bone regeneration

One successful therapeutic approach in bone tissue engineering is combining a suitable material with a growth factor to regenerate the bone. Bone morphogenetic proteins BMP-2 and BMP-7 delivered with collagen are FDA approved growth factor based bone therapies. (Medtronic; Stryker). Bone morphogenetic protein-2 was discovered by Dr. Marshall Urist [52]. He showed the potential of BMP-2 to induce bone formation. BMP-2 is a growth factor of the TGF-beta family and it is involved in bone organogenesis. However, its function is not only inducing bone formation, but it is also involved in many developmental and physiological events. Among many examples, it is known that BMP-2 is required for early heart development [53]. BMPs have been shown to regulate the action of follicle stimulating hormone in the ovaries [54]. At a molecular level, different modes of cross-talk exists between TGF-β/BMP and the signalling pathways of Mitogen-activated protein kinase, phosphatidylinositol-3 kinase/Akt, Wnt, Hedgehog, Notch, and the interleukin/interferon-gamma/tumor necrosis factor-alpha cytokines pathways [55]. Some of these pathways have been shown to regulate the effects of BMP-induced signalling in bone dynamics [56]. Such a

potent growth factor therefore should be spatio-temporally controlled. In body, TGF-β/smad pathway is controlled by complex expression of intracellular and extracellular inhibitors and activators.

BMP-2 soaked collagen sponge was first introduced in the United States in 2002 as approved by Food and Drug Administration (FDA) for anterior lumbar interbody fusion in a titanium cage[57]. In 2004 it was also approved for tibial nonunions as an alternative to autograft, and in 2007 for oral maxillofacial reconstructions [58, 59]. However, independent reviews stated a reporting bias in the industry-sponsored publications [60, 61]. In addition several adverse events associated with BMP-2 were reported and some of them were life-threatening, especially in anterior cervical spine fusions [61]. These were cervical and soft tissue swelling, airway compromise, and need for reoperation [62]. As a result, FDA issued a Public Health Notification about BMP-2 use in 2008 [63]. Later, these adverse events have been associated to the poor release profile of BMP-2 with a high initial burst release and supraphysiological doses of BMP-2 [64]. Due to the fast release of BMP-2 (around 50% in the first two days) a high loading concentration of the protein was necessary to achieve effective dose in the following days [65]. It is many times postulated that with a good carrier for BMP-2, protein release can be modulated to be more effective [64, 66]. In this way, the initial loaded dose can be decreased thereby adverse effects are expected to decrease.

Aim and outline of this thesis

In this thesis, we aim to design and compare different biomaterials in terms of growth factor (BMP-2) release profile and bone regenerative capacity with a final goal to develop biomaterials that can induce or augment bone healing. My research question is: Which design of slow release system with which release profile will induce bone healing?

Chapter 2 reviews the current osteogenic growth factor delivery systems with special attention to bone morphogenetic protein-2 (BMP-2). In this chapter we review the gene and protein delivery strategies mentioning advantages and drawbacks of each system and new technologies allowing protein delivery with specific coupling to the scaffolds.

In chapter 3a, the development of a slow release system for an osteogenic protein, such as BMP-2, is demonstrated. Using recombinant collagen I based recombinant peptide (protein) (RCP) microspheres and varying the characteristic of these microspheres we modulate the release profile of BMP-2. Furthermore, we study the molecular interaction between BMP-2 and RCP directly by means of surface plasmon resonance experiments. In Chapter 3b, microspheres carrying different concentrations of BMP-2 are tested in rats in an ectopic model to study bone formation.

For chapter 4, we develop different in situ gelling hydrogels to deliver BMP-2 carrying microspheres. The purpose of the hydrogel is to keep the microspheres in situ, fill a defect and create a scaffold for the infiltrated cells to deposit their own matrix. We compare the performance of various hydrogel-microsphere composites with respect to physical chemical characteristics, BMP-2 in vivo release, bone formation, cell infiltration and inflammatory characteristics. The alginate microsphere formulation appears to be the best hydrogel for bone formation and this formulation is selected for the study in chapter 5.

In chapter 5, we hypothesize that the dose of BMP-2 delivered with RCP microspheres in an alginate gel has an effect on bone formation in terms of bone volume. This hypothesis is first tested using four doses of BMP-2 in an ectopic bone model in rats. Later two doses of BMP-2 are tested in calvarial defect model in rats.

In chapter 6, the parameters that can be further improved in a biomaterial are discussed. Degradation rate, interaction with the matrix and drug release profile of our material are compared to those described in literature. As a future perspective, application areas are proposed and feasibility of clinical translation is discussed.

Finally, in chapter 7 I summarize the findings of the research performed for this thesis.

CHAPTER 2

HOW TO USE BMP-2 FOR CLINICAL APPLICATIONS?: A REVIEW ON PROS AND CONS OF EXISTING DELIVERY STRATEGIES

Didem Mumcuoglu[1,2§], Claudia Siverino[3§], Barbara Tabisz[3§], Bas Kluijtmans[1], and Joachim Nickel[2,3]

1 FUJIFILM Manufacturing Europe B.V., P.O. Box 90156, 5000 LJ Tilburg, The Netherlands
2 Department of Orthopaedics, Erasmus MC, University Medical Center Rotterdam, The Netherlands
3 Wuerzburg branch of the Fraunhofer-Institute Interfacial Engineering and Biotechnology, IGB, Translational Center Wuerzburg ´Regenerative therapies in oncology and musculoskelettal diseases`, Roentgenring 11, D-97070 Würzburg, Germany
4 University Hospital Wuerzburg, Chair Tissue Engineering and Regenerative Medicine, Roentgenring 11, D-97070 Wuerzburg, Germany
§   Authors contributed equally to this work.

INTRODUCTION

Healing of bone fractures describes a remarkable process in that the injured tissue heals without scar formation, thus typically resulting in a complete regeneration of the bone´s anatomy and function [67]. Long bone fractures are reported to occur in the western world at an incidence rate of 300 - 400 cases per 100,000 individuals per year [68, 69] and heal in most cases without surgical intervention within 20 weeks [70]. The needs for a progressive union of bone fractures have been identified and defined as a so-called diamond shaped concept comprising the parameters: adequate cellular environment, sufficient growth factors, bone matrix and mechanical stability. Patients lacking one of these parameters might develop complications during the healing process, which subsequently can result in a delayed or even non-union of the fracture [71]. The incidence of non-union fractures has been reported to range from 4 - 10 % [70, 72]. Non-union fractures are associated to reductions in the patient´s general life quality but also to concomitant inconveniences and costs due to prolonged hospitalization and secondary interventions. It is therefore of great interest to develop new therapeutic concepts that positively affect bone healing.

In the past, the main focus for a regenerative stimulation of non-union fractures was laid on the use of autograft, allograft, and xenograft bone. Of these, autografts were considered as golden standard as these are osteogenic, osteoconductive, and osteoinductive [73-75]. However, the use of autografts is limited due to the given volume quantities and due to donor site morbidities which are frequently observed and typically accompanied by chronic pain [76]. Other major complications which occurred upon extraction of autograft bone are vascular injuries, deep infections, or neurologic injuries at the donor site [77].

Another regenerative approach which recently gained attention as alternative to autograft bone in clinical settings is the use of platelet-rich plasma (PRP). This method in principle utilizes intrinsic growth factors of platelet concentrates in order to stimulate and accelerate a healing response [78]. However, despite the efficacy of PRP in *in vitro* and *in vivo* scenarios, its use and delivery in terms of bone regeneration have yet not been optimized. A significant drawback of such preparations is that optimal doses for administration as well as the identity of the active substances within the concentrates are largely unknown [79].

Extensive studies focusing on the underlying molecular mechanisms of fracture repair identified some specific factors to be involved in the healing process like parathyroid hormone (PTH), hypoxia-inducible factor 1a (HIF-1a), factors modulating the Wnt signaling pathway, and bone morphogenetic proteins (BMPs) [80]. The use of defined compounds like such growth factors allows more precise treatment of bone fractures and are financially advantageous since high amounts of these factors can be prepared in appropriate recombinant expression systems [81]. Here, the most promising growth factor candidates are bone morphogenetic proteins (BMPs), which were originally identified by their capabilities to induce the formation of bone when implanted at ectopic sites [52, 82].

BMPs belong to the large TGF-beta superfamily of secreted growth factors which play an important role in early embryonal development but are also crucial for the maintenance and regeneration of tissues and organs in the adult organism [83-85]. The existence of BMPs in all vertebrates as well as non-vertebrate animals highlights the importance of these factors for a multitude of biological processes, which recently gave rise to the suggestion to rename the term "bone morphogenetic protein" into "body morphogenetic protein" [86]. This renaming would also eliminate the misinterpretation that all BMPs are truly osteogenic. BMPs which indeed induce bone formation can be, based on sequence homology and receptor usage, divided into three subgroups, the BMP-2, -4; the BMP-5, -6, -7; and the BMP-9, -10 subgroup, respectively [87, 88]. Other proteins which are, based on a historical context, also called BMPs are either not osteogenic or their precise function has yet not been fully elucidated. For instance, BMP-1 (also known as Mammalian tolloid protein (mTLD) or Procollagen C-proteinase (PCP)) represents a metalloprotease and does not share structural similarities with other TGF-β superfamily members [89]. Further examples are provided by BMP-3, BMP-13 (also known as GDF-6) and BMP-14 (also known as GDF-5) which function, at least partially, as BMP antagonists/inhibitors rather than being agonistic on their own [90-92].

Signal transduction by TGF-β superfamily members is typically initiated by binding to two types of serine/threonine kinase receptor chains termed type I and type II [93-95]. Upon complex formation, the constitutively active type II receptor activates the type I receptor which subsequently leads to an activation of the so-called canonical SMAD signalling pathway [96, 97]. Disregarding cross-talks with other connected signalling cascades (like e.g. the MAP-Kinase signalling pathway) only two different SMAD pathways, the so-called SMAD-2/-3 or the SMAD-1/-5/-8 pathway, are established. Which of the two canonical pathways finally gets activated solely depends on the individual type I receptor (the particular signalling receptor) being present in the signalling active ligand-receptor complex. Thus, within this superfamily a strong signal convergence starting from a manifold of ligands and ending principally in the activation of only two different SMAD signalling pathways is established which appears even more limited as far as osteogenic BMPs are concerned [98]. Despite differences in the preferential receptor usage observed for the particular osteogenic ligands, signalling occurs in all cases via the SMAD-1/-5/-8 pathway. For BMP-2 and -4 -10, signalling is mediated by the type I receptors (BMPR-IA or IB) whereas the BMP-5/-6/-7 subgroup utilizes ActR-I (Alk2) for signalling (for review, see Katagiri *et al.* [99]). For BMP-9 high affinity binding to ALK1 has been reported but signalling can also occur via ActR-I [100]. The obvious discrepancy between the number of ligands (more than 20 BMP members have been identified in mammals to date) and the limited amount of receptors raises important questions especially how these proteins can share so many different cellular functions and furthermore how those can act as morphogens during embryogenesis. Different temporal and/or spatial expression patterns might best explain this issue but since double knock-outs of ligand genes often lead to more severe phenotypes than observed for the individual

single knock-outs the existence of at least partial compensation must be taken into consideration. It therefore seems plausible that cellular signalling is modulated massively at several cellular levels (for review see Nickel *et al.* [98]). Extracellularly so-called modulator proteins (e.g. Noggin, Chordin, etc.) can bind to the ligand thereby preventing its interaction with the receptors as shown for Noggin [101] or Follistatin [102]. Thus, ablation of the interaction of the osteogenic factors to Noggin also indirectly increases the osteogenic potential of the particular ligand [103].

Aside from these modulators, the biological activity of BMP-2 or -7 is also regulated by their capability to bind to components of the extracellular matrix (ECM) such as heparin or heparan sulfates [104, 105]. *In vivo*, the ECM seems to function as reservoir by adsorbing the ligands from the three-dimensionality of the interstitial liquid thereby increasing the ligands concentration on the cell surface. The matrix serves as a store allowing a slow release of the ligand over prolonged periods of time. Hence modulating the binding strength of the growth factors to the ECM could result in altered bioactivities which indeed has already been observed *in vitro* and *in vivo* [106].

Taken together, the different aforementioned parameters which concertedly define the particular ligand´s osteogenic potential have been addressed in several pre-clinical and clinical trials. They generally aimed to produce osteogenic formulations allowing the application of the growth factor to defect sites. For that purpose, they use systems which concomitantly control the factor´s release to achieve sufficient high local concentrations over the period of time needed to heal the defect.

This review sheds light into the design of the different systems to deliver BMP-2 for *in vivo* applications. As outlined above, the control over the growth factor´s bioactivity and spatial-temporal presence is obviously crucial for bone healing but seems extremely difficult to achieve.

Growth factors like BMP-2 can principally be brought to injured site in two different ways. At first, DNA that encodes for the particular growth factor can be delivered either in form of a suitable expression plasmid or integrated into a viral particle or the genetic information is already introduced into an acceptor cell´s genome in order to express the particular growth factor at the site of action. As second method, the gene product, i.e. the recombinant expressed growth factor itself or peptide mimicking its specific bioactivity, is applied ectopically to the injured site. For an overview, see Figure 1.

Gene therapy offers a multitude of different applications ranging from cancer to various infectious diseases, cardiovascular or other monogenic disorders. Due to its generic potential, over 1800 clinical trials involving gene therapy were conducted by 2012 [107]. Also in bone regeneration the potential of gene delivery is still under investigation. Principally, as mentioned before the genetic information can be delivered by a vector to the injured site where cells will take it up and start protein expression, or by the delivery of cells

that are already transfected with an appropriate vector *ex vivo* which, after implantation, will express the protein at the site of injury.
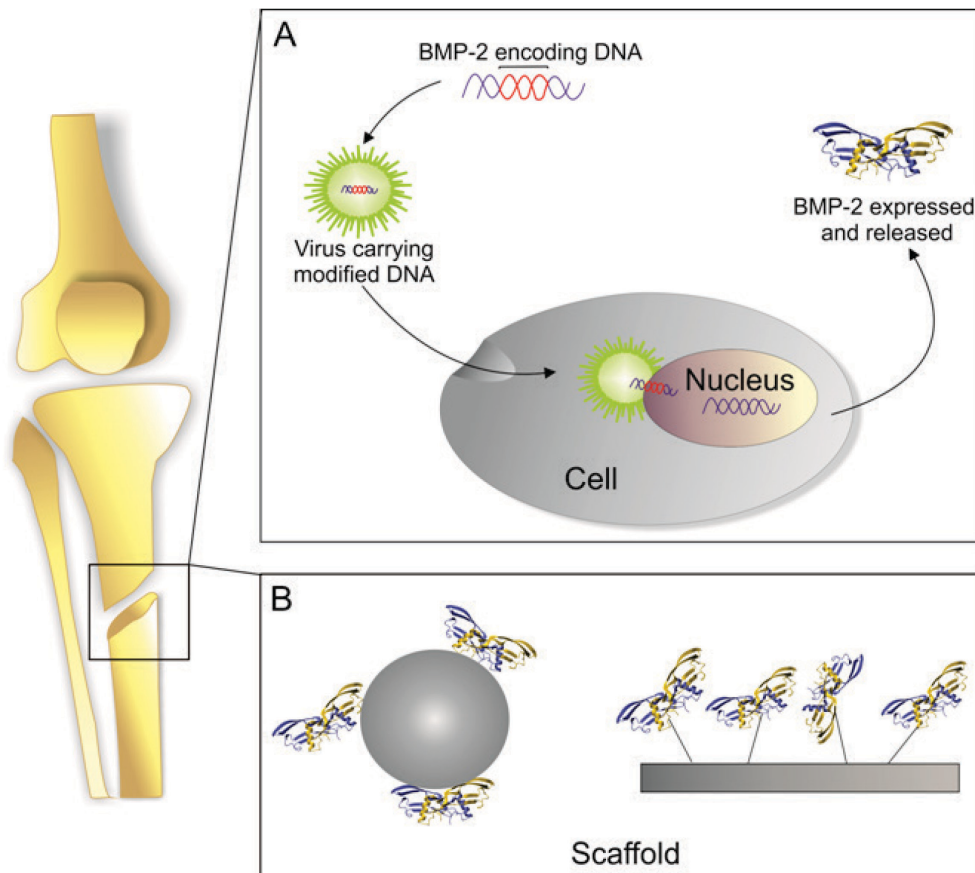
Figure 1. Main principles for growth factor delivery. (A) cDNA encoding for the desired growth factor is introduced into the cells e.g. via plasmids or viral vectors and is translated and secreted at the site of injury. **(B)** The protein is deposited at the site of injury in a form of depot e.g. in form of functionalized scaffolds.

In the following, both techniques are discussed in detail comparing the feasibility and drawbacks of each technique in scope of bone regeneration by application of the best investigated osteogenic factor, BMP-2, as well as potential ways to further improve each technique.

BMP-2 DELIVERY USING BMP-2 ENCODING cDNAs

General aspects of various DNA delivery methods

The choice of the growth factor to be expressed is very important since the single gene to be delivered, here that of BMP-2, must initiate an apparently high complex process resulting finally in the full restoration of the bone defect. For more complicated cases (e.g. where a large defect area needs to be repaired) gene delivery of a combinations of BMP-2 along with

factors of other growth factor families (e.g. VEGF) [108] or combinations of BMP-2 and transcription factors (e.g. BMP-2 and Runx2) seems advantageous [109]. Co-expression of BMP-2 and transcriptional factors being specific for bone tissue such as Runx2 might provide more efficient bone regeneration since it regulates expression of other osteogenic factors that drive e.g. the osteogenic differentiation of mesenchymal stem cells [110]. However, the osteogenic gene to be delivered is not the only parameter to be considered. Also the choice of the vector or the matrix that will determine the transfection efficiency of the gene and the residence time is equally important. A major concern of gene therapy is the stable and controllable overexpression of the delivered gene. In order to prevent extreme expression levels, which in terms of BMP-2 delivery might result in unwanted off-target effects, constructs with inducible promoters - such as tetracycline-sensitive promoters (TetON) - might be favorable [111].

In general, the vectors that are used for gene therapy can be subdivided into two classes: viral and non-viral vectors. The use of viral and non-viral vectors for tissue engineering has been reviewed elsewhere [112-114] but advantages and disadvantages of the particular expression systems are important to note. Viral vectors - as the name suggests - are derived from viruses (i.e. adenovirus; lentivirus) and have higher transfection efficiencies than non-viral vectors. However, due to safety concerns, the use of viral vectors in clinics is still under debate. Safety concerns address immunogenicity of particular viruses which indeed differ amongst different virus types. The adenovirus, which was one of the first used vector systems for gene delivery, may induce inflammatory or antigenic responses due to expressed viral hull proteins [115], whereas adeno-associated viruses (AAV) are considered to be safer since viral proteins are not expressed in the receiver cell (for review, see Buning *et al*. [116]). On the other hand, retroviruses or lentiviruses might induce insertional mutagenesis which limits their general potential for gene therapy. The use of adenovirus or AAV in bone regeneration at this stage seems more feasible since it poses less risks and it provides transient expression for several weeks matching the time frame for bone defect to heal [112].

Due to the mentioned safety concerns, a promising alternative relies on the use of liposomes that act as a vehicle for non-viral vectors (plasmids) and might reach adequate efficacy with coincident lower risks compared to viral vectors. Besides safety, liposomes are easy to prepare and their use is not constrained by the size of the used DNA [117]. Both, viral or non-viral vectors can be applied to the injury site either directly or embedded within a matrix/scaffold.

Delivery of BMP-2 encoding genes by direct injection of viral or non-viral vectors or by application of DNA-functionalized matrices

Different DNA delivery methods have been investigated *in vivo* using different animal models. In rodents, the injection of adenovirus carrying the BMP-2 gene resulted in

successful delivery and as a result of BMP-2 over-expression improved osteogenesis in the defect area could be observed [118]. However, in other animal studies the same adenoviral system failed [119]. In these cases, a high level of BMP-2 expression was observed within the first week after implantation which strongly decreased in the following weeks. Inflammatory cells were found in the defect area which showed an immune response against BMP-2 and/or the adenoviral vehicle which might explain the observed retardation of osteogenesis [119]. This study revealed the importance of larger animal studies before conducting clinical trials which is also recommended by FDA guidelines [120].

In order to improve the efficacy of the applied vehicles, they might be shielded from the recipient´s immune system using so-called stealth (PEGylated) liposomes. Another method to increase the transfection efficiency of the vehicle relies on the use of cell penetrating peptides (CPPs) [121]. Also targeted delivery of the vehicles specifically to bone tissue would result in a homing of the transgene to the defect site. A very interesting new idea for efficient gene delivery is based on "designer" histones serving as targeting molecules thus aiming to improve the osteogenic capacity of growth factors [122]. Taken together, more sophisticated designs of vectors (e.g. with stealth liposomes, CPPs, inducible systems or targeting molecules) hold more potential if used in direct gene delivery approaches. But, the development of suitable delivery systems is not easy since the individual design strongly depends on the application itself and the clinical outcome of such a complex design is hard to predict. Different ways to improve gene delivery systems in general are detailed elsewhere [123] but one important improvement to be noted relies on the encapsulation of the vector within a biomaterial or functionalizing the material´s surface with DNA encoding for the desired protein [123]. Those matrices are called "gene-activated" matrices (GAMs) and their applications have been extensively tested either in a form of hydrogels [124] or implant coatings [125]. In one example, BMP-2 encoding cDNA was embedded within alginate hydrogels which serves as a potent transfection agent and as a good scaffold material at the same time [126]. Advantages of such matrices are the long shelf-life of the material (possibility of freeze-drying), and ability to function as a defect filler [114].

For the regeneration of more complex tissue structures like the bone-cartilage interface, scaffolds comprising two layers were designed, one of which consisted of a "chondrogenic plasmid" (TGF-β1)- functionalized chitosan-gelatin and the other an "osteogenic plasmid" (BMP-2)-functionalized hydroxyapatite/chitosan-gelatin [127]. Mesenchymal stem cells were also seeded in each layer of the gene activated matrix. Detailed analyses of this system revealed that the used stem cells differentiate towards chondrocytic or osteoblastic lineages depending on the layer they were positioned. Furthermore, a successful regeneration of an osteochondral defect could be achieved using this construct in a rabbit knee model.

The different natural or synthetic scaffold materials being used for bone regeneration are not in scope of this review article. However, since the scaffold also actively takes part in the regeneration process, the characteristics of each biomaterial should be considered,

compared and selected for a specific application. Among different natural polymers, insoluble collagen-based bone matrices (ICBM) have been widely used which is based on the fact that that bone organic matrix principally consists of collagen (90%) [128]. The drawback of this matrix relies on remnants of immunogenic molecules that might challenge the host´s immune system. Other natural matrices which are represented by in situ gelling systems like alginates or peptide nanofibers are injectable, thus allowing easy filling of the defect area. Although a matrix is important to fill the defect area and localize cells and growth factors at the site, it does not always result in better healing process which depends strongly on the chosen scaffold. For instance, in a study where either untreated or adenoviral transduced cells expressing BMP-2 were injected either directly or embedded within alginates into a bone defect in nude rats, the alginate scaffold clearly impeded BMP-2 induced bone formation [129]. This study nicely demonstrates that parameters like the choice of the cells to be introduced or the selected scaffold material only seem to fine-tune the outcome of the individual experiment but the initial trigger of this complex process is provided by the applied osteogenic growth factor.

Gene delivery by cells *ex vivo* transfected with BMP-2 encoding cDNAs.

Cell mediated gene therapy is another approach in which cells are transfected *ex vivo* with the cDNA encoding for the desired growth factor and are subsequently administered to the injury site for tissue regeneration. The disadvantages of cell based gene therapy compared to acellular approaches are related to costs and also the necessity to obtain sufficient amounts of suitable autologous cell material. Furthermore, the procedure is more difficult to perform than the before mentioned acellular approaches, it is more time-consuming due to the necessity to expand the autologous cells. Additionally, the work has to be done according to the guidelines of Good Manufacturing Practice (GMP). However, there are also noteworthy advantages, since the delivered cells themselves might actively participate in the regeneration process. Due to complications associated with allogenic cell sources, the use of autologous cells is the gold standard in the clinics so far [130]. But, there is also a drawback of this technique. An additional treatment or surgery is required in order to obtain these cells being often accompanied by a significant tissue morbidity at the site of explantation [131]. The current practices and studies in bone and cartilage regeneration generally involve mesenchymal stem cells (MSCs) derived either from bone marrow or other sources. Owen and co-workers already showed in the late 1980s that bone marrow derived stem cells (BMDSCs) can be differentiated towards different cell types including bone [132]. More recently, an alternative, powerful method was established to re-program non-stem cells to so-called "induced pluripotent stem cells" (IPSCs). Here, somatic cells (e.g. adipocytes which can be obtained easily by liposuction) are dedifferentiated to so-called induced pluripotent stem cells (iPSCs) which subsequently are again differentiated to MSCs [133]. This new method is not yet in clinical use, but first clinical trials using IPSCs for macular degeneration have been initiated in Japan [134]. In one of the early clinical studies addressing the treatment of bone disorders, the transplantation of allogenic MSCs has been

investigated in children with osteogenesis imperfecta. In this study, the allogenic BDMSCs were shown to improve the velocity of bone growth in five of the six patients [135] which led to several follow-ups in the field of bone regeneration. Recently, a clinical trial has investigated the effect of BMDSCs for craniofacial bone regeneration. Here, accelerated alveolar bone regeneration could be observed in a jawbone defect thereby eliminating the need for secondary bone grafting [136]. While usage of BDMSCs progresses in clinical trials aiming for bone regeneration, pre-clinical studies already involve MSC-based gene delivery. In one of these pre-clinical studies, bone marrow derived cells were co-transfected with cDNAs encoding for BMP-2 and vascular endothelial growth factor-165 (VEGF-165) in order to induce bone regeneration by means of BMP-2 mediated osteogenesis and VEGF mediated angiogenesis [137]. The cohort expressing both growth factors simultaneously was found to be better in terms of the formation and deposition of newly formed bone compared to the cohorts expressing only one of the two growth factors in rabbit orbital defect model [137]. The delivery of VEGF in combination with the osteogenic BMP-2 induces neo- vascularization of the newly formed bone tissue thus enabling superior supply of nutrients [138].

Harvesting bone marrow is not an easy procedure since it often causes post-operational pain. Therefore, alternative stem-cell sources, such as adipose tissue, have been intensively investigated. In a study employing BMP-2 transfected adipose stem cells, their potential for bone regeneration was clearly demonstrated. When rats were treated with the transfected stem cells being embedded into alginate gels, complete bone healing was observed in a cranial defect model [139]. Thus, due to the easy of collection adipose tissue derived stem cells are preferred over BMDSCs at least for this application.

However, most of the clinical trials utilizing MSCs for bone regeneration were not successful. Meijer et al. [130] stated possible reasons and identified important parameters as the number of cells with osteogenic capacity, the bio-compatibility of the used scaffolds, the presence of osteogenic factors, and vascular supply. Furthermore, it was also reported that results of pre-clinical trials in most cases could not serve as layout for the clinical studies since differences in e.g. the regeneration time of rodents and humans produced different experimental outcomes [130].

In MSC mediated gene delivery, one of the critical issues is the localization of the modified cells, and consequently the localization of the expressed protein. However, when MSCs were injected, it was observed that the injected cells do not easily home to bone and 98% of the injected MSCs are lost through liver and spleen [140]. To overcome this problem, the cells might be transfected to co-express an osteogenic growth factor like BMP-2 along with bone-homing proteins e.g. CD49d [141].

DELIVERY OF RECOMBINANT BMP-2

General aspects

Growth factors which can be delivered to the site of injury might recruit endogenous stem cells to the site of action which upon exposure to the ligand undergo differentiation, thus inducing bone healing in situ. An FDA approved product, INFUSE® Bone Graft, which contains BMP-2 being adsorbed to a collagen sponge has been clinically used in spinal cord injuries. However, some adverse events such as infections, severe swelling, heterotopic ossification or urogenital problems have been observed after surgery [62, 142, 143] which are discussed to be related to the supraphysiological amounts of the growth factor being administered. This leads to the hypothesis that these adverse events might be eliminated by reducing the delivered growth factor amount to a suitable yet clinically relevant dose. Therefore, the development of a delivery system that provides a sustained release of the protein at sufficient concentrations is a challenge of high priority. An overview on the various BMP-2 delivery strategies is depicted in Figure 2. These strategies will be discussed in more detail in the next sections.
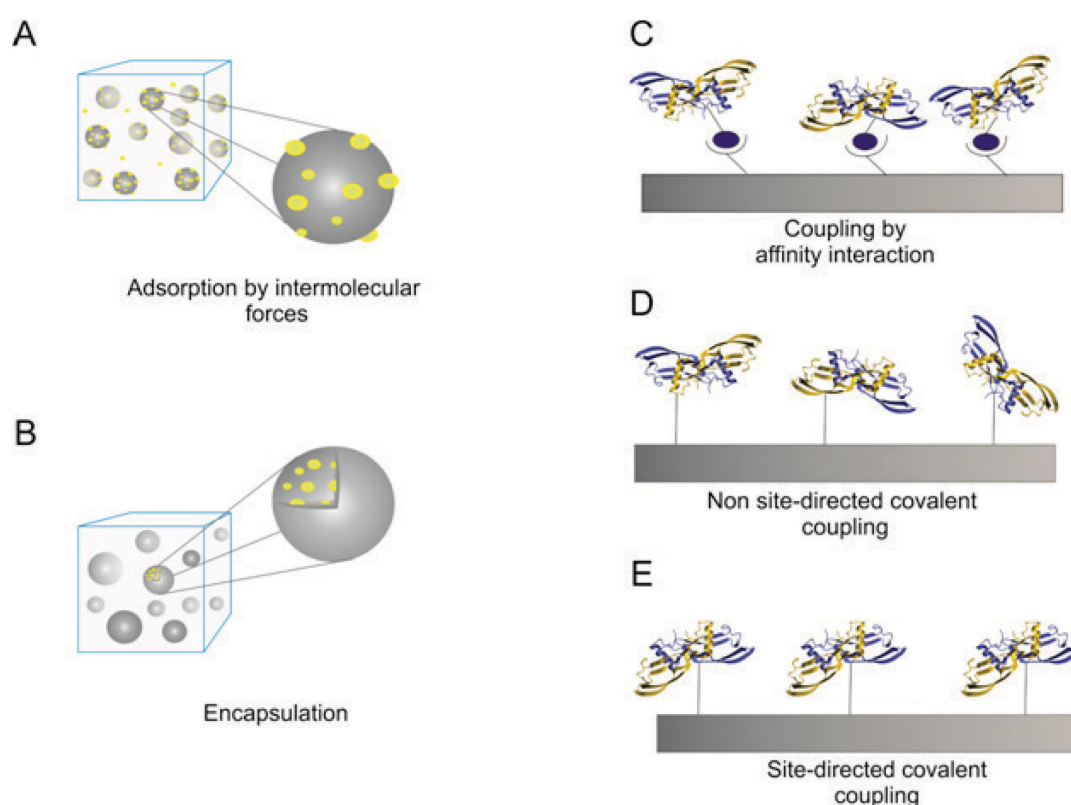
Figure 2. Delivery strategies for recombinant expressed BMP-2 or BMP-2 variants

The cartoons illustrate the different immobilization strategies as indicated **(A)** BMP-2 can be adsorbed to solid surfaces or encapsulated into e.g. hydrogels **(B)**. Higher coupling specificities can be achieved by affinity interactions e.g. using biotinylated BMP-2 being coupled to streptavidin coated matrices **(C)**. Covalent coupling can be achieved non site-

directed to structures being activated e.g. by NHS esters **(D)** or site-directed via click chemistry **(E)**.

Non-covalent binding strategies

Delivery of encapsulated or adsorbed BMP-2

In vivo, growth factors interact with receptors present on the cell surface in a non-covalent manner. The signalling molecule, such as BMP-2, is in most cases soluble (i.e. not membrane bound) and thus can diffuse or be actively transported to responsive cells. Therefore, many research laboratories emphasized on non-covalent binding strategies which utilized growth factors being adsorbed to or encapsulated in a broad variety of suitable scaffold materials.

Natural polymers such as collagen have several advantages. For example, they have endogenous enzyme cleavage sites and the degradation time of the material follows the endogenous remodelling time of collagenous tissues. Collagen sponges represent the earliest and best studied materials used for BMP-2 delivery. A disadvantage of this material relies on so-called early burst effects which are often observed upon administration [144]. In order to obtain a sustained release of the protein and decreasing this initial burst release phenomenon, genipin-crosslinked gelatin microparticles have been designed. Gelatin microparticles showed lower burst releases compared to poly(lactic-co-glycolic acid) (PLGA) microparticles *in vitro*. A composite scaffold of these gelatin microparticles embedded in poly(propylene fumarate) (PPF) showed a sustained release of BMP-2 *in vivo* in a subcutaneous mouse model. This study also demonstrated that microspheres encapsulated within a scaffold provide a better control of growth factor release compared to the scaffold alone [145]. In order to produce fully synthetic biodegradable materials, mimics of natural polymers such as collagen have been designed. In one of these studies, matrix metalloproteinase (MMP) cleavage sites and RGD (Arg-Gly-Asp) moieties were introduced into polyethylene glycol (PEG) polymers. Here, the release of BMP-2 was shown to be induced by MMP-2 mediated degradation *in vitro*. The effect of these hydrogels containing 5 µg of BMP-2 on bone healing was studied using critical-sized calvarial defect model in rats. The MMP-sensitive, BMP-2-loaded hydrogel induced formation of new bone comparable to BMP-2 loaded collagen sponges (Helistat®) [146]. Another more complex material which was also studied in the context of bone regeneration, is a MMP cleavable PEG hydrogel functionalized with an α2β1 integrin-specific peptide (GFOGER; single letter amino acid code, O = hydroxyprolin). This material was shown to be effective for bone-healing in a mouse critical size defect model even in the absence of BMP-2 but doping the hydrogel with low BMP-2 doses (0.03 µg) resulted in higher bone formation capabilities and complete bridging of bone gaps after 8 weeks [147]. Hybrid nanofiber mesh/alginate delivery systems containing RGD (Arg-Gly-Asp) have been compared to collagen sponges for BMP-2 release [148]. Bone formation at 8 weeks post-surgery was significantly increased in the nanofiber mesh/alginate group compared to the collagen sponges at the same dose (1.0 µg rhBMP-2).

In order to obtain 3D scaffolds with defined and reconstructable structures, Lee *et al*. [149] created polymeric 3D scaffolds by solid free-form fabrication (SFF) technology, computer-aided design (CAD) and computer-aided manufacturing (CAM) techniques. BMP-2 loaded microspheres were encapsulated within these microstereolithography-produced scaffolds and after 7 days BMP-2 started to be released linearly. When the performance of the construct was studied in a rat cranial bone defect model, around 75% bone formation was observed after 11 weeks [149].

The detailed description of the results, using different combinations of BMP-2 and materials as mentioned before, led to the assumption that the material type has a major impact on the success of bone regenerative approaches. These material related effects become obvious by comparing e.g. brushite and PLGA controlled release systems loaded with the same doses of BMP-2. PLGA appeared significantly more osteogenic than brushite which is attributed to the slow resorption rate of brushite [150]. As a consequence, BMP-2 is not released in sufficiently high concentrations which might indicate the requirement of an at least minimal burst release. On the other hand, the hard brushite material might also impede the migration of invading cells which are essential for the process of bone regeneration.

Delivery of BMP-2 utilizing affinity interactions

One of the strategies for protein immobilization relies on affinity interactions of specifically tagged proteins with appropriately functionalized surfaces. Unlike covalent coupling, affinity interactions are weaker, with the strength depending on the particular interaction partners. In most cases, the interaction can be affected e.g. by changing pH values, the temperature of the solution, or by using a competitive ligand. *In vivo*, these parameters can certainly only be altered to a limited extent. However, there are profound advantages of such approaches relying on a high specificity of the interaction, a mainly uniform orientation of both interacting partners, mild coupling conditions and a broad availability of various commercially available affinity tag systems. Reversibility of affinity interactions may be advantageous when the controlled release of the growth factor is crucial, for instance if the ligand has to be internalized from the effector cell to gain full signaling capabilities.

Nevertheless, there are also some limitations that one needs to consider when choosing the affinity-tag coupling strategy, such as laborious protein engineering, overall cost of affinity ligands, the possibility of changing the proteins properties, an unpredictable release of the immobilized growth factor or limited possibilities for tag positioning. Usually affinity tags are placed on either N- or C-terminus of a protein to minimize changes in its biological activity. Though, positioning of an affinity tag at either the N- or C-terminus of the protein sequence may be in some cases detrimental for its trafficking and folding.

Common affinity immobilization approaches can be performed via a vast number of different molecular fusion tags, such as small charge-based (poly-arginine or poly-histidine-)

affinity tags, epitope tags based on the interaction with antibodies (hemaglutinin (HA), Myc, FLAG™, V5 epitope), protein fusion tags (Protein A, Small Ubiquitin-related MOdifier (SUMO), glutathione *S*-transferase (GST), maltose binding protein (MBP), calmodulin binding protein (CBP), certain protein domains (cellulose binding domain, chitin binding domain), biotinylation (based on strong biotin-avidin affinity), and many others [151-154].

As already mentioned, BMP immobilization has been broadly exploited in terms of physical adsorption, encapsulation and non-specific covalent immobilization. Nevertheless, addition of fusion tags was in context of BMPs employed mostly for protein purification (histag [155], maltose binding protein [156]), or detection and enrichment purposes [157, 158], and only in a few cases designed to enable a more permanent immobilization on scaffolds. Insertion of any kind of tag within the mature part of thr BMP sequence is strongly restricted to the N-terminus, which is caused by the buried architecture of its C-terminal end. Because of the specific domain arrangement of BMP proteins comprising a pro- and a mature-domain, insertion of any tag used in an eukaryotic heterologous expression system is thus strongly restricted to the N-terminal end of the mature part as well which might impose hindrance in the intracellular protein trafficking and proper processing of the mature peptide.

BMP-2 immobilization via His-tags

One of the best explored affinity tags used in protein science is a strain of 6 histidines, demonstrating a high affinity towards bivalent metal ions. An application for BMP-2 immobilization via an introduced his-tag was reported by Zhao *et al*. [159]. BMP-2 was expressed as fusion protein with 6 histidines (his6-tag) fused to the N-terminal end of the mature part of human BMP-2. 10 μg of the tagged BMP-2 protein was loaded onto a demineralized bone matrix (DBM) which was covalently decorated with pentahistidin antibodies (so-called MAbs-DBM). The antibodies were used to enhance the loading capacity of the demineralized scaffold. These scaffolds were subsequently tested in cell based assays for osteogenic differentiation using C2C12 cells and also *in vivo* for inducing ectopic bone formation in male Sprague–Dawley rats. The results clearly showed that his-tag immobilized BMP-2 was able to induce alkaline phophatase (ALP) activity in C2C12 cells in a dose dependent manner independent of whether it was adsorbed to the undecorated demineralized scaffold or bound to the pentahistidin antibody decorated scaffold. However, his-tag-BMP-2 bound to MAbs-DBM induced higher ALP signals at the same BMP-2 dose. *In vivo*, after two weeks of implantation his-tag-BMP-2/DBM and His-BMP-2/MAbs-DBM both induced formation of ectopic bone in proximity to the scaffolds which could not be observed in case of unloaded scaffolds. Moreover his-tag-BMP-2/MAbs-DBM revealed thicker layers of bone tissue and higher levels of calcification [159].

BMP-2 immobilization via bi-functional peptide linkers

Hamilton and co-workers have recently established a phage display procedure for the isolation of short bi-functional collagen and BMP-2 binding peptides [160]. For this purpose, they employed a biotinylated BMP-2 (linked by conventional N-Hydroxysuccinimide(NHS)-coupling techniques), which was then immobilized to a streptavidin-coated 96-well microplate. Ten different phage display libraries, designed with a central specific amino acid core motif were screened for peptides that bind to BMP-2. The identified BMP-2-binding peptides were then individually combined with a collagen-binding peptide sequence (generated in previous work [161]) by a flexible linker. Such bifunctional peptides were mixed with BMP-2 supplied with an injectable collagen gel. The osteogenic properties of the construct (200 µl of collagen gel containing 2 mg of BMP-2) were investigated *in vivo*. Two weeks after surgery approximately 25% of the implant was covered with new bone in the peptide-containing group, whereas no bone formation was observed in the control group (without the bi-functional peptide). Further analyses revealed that binding of the BMP-2-binding peptides to BMP-2 was not affected by the presence of human plasma since plasma components theoretically could interact and thus compete for the binding of the peptide to BMP-2 [160].

BMP-2 immobilization via interaction with heparin/chitosan

Heparin, also known as a heparan sulphate is a highly sulfated glycosaminoglycan, carrying a strong negative surface charge. It is stored mainly in mast cells of the immune system and appears in the extracellular matrix of eukaryotic cells where it interacts with multiple growth factors and serves as an antibacterial and hydrating factor for the cellular matrix [162]. Owing to its strong affinity towards BMP-2, a number of BMP immobilization approaches using heparin/heparin-binding-site interaction emerged in the recent years.

In a paper by Kim *et al*. [163] titanium dental implants were covalently covered with heparin by using classical EDC/NHS-mediated coupling chemistry. The work focused on the development of a dental implant with antibacterial properties and enhanced osteogenic function. The BMP-2 binding to the heparin-grafted titanium discs was accomplished by immersing it in a BMP-2 solution (10 or 50 ng/mL) for 24 h at ambient temperature. *In vitro* tests showed reduced inflammatory potential as analyzed in a murine macrophage cell line, a sustained release of BMP-2 from the heparin-titanium discs and stimulated osteoblast function which was further proven by significantly higher ALP activities and calcium contents in cells grown on BMP-2 (50 ng)-immobilized titanium surfaces. Similar approaches to functionalize titanium surfaces were performed by Lee *et al.* and reported in 2012 [164].

Also recently, a similar approach for BMP-2 immobilization on polycaprolactone fibers was published in which their potential to induce osteogenic differentiation of periodontal ligament cells was studied [165]. The polycaprolactone fiber surface was functionalized with heparin-dopamine and further coated with BMP-2. The publication reports sustained BMP-2

release profiles over 28 days with no evident cytotoxicity against periodontal ligament cells (PDLCs). Fibers with immobilized BMP-2 significantly induced osteogenic differentiation with a significant increase in ALP activity, calcium deposition and mRNA expression levels of osteocalcin and osteopontin compared to the unmodified PCL fibers [165]. A subsequent *in vivo* study demonstrated that the implanted BMP-2/Hep–DOPA/PCL/PLGA scaffolds implanted into rat femur defects induced more bone formation compared to that of BMP-2/Hep/PCL/PLGA- and PCL/PLGA scaffolds [166]. Similarly, BMP-2 has also been immobilized onto calcium coated chitosan scaffolds [167]. These *in vivo* studies were performed in New Zealand male rabbits. Defects of 4 mm in diameter were drilled into tibiae maesetae of both legs and the scaffolds were implanted into the deficient area. The osteogenic potential of the scaffold was analysed 3 weeks after implantation. The results showed that BMP-2 remained active in the chitosan scaffolds and its release kinetic was dependent on the presence of calcium phosphate salts. Chitosan scaffolds containing both calcium phosphate salts (CPS) and BMP-2 were more osteoinductive than their counterparts alone [167].

BMP-2 immobilization via biotin-streptavidin interactions

A complex of biotin bound to streptavidin is the strongest known non-covalent biological interaction, with a dissociation constant (K_D) of 10^{-13} M [168]. The complex formation is robust and binding may only be disrupted by harsh, denaturing conditions. For this reason biotin and streptavidin are a very convenient choice for protein immobilization. In context of BMP-2 immobilization, biotin-streptavidin interaction has been used to study the biological activity of bound BMP-2 [169], as well as for quantifying small amounts of immobilized BMP-2 on various materials [170]. Recently, a continuous surface BMP-2 gradient was constructed using biotin-streptavidin interaction, to enable cell screening studies [171]. However, since the production of streptavidin is cost-intensive, such approaches were in the past mainly addressed in basic research for e.g. protein purification or protein quantification.

BMP-2 immobilization via synthetic oligonucleotides

In an *in vitro* study conducted by Schliephake and co-workers [172] a set of complementary DNA strands was used for BMP-2 immobilization. The aim of the study was to investigate whether oligonucleotides could be suitable to immobilize and slowly release osteogenic growth factors, and thereby enhance the osteogenic potential of titanium implants. 60-mer non-coding DNA oligonucleotides were fixed to titanium surfaces by anodic polarization. Conjugation of BMP-2 with complementary sequences was achieved by chemical crosslinking using disuccinimidyl suberate (DS) as linker molecule. The functionalized BMP-2 was then hybridized to the titanium-anchored oligonucleotides at room temperature (the coupling scheme is similar to that of biotinylated BMP-2 interacting with strepatavidin, see figure 2C). *In vitro* experiments were performed using human bone marrow stromal cells (hMSCs). Release studies over 28-days showed a continuous release of BMP-2 from the

titanium surface. Also proliferation of cells was significantly increased and the osteogenic markers, osteopontin and alkaline phosphatase, were upregulated. Additionally, BMP-2-conjugated scaffolds revealed significantly higher number of focal adhesion points. Released BMP-2 was tested for its biological activity which was shown to be comparable to non-conjugated BMP-2, proving that the conjugation process did not affect its biological activity.

As many affinity binding approaches clearly showed that an increase of the affinity of BMP-2 to particular scaffolds enhances the osteogenic potential of the construct, several research groups have focused on covalent binding of the growth factor onto various materials.

Delivery strategies using covalently coupled recombinant BMP-2

Most of the injectable BMP carriers are unable to retain BMP at the site of injection. As a consequence, most carriers lose 50% or more of pre-loaded BMP after a few days *in vivo*. The delivery of a covalently immobilized growth factor would therefore offer the advantage of a controlled and sustained influence on cell behavior in comparison with soluble or slowly released proteins.

Implanting constructs being functionalized with covalently bound BMP-2 [173] demonstrated the easy delivery of this growth factor with a homogeneous distribution on the implant surface, primarily circumferential bone induction, rapid gap filling by trabecular bone within 4 weeks and an easy control and avoidance of ectopic bone formation. Covalent immobilization of BMP-2 and epidermal growth factor (EGF) has also been achieved on titanium dioxide (TiO_2) nanotube surfaces by N,N-carbonyldiimidazole (CDI) coupling either via direct binding to amine groups of the growth factor or via spacers such as 11-hydroxy-undecylphosphonic acid (PhoA) [174]. Coupling proteins via N,N-carbonyldiimidazole is non-site directed and may result at least partially in deactivation or denaturation of the coupled proteins. BMP-2 coating did not contribute to cell proliferation, attachment, adhesion or proliferation as shown for EGF if exposed to bone marrow derived MSCs. These findings indicate that these cellular activities are not triggered by BMP-2 or that the cells in general might be BMP-2 insensitive.

Since naturally occurring growth factors only contain a limited subset of reactive groups (NH_2-, OH- COOH-, and SH-groups) being present in sidechains of particular amino acids, the chemical coupling reactions have to address the individual demands of these functional groups for coupling. In order to extend the spectrum to a broader variety of potential coupling chemistries, bi-functional linkers have been designed for coupling of growth factors to scaffolds. Several coupling methods have recently been developed to further control the orientation of the growth factors to be immobilized including usage of cysteine-containing tags, peptide aptamers and fibrin or collagen substrates [175]. However, these methods entail protein modifications thus can also affect the outcome of individual cellular responses. Recently, Tabisz *et al.* [176] published a strategy for site-directed coupling of BMP-2 to scaffolds by click-chemistry utilizing an artificial amino acid, which had been

introduced during bacterial expression by amber codon suppression [177]. The constructed BMP-2 variant showed the same bioactivity compared to wildtype BMP-2 and could be coupled site-directed and biologically active coupled to solid surfaces. This technique allows an interesting alternative since the linker used for coupling already gets introduced into the protein upon protein expression thus avoiding secondary modifications. Another hallmark of this technique is that the position of the artificial amino acid is not restricted to the N-terminus of BMP-2 thus allowing a positioning which certainly will not impede the binding of BMP-2 to its cognate receptors.

Engineered surfaces decorated with site-directed and covalently bound BMP-2 being immobilized via optimized linkers might represent an excellent alternative in order to maintain the growth factor´s biological activity. Other surfaces, for instance gold surfaces have been first decorated with a hetero-bifunctional linker which subsequently were exposed to BMP-2. For tracking purpose, BMP-2 has been iodinated with Na^{125}I prior to coupling. The activated surfaces were used in cell based assays using C2C12 cells [178]. Also here, the covalently immobilized BMP-2 activated BMP-dependent signal transduction, thus resulting in the expected cellular responses like suppression of myotube formation and upregulated ALP expression. Specific BMP-2 binding peptides have been screened and used as part of an engineered hetero-bifunctional spacer enabling the simultaneous binding to BMP-2 and collagen [160]. In cell based assays, the bifunctional linker increased the retention of BMP-2 within a collagen matrix and led to increased osteogenic activities. But, it is not clear if BMP-2 can bind its cognate cellular receptors while still bound to the peptide or if BMP-2 has to be first released for interaction with these receptors. However, *in vivo* results demonstrate that the presence of the linker significantly increased osteogenic activity [160].

Delivery strategies using covalently coupled BMP-2 derived peptides

The use of peptides mimicking BMP-2 specific bioactivities might represent an attractive alternative for the costly recombinant growth factors [179]. Synthetic BMP-2 peptides might circumvent the use of native proteins that may undergo degradation and denaturation *in vivo*. But, due to the dimeric nature of the BMPs, the binding epitopes for the type I- (wrist epitope) and the type II receptor (knuckle epitope) exist twice. So, to achieve full receptor activation, the native ligand has to bind to two type I- and two type II-receptor chains forming a heterohexameric ligand-receptor assembly [180]. Thus, mimicking these capabilities with a simple peptide seems not feasible. However, coupling of a synthetic peptide corresponding to amino acids located within the knuckle epitope by EDC/NHS chemistry to alginate gels induced prolonged ectopic calcification for up to 7 weeks in rat calf muscle whereas BMP-2-doped collagen gel showed maximum ectopic calcification already after 3 weeks but the formed calcified ossicles disappeared after 5 weeks [181]. The peptide-functionalized alginate scaffold also induced ALP activity (ALP) in a murine osteoblast cell line. Furthermore, it could be demonstrated that upon exposure to this

construct SMAD signaling is initiated resulting e.g. in the upregulation of osteopontin expression and an increased mineral deposition in murine mesenchymal stem cells [182]. Compromised bone growth often occurs in the immediate vicinity of metallic implants, leading to weakened bone quality and implant failure. BMP-2 peptides covalently bound to glass, titanium, cobalt chromium (CoCr) and gold substrate have been shown to enhance and accelerate the growth and differentiation of osteoblasts and other cell lines. Chemical immobilization of synthetic peptides onto titanium implants was conducted to evaluate the *in vitro* and *in vivo* osteointegration capacity [183]. A peptide mimicking both, the wrist and the knuckle epitope was chemically synthesized using a so-called F-moc chemistry with an additional N-terminal modification by a cysteine-containing spacer which eases chemical conjugation onto implant surfaces. This peptide covalently coupled to titanium discs showed in MC3T3-E1 cells higher proliferation and upregulated expression of osteogenic markers such as ALP compared to the control disc. Importantly, the peptide modified implant material introduced into canine mandibles showed a significant increase of bone growth, thereby confirming that biochemical modifications of Ti surfaces can indeed increase the rate of bone healing compared to untreated Ti surfaces. Potentially useful findings have also been reported for CoCr alloy implants, where the presence of a BMP mimicking peptide (coupled via a cysteine amino acid at the N-terminus) showed twofold increase in ALP activity after 2 weeks of incubation and a fourfold increase in calcium content after 3 weeks of incubation compared to controls [184]. Peptides mimicking the knuckle epitope of BMP-2 have also been immobilized on anodized nanotubular titanium [185]. Results showed increased osteoblast adhesion compared to non-functionalized anodized titanium. This *in vitro* study adds anodized materials that hold nanometer surface textures to the growing list of materials that promote osteogenesis.

Several reports found in the more recent literature have demonstrated that surface textures in the nanometer-scale topography can influence proliferation and differentiation of embryonic and mesenchymal stem cells. Therefore, nanoscale topographies in combination with growth factors may promote proliferation or lineage differentiation of stem cells. To develop these substrates, the factors have to be immobilized directly on the surface of the substrate. One study showed that nanopatterned polyurethane acrylate (PUA) substrates uniformly coated with poly(glycidyl methacrylate) (pGMA) by initiated chemical vapor deposition (iCVD) followed by covalent immobilization of BMP-2 peptides results in a much more efficient BMP-2 peptide immobilization than e.g. physical adsorption. Results of Alizarin Red S staining, immunostaining, and quantitative real-time polymerase chain reaction (qRT-PCR) revealed that hMSCs cultured on such nanopatterned surfaces enhanced osteogenic differentiation [186]. However, despite the studies demonstrating the influence of peptide-modified surfaces on cellular behavior *in vitro*, there is relatively little evidence reporting their effects on osteogenesis and osteoclastogenesis (remodeling) *in vivo*.

COMPARISON OF GENE AND PROTEIN/PEPTIDE DELIVERY STRATEGIES

In an *in vitro* study, gene delivery of BMP-2 and ectopic delivery of the recombinant BMP-2 protein were directly compared. Interestingly, both approaches showed comparable mineralization results. A difference was observed in osteogenic protein expression levels where BMP-2 transfected cells expressed more osteopontin compared to the cells treated with same amount of recombinant BMP-2 protein in the cell culture medium [187]. Both, gene and protein delivery have advantages and drawbacks. Gene delivery provides supply of proteins for a relatively long time and the expression period can be controlled by inducible expression vectors. But a safety concern remains about the use of viral vectors in clinics. When non-viral vectors are considered, transfection of long DNA fragments appears difficult to perform and the efficiency may not be enough to realize complete bone restauration. In gene delivery, the protein is continuously produced by the cells and therefore stability is not an issue. However, in the development of protein delivery systems, the stability of the protein in the period of at least several weeks should always be considered and assured. Besides, the required dose and release kinetic should be assigned correctly for successful clinical outcomes.

As suggested, both systems need further improvements, more characterization of the improved systems and solid pre-clinical data to pursue with clinical trials.

FUTURE PERSPECTIVES

The complexity of tissue engineering in the field of bone regeneration inspired numerous investigators to date and as more investigations are conducted more complexity arises [188]. For the generation of innovative products more advanced engineering strategies of biomaterials probably including cells as well as growth factors are required. Controllable and reproducible production techniques of innovative materials have to be elaborated on products acting osteogenic on their own. Ideally, these materials are applied together with cells, either actively taking part in the regeneration of the bone defect and/or secreting the signalling molecules which act as initial trigger of a whole cell-cell communication cascade resulting finally in the recruitment of osteoprogenitor cells from the surrounding tissue. This initiating signal is most-likely provided by BMP-2 as described in this manuscript since application of this protein (or another osteogenic BMP) at ectopic sites (e.g. in muscular tissue) results in the formation of an ossicle by mechanisms being similar to those occurring in natural bone growth and repair. Ideally, the provided signal is sufficiently active for the period of time the bone defect needs to heal. In principal, this can be achieved best by genetically manipulated cells but due to immunological concerns, autologous cells are required. Alternatively, the signal can be provided by the application of recombinant BMPs. Here, numerous trials have been conducted within the last decades all of which faced the same problem relying on the general (bio-) chemical properties of this class of growth factors. As these proteins can induce the formation of ectopic bone, it has to be assured

that responsive tissues (e.g. muscular tissue) are not exposed to these proteins even in situations of bone fractures. For that purpose, the osteogenic BMPs are evolutionary "designed" as badly soluble proteins which additionally bind strongly to components of the extracellular matrix. Local administration of huge amounts must consequently result in a kind of precipitate rendering the majority of the protein biologically inactive. This inactive clot is typically eliminated by several environmental mechanisms. The design of 2nd generation BMPs should, therefore, focus on protein variants which in general provide higher bioactivities over longer periods of time. This can be achieved by enhancing the individual binding affinities of the ligand to the cell surface receptors by rational structure based design. Due to enhanced binding affinities, the applied dose of the BMPs being required can be significantly reduced but the protein modification bears the risk to induce immunological responses. Another way to keep the growth factor´s signalling capacities biologically active and locally in place might be provided by tight binding of the factor to suitable scaffold structures. As discussed in this review this might be realized addressing the material side (with scaffolds being optimized for BMP binding) and/or addressing the growth factor side (by a covalently bound BMP which ideally is coupled to the matrix side directly), thus enabling a robust and reproducible decoration of the chosen matrix. If initial steps of the regeneration process involve the migration of stem cells being recruited by a growth factor gradient, the coupling of this factor should - at least partially - occur via linkers which are cleavable by e.g. matrix-metalloproteinases.

In conclusion, by addressing the key problems which have been identified to date it seems feasible to create either cell-based or cell-free delivery systems for BMP-2 which in the near future can routinely be used in clinics in case of complex traumas and other cases requiring medical intervention.

CHAPTER 3A

COLLAGEN I DERIVED RECOMBINANT PEPTIDE MICROSPHERES AS NOVEL DELIVERY VEHICLES FOR BONE MORPHOGENETIC PROTEIN-2

Didem Mumcuoglu[1,2], Laura de Miguel[1], Shehrazade Jekhmane[1,3], Claudia Siverino[4,5] Joachim Nickel[4,5], Thomas D. Mueller[6], Johannes P. van Leeuwen[7], Gerjo J. van Osch[2,8], Sebastiaan G. Kluijtmans[1]

1 Fujifilm Manufacturing Europe B.V., The Netherlands
2 Department of Orthopaedics, Erasmus MC, University Medical Center Rotterdam, The Netherlands
3 Department of Physical Chemistry and Soft Matter, Wageningen University, The Netherlands
4 Department for Tissue Engineering and Regenerative Medicine, University Hospital Wuerzburg, Germany
5 Fraunhofer IGB, Translational Center Wuerzburg, Germany
6 Department for Molecular Plant Physiology and Biophysics, Julius-von-Sachs Institute of the University Wuerzburg, Germany
7 Department of Internal Medicine, Erasmus MC, University Medical Center Rotterdam, The Netherlands
8 Department of Otorhinolaryngology, Erasmus MC, University Medical Center Rotterdam, The Netherlands

Abstract

Bone morphogenetic protein-2 (BMP-2) is a powerful osteoinductive protein; however, there is a need for the development of a safe and efficient BMP-2 release system for bone regeneration therapies. Recombinant extracellular matrix proteins are promising next generation biomaterials since the proteins are well-defined, reproducible and can be tailored for specific applications. In this study, we have developed a novel and versatile BMP-2 delivery system using microspheres from a recombinant peptide based on human collagen I (RCP). In general, a two-phase release pattern was observed while the majority of BMP-2 was retained in the microspheres for at least two weeks. Among different parameters studied, the crosslinking and the size of the RCP microspheres changed the *in vitro* BMP-2 release kinetics significantly. Increasing the chemical crosslinking (hexamethylene diisocyanide) degree decreased the amount of initial burst release (24 h) from 23% to 17%. Crosslinking by dehydrothermal treatment further decreased the burst release to 11%. Interestingly, the 50 and 72 µm-sized spheres showed a significant decrease in the burst release compared to 207-µm sized spheres. Very importantly, using a reporter cell line, the released BMP-2 was shown to be bioactive. SPR data showed that N-terminal sequence of BMP-2 was important for the binding and retention of BMP-2 and suggested the presence of a specific binding epitope on RCP (K_D: 1.2 nM). This study demonstrated that the presented RCP microspheres are promising versatile BMP-2 delivery vehicles.

Keywords: bone morphogenetic protein-2, microspheres, protein delivery, bone regeneration

INTRODUCTION

Bone has a high self-regeneration capacity and most of the fractures can heal without any scar formation [36]. However, in critical-size bone defects, a surgical procedure with use of bone grafts is required [189, 190]. To replace the use of natural bone in clinics, there has been a tremendous effort to develop biomaterial based synthetic bone substitutes [191]. The biomaterials have been used in combination with growth factors to create an osteoinductive environment and to induce substantial amount of bone formation. These osteoinductive growth factors are known to recruit osteoprogenitor cells and guide their differentiation during the regeneration of the bone [192]. Bone morphogenetic protein-2 (BMP-2) and bone morphogenetic protein-7 (BMP-7) are growth factors that are already clinically used in bone regeneration [193]. BMP-2 adsorbed onto a collagen sponge matrix has been approved by the FDA for spinal applications [194]. However, off-label use [195] of BMP-2 especially in the cervical spine fusion resulted in adverse events such as hematoma, swallowing/breathing difficulties or swelling without hematoma [196]. Therefore, to obtain better clinical outcomes utilizing BMP-2, it is crucial to reduce the applied dose and/or to regulate its spatio-temporal delivery using appropriate delivery systems [148].

Several materials, especially natural biopolymers, have been investigated as controlled release systems for BMP-2 [150, 197-199]. Natural biopolymers are often chosen as a delivery system in tissue engineering not only due to their biocompatibility and biodegradability, but also due to their intrinsic features mimicking the extracellular matrix. As such, collagen was widely studied since it is a major component of the organic bone matrix [200]. However, in case of collagen sponge, one of the first natural scaffolds used for BMP-2 delivery, an early burst release of BMP-2 is typically observed[144]. More sophisticated BMP-2 release systems based on collagen's degradation product, gelatin have been developed [201]. For example, genipin-crosslinked gelatin microspheres have been shown to provide a slower release compared to PLGA microspheres [145]. However, animal-derived collagen or gelatin-based materials bear the risk of antigenic response, and batch-to-batch variability which complicates their clinical translation [202].

We have previously developed a human collagen type I-derived recombinant peptide (RCP) as designer biomaterial, which is produced by a fermentation process using genetically modified yeast *Pichia pastoris* [203].The major advantage of RCP over animal-derived proteins is that genetically engineered RCP offers a versatile and powerful platform to create functional (collagen-based) peptides with a low immunogenic response. The specific RCP variant used in this study is enriched with several RGD units. RCP-based microspheres have been shown to support cell attachment and cell proliferation [204]. Furthermore, RCP is advantageous over animal-derived collagen/gelatin not only for enhanced cell binding, but also for its well-defined protein sequence, the reproducibility of the production process, and low immunogenicity [205]. Previous *in vivo* studies have shown that RCP-based

microspheres do not elicit a strong immune response or foreign body reaction when injected subcutaneously [206].

In this study, we developed novel RCP microspheres for a defined release of recombinant BMP-2. The aim of this research was to identify the parameters that control BMP-2 release kinetics. Detailed understanding of different parameters affecting these release kinetics is required for the final design of a controlled release system. Based on literature, we selected crosslinking [201], particle size [207] and pore size [208] as potential parameters to modulate release. Hence, we used different crosslinking techniques and different preparation methods to create a small library of microspheres. In brief, the effect of crosslinking was studied by using high and low amounts of chemical crosslinker (hexamethylene diisocyanide); and long and short dehydrothermal treatment. The effect of size was studied creating three different sizes of spheres: 50 and 72 and 207 µm; and pore size studied by creating pore sizes of 1 µm, 10 µm and macropores (>10µm). These microspheres were subsequently loaded with BMP-2 by adsorption and their release profiles were investigated by ELISA. Furthermore, the bioactivity of the released protein was confirmed by cellular assays using a reporter C2C12 cell line. To gain better understanding of the interaction between BMP-2 and RCP on a molecular level a Surface Plasmon Resonance (SPR) study was performed using multiple BMP-2 variants.

MATERIALS AND METHODS
Materials

Recombinant peptide (RCP) based on human collagen I, commercially available from Fujifilm as Cellnest™, was produced by a fermentation process using genetically modified yeast *Pichia pastoris* as described previously [203, 206]. RCP comprises 571 amino acids, has an isoelectric point (pI) of 10.02 and a molecular weight of 51.2 kDa. The mature part of rhBMP-2 (amino acids 283 to 396 plus an N-terminal Met-Ala) was expressed in E. coli, isolated from inclusion bodies, renatured and purified as previously described [209]. In the variant EHBMP-2 the N-terminal segment of the mature part of BMP-2, which contains two triplets of basic amino acid residues (QA KHK Q RKR …), was replaced by a non- basic dummy sequence of identical length [104]. In T4BMP-2 the N-terminal sequence motif harboring two basic triplets (shown above) was doubled (QA KHK Q RKR A KHK Q RKR…) [210]. Both protein variants were expressed and purified identical to wildtype BMP-2 [209]. For use in SPR, the extracellular domain of the BMP type I receptor BMPR-IA (BMPRIA$_{ec}$) was expressed in E.coli and purified as described [209].

Hexamethylene diisocyanide (HMDIC), corn oil, calcium carbonate (CaCO$_3$), picrylsulfonic acid (TNBS,5% w/v solution in H$_2$O), bovine serum albumin (BSA) and collagenase from *Clostridium histolyticum* were purchased from Sigma-Aldrich (St. Louis, MO, USA). Ethanol, acetone and hydrochloric acid were purchased from Millipore (Billerica, MA, USA). ELISA development kit and reagents were ordered from Peprotech (Rocky Hill, NJ, USA). Gibco

products: Dulbecco's Modified Eagle's Medium (DMEM) and penicillin-streptomycin were ordered from Thermofisher Scientific (Waltham, MA, USA). SteadyLite Plus was ordered from Perkin Elmer (Waltham, MA, USA). MilliQ water was used in the experiments.

Preparation of RCP microspheres

RCP microspheres were produced by emulsification using calcium carbonate ($CaCO_3$) crystals as pore-forming agent. Briefly, a 20% (w/v) aqueous RCP solution was mixed with $CaCO_3$ powder (fine powder with particle size of <1 μm or 10 μm) in a 1:1 weight ratio of RCP to $CaCO_3$. The suspension was added dropwise to preheated corn oil at 50°C while stirring the emulsion at 800 rpm for 20min. Then, the emulsion was cooled using an ice bath and the emulsified microspheres were washed three times with acetone. After overnight drying at 60°C, microspheres were sieved to the desired size (Sieves Retsch GmbH, Haan, Germany). In the experiments 32-50 μm, 50-72 μm or 200-300 μm sieve fractions of microspheres were used. Subsequently, the microspheres were crosslinked. DHT (dehydrothermal) crosslinking was conducted at 160°C in vacuum (~$5x10^{-3}$ mbar) for 1 day or 4 days. Hexamethylene diisocyanide (HMDIC) crosslinking was conducted by suspending 1 g of spheres, and 1mL of HMDIC (high) or 30 μL of HMDIC (low) in 100 mL ethanol for 1 day. (High HMDIC corresponds to an excess amount of chemical crosslinker, while low HMDIC corresponds to less than the amount required to crosslink all amino groups present in the RCP). After crosslinking, the $CaCO_3$ porogen was removed by suspending the microspheres in 0.23 M HCl for 30 min until the formation of carbon dioxide stopped. The microspheres were washed repeatedly with water until a neutral pH was achieved. Complete removal of $CaCO_3$ was confirmed by Energy-dispersive X-ray spectroscopy (EDX) mapping of calcium on spheres (Jeol JSM-6335F Field Emission Scanning Electron Microscope). In order to produce 200-300 μm microspheres, the viscosity of corn oil was decreased during emulsification by adding n-heptane. Macroporous microspheres with pores larger than 10 μm were produced by a double emulsification method as described elsewhere [211]. No $CaCO_3$ porogen was used in the preparation of these macroporous microspheres.

Characterization of microspheres

The microsphere size was measured by a particle size analyzer (Mastersizer 2000, Malvern instruments, Malvern, United Kingdom). Dry microspheres were resuspended and measured in ethanol. The swollen sphere size was determined after overnight incubation in pure water. All measurements were performed in triplicate. The average microsphere size was calculated based on volume weighted mean. The size distribution of spheres is indicated as 10% (D0.1), which means 10% of spheres are below this size; and 90% (D0.9), which means 90% of spheres are below this size. The swelling ratio for each type of microsphere was calculated using the ratio of swollen diameter in water (dt) to dry diameter (do) and subsequently converted to volume $(dt/do)^3$.

Carboxyl and amine groups of RCP are crosslinked by DHT; whereas, only amines are crosslinked by HMDIC. Therefore, the degree of crosslinking was determined by measuring the residual free amines of the microspheres using a colorimetric assay, based on 2,4,6-trinitrobenzenesulfonic acid (TNBS). TNBS reacts with primary amines including both terminal α-amino groups and side chain ε-amino groups [212]. The absorbance was measured at 345 nm using a CARY 50 UV-Vis spectrophotometer (Agilent Technologies, Santa Clara, CA, USA). The experiment was done in triplicate and non-crosslinked RCP was used as a reference to calculate the reduction of amino groups upon crosslinking. The morphology and distribution of microspheres were visualized by a Jeol JSM-6335F Field Emission Scanning Electron Microscope with an accelerating electron voltage of 2.5-5.0 kV. Samples were coated with 10 nm Pt.

BMP-2 loading, release and bioactivity

The experimental setup for BMP-2 release measurements was adapted from Poldervaart *et al*. [213]. BMP-2 loading was performed in 1.5 mL Eppendorf LoBind tubes, where 75 μL of rhBMP-2 solution with a concentration of 12 μg/mL was added on top of 15 mg dry microspheres and incubated overnight at 4 °C to allow adsorption of BMP-2 during the swelling of microspheres. During this incubation, all liquid is absorbed by the microspheres. The above loading ratio corresponds to 60 ng BMP-2 per mg microspheres. In the "loading dose experiment" the concentration of the BMP-2 solution was varied to obtain 6, 60 and 600 ng BMP-2 per mg microspheres. For the experiment comparing microspheres with different pore size, the same number of microspheres instead of same weight was used to correct for differences in microsphere density. The number of spheres per mg was calculated by counting the spheres under the microscope. For the mentioned experiment, 900 ng of BMP-2 was loaded onto 15 mg 1 μm porous spheres, 15 mg 10 μm porous spheres, and 7.7 mg macroporous spheres.

To initiate the release assay next day, 925 μL release medium containing DMEM, 1% BSA and 1% penicillin-streptomycin was added on top of the swollen microspheres. BSA was used to prevent adsorption of BMP-2 to the tubes and penicillin-streptomycin was used to prevent bacterial growth potentially resulting in degradation of RCP. The tubes were placed on a tube rotator at 37°C and the release was followed for 2 weeks by refreshing medium at regular time intervals. For the refreshment, the complete release medium (900μL) was collected after centrifugation at 3000 rpm for 5 min and replaced with fresh medium (900μL). Released rhBMP-2 was quantified by ELISA using the rhBMP-2 ELISA development kit (Peprotech) according to the supplier´s protocol. Released BMP-2 was calculated using a standard calibration curve. The percentage of released BMP-2 was calculated relative to the positive control, which is BMP-2 solution at the same concentration (900ng/mL) without microspheres kept at the same conditions as the release samples. After 2 weeks the release assay was finalized by degradation of the microspheres to liberate the remainder of BMP-2 inside the microspheres. Hereto, 900 μL of a collagenase solution (2mg/mL DMEM) was

added to the microspheres. After overnight incubation the BMP-2 concentration was analyzed again by ELISA. The positive control at the same concentration was also treated with collagenase to calculate the percentage of BMP-2 released.

The bioactivity of the released BMP-2 was determined employing a cell assay using C2C12-BreLUC cells. The cell line is genetically modified with a reporter gene construct harboring a BMP-responsive element to control luciferase expression in a dose-dependent response to BMP-2 stimulation. This type of construct has previously been used as a reporter for different bone morphogenetic proteins in different cell lines [214, 215]. Cells were maintained in DMEM with 10% fetal calf serum, 1% penicillin-streptomycin and 0.5% G418. For the assay, 5×10^3 cells per well were seeded in 96 well plates and after 30 min the release medium was added to cells. A standard calibration curve with BMP-2 was made. After 24 hours of incubation, SteadyLite Plus kit components were added according to the manufacturer's protocol and 15 min after cell lysis, the luminescence signal was measured for 6 s using a Wallac VICTOR Multilabel reader (Perkin Elmer, Waltham, MA, USA). Sample BMP-2 concentrations were calculated based on BMP-2 standard calibration curve.

Surface plasmon resonance (SPR) spectrometry

A ProteOn XPR36 biosensor system (Bio-Rad, Hercules, CA, USA) was used for all surface plasmon resonance interaction experiments. Measurements were performed at 25°C using 10mM HEPES pH 7.4, 3.4mM EDTA, 0.005% (v/v) Tween-20 supplied with different NaCl concentrations (150 mM and 500 mM) as running buffer, the flow rate for interaction data acquisition was set to 50µL min^{-1}. For interaction analyses BMPRIA$_{ec}$ protein was biotinylated in a 1:2 stoichiometric ratio using Sulfo-NHS-LC-biotin (Pierce, Thermo Fisher Scientific, Rockford, IL, USA) following the manufacturer's protocol. For immobilization, a GLC sensor chip was first activated using EDC/Sulfo-NHS (Bio-Rad, Hercules, CA, USA) according to manufacturer's recommendation, then streptavidin (Sigma-Aldrich, St. Louis, MO, USA) was perfused over the activated sensor surface at a concentration of 40ug mL^{-1} until resonance unit (RU) levels reached 2000 to 2200 RU. The biotinylated receptor ectodomain was subsequently immobilized onto this streptavidin sensor surface at a density of approximately 500 RU. RCP (100 µg/mL) was coupled directly to the EDC/NHS activated chip matrix at a density of 1300 RU. For a single kinetics measurement six different analyte (BMP-2) concentrations starting at 50nM (log2 dilution series) were used. The association time was set to 180s; dissociation data were obtained from perfusion with running buffer for 120s. Interaction data were acquired employing the so-called single-shot kinetic setup specific to the ProteOn XPR36 SPR system, which allows measuring all six analyte concentrations simultaneously. After each BMP-2/BMP-2 variant perfusion, the sensor chip was regenerated with three subsequent 120s pulses injecting 100mM glycine pH 2.5, 10mM glycine pH 1.5 and 4M MgCl$_2$ at a flowrate of 50µL min^{-1}. Bulk phase effects (buffer jumps, etc.), non-specific binding of the analyte to the chip matrix, the interaction of the analyte to a streptavidin surface on a control flow channel and the interaction at the, so-called, non-

modified interspots were subtracted from all binding data. Equilibrium binding constants (K_d) were calculated by fitting the association and dissociation phase of the sensograms using a grouped regression analysis of the rate constants (k_{on}, k_{off}) and employing a simple 1:1 Langmuir-type interaction model. Fitting analyses were considered successful when Chi^2 values were less than 10% of the maximal signal amplitude. Standard deviation of the kinetic rate and equilibrium binding constants were derived from three independent experiments using five-six different analyte concentrations. For clarity, only the SPR curves at 25 nM BMP-2 protein (wildtype or variants thereof) are shown in the results.

Study design

Eight different types of microspheres were produced by changing the preparation or crosslinking method, or the material. First, 50-72 μm microspheres were crosslinked by 4 different methods: HMDIC high (MS#1), HMDIC low (MS#2), DHT 4 day (MS#3) and DHT 1 day (MS#4). Effects of sphere size and pore size were investigated using HMDIC-high crosslinked spheres only. To investigate the effect of sphere size three different sizes of microspheres were produced: 32-50 μm (MS#5), 50-72 μm (MS#1) and 200-300 μm (MS#6). The effect of porosity and pore size was investigated using the large 200-300 μm-sized microspheres because producing macroporous spheres was only possible at this size. Microspheres with different porosity were produced by 1 μm $CaCO_3$ (MS#6), 10 μm $CaCO_3$ (MS#7) pore leaching or by the double emulsification method (MS#8). We have used this library of different microspheres to study the influence of physicochemical characteristics of spheres on BMP-2 release (as summarized in Table 1).

Statistical analyses

Differences in release for each time point were analyzed by one-way ANOVA. Linear regression analysis was done after plotting cumulative release (%) vs. $\log_2$ (time) and corresponding r^2, slope values were calculated. Two-phase decay model in Graphpad Prism was used to analyze the rate of release kinetics. Experiments were run in triplicate, statistical significance between means is shown with asterisks corresponding to * = $p < 0.05$, ** = $p < 0.01$, *** = $p < 0.001$.

Table 1. Characteristics of RCP microspheres in terms of size (dry and swollen in water) and residual amines after crosslinking

	Microsphere type			Characterization					
Name	Sieve size	Crosslinking type	Introduced pore size	[i]Dry average diameter d_o (µm)	[i]Dry size range 10%-90% (µm)	[ii]Swollen average diameter d_t (µm)	[ii]Swollen size range 10%-90% (µm)	[iii]Swelling ratio $(d_t/d_o)^3$	[iv]Average residual amino groups ± SD (mmol/100g)
MS#1	50-75 µm	HMDIC high	1 µm pores	71.9	50.5 - 96.3	74.7	52.4 - 100.3	1.1	14.6 ± 0.5
MS#2	50-75 µm	HMDIC low	1 µm pores	70.3	49.3 - 94.2	75.9	53.4 - 102.0	1.3	28.0 ± 4.8
MS#3	50-75 µm	DHT 4 day	1 µm pores	65.6	46.1 - 88.2	72.7	50.7 - 97.5	1.4	41.3 ± 2.1
MS#4	50-75 µm	DHT 1 day	1 µm pores	68.6	48.1 - 91.9	78.9	55.5 - 105.5	1.5	47.1 ± 2.7
MS#5	32-50 µm	HMDIC high	1 µm pores	50.3	35.0 - 67.7	53.0	36.9 - 71.0	1.2	13.8 ± 0.6
MS#6	200-300 µm	HMDIC high	1 µm pores	206.6	144.8 - 276.7	281.5	202.9 - 369.2	2.5	15.0 ± 0.3
MS#7	200-300 µm	HMDIC high	10 µm pores	258.4	186.5 - 342.7	290.9	210.7 - 382.3	1.4	11.0 ± 0.9
MS#8	200-300 µm	HMDIC high	Macropores	269.2	172.7 - 383.0	364.3	254.8 - 488.8	2.5	26.6 ± 1.2

[i] Sphere size was measured in ethanol. The size range shows the sphere size distribution in which 10% of the spheres are smaller and 10% of the spheres are bigger than this range. [ii] Sphere size was measured in water. The size range shows the sphere size distribution in which 10% of the spheres are smaller and 10% of the spheres are bigger than this range. [iii] Swelling ratio was calculated by using this formula $(d_t/d_o)^3$; where d_t is the average swollen size and d_o is the average dry size. [iv] Average residual amino groups were analyzed by TNBS assay in triplicates and standard deviation (SD) is shown.

RESULTS
Preparation and characterization of the microspheres

In order to investigate the effect of several parameters on BMP-2 release, a small library of RCP microspheres was created, comprising spheres differing in size, pore size or the crosslinking technique used. These microspheres were extensively characterized in terms of their morphology, size distribution and the number of residual amino groups (Table 1). The size uniformity was confirmed by laser diffraction. The smallest spheres prepared in this study had an average 'dry' diameter of 50 µm (MS#5) and the largest spheres of 269 µm (MS#8). This wide variation in sphere size allowed us to investigate the effect of size on BMP-2 release over a broad size range. The degree of crosslinking was investigated by analyzing the residual or non-reacted amines using the colorimetric TNBS assay. In this assay, the non-crosslinked RCP was used as a reference. Theoretically, non-crosslinked RCP contains 65 mmol/100 g primary amines in the form of lysine. HMDIC-high crosslinking conditions using a large excess of reactive isocyanate groups led in general to a reduction of more than 80% of these RCP primary amines (MS#1, MS#5-7). As expected, a lower amount of HMDIC increased the number of unreacted primary amine groups significantly (MS#2 vs MS#1). Crosslinking by heat (DHT) resulted in a smaller reduction of primary amine groups than HMDIC crosslinking. The MS#4 sample with a shorter DHT crosslinking time in comparison with MS#3 contained more residual amines. The swelling ratio of different crosslinked spheres at the same size (MS#1-4) showed a clear relation with crosslinking; less crosslinking resulted in more swelling.

Influence of the loading dose on BMP-2 release

To investigate the effect of the loading dose on protein binding and release, 50-75 µm HMDIC high 1 µm porous microspheres (MS#1) were loaded with three doses of BMP-2: 6 ng BMP-2 per mg microspheres, 60 ng BMP-2 per mg microspheres and 600 ng BMP-2 per mg microspheres. As shown in Figure 1, the percentage of released BMP-2 during the first two days was independent of the loading dose and fits a one-phase exponential decay exhibiting an r^2 value >0.91. Irrespective of the 100-fold difference in loading dose the dissociation rate K was similar for the three conditions, between 10^{-5} and 10^{-6} s^{-1}. In the following experiments we employed 60 ng BMP-2 per mg microspheres unless specified otherwise.
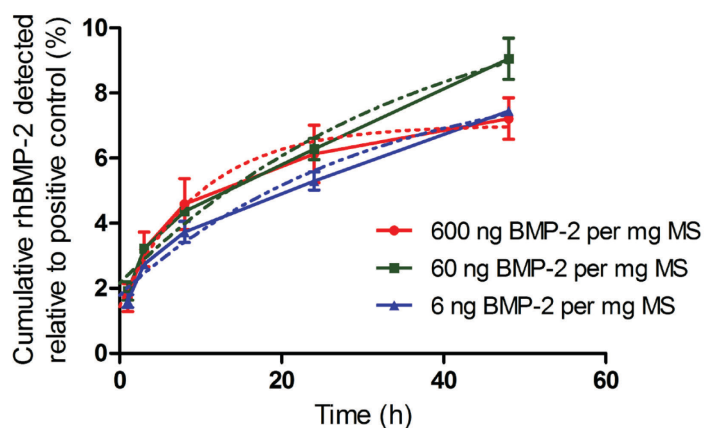
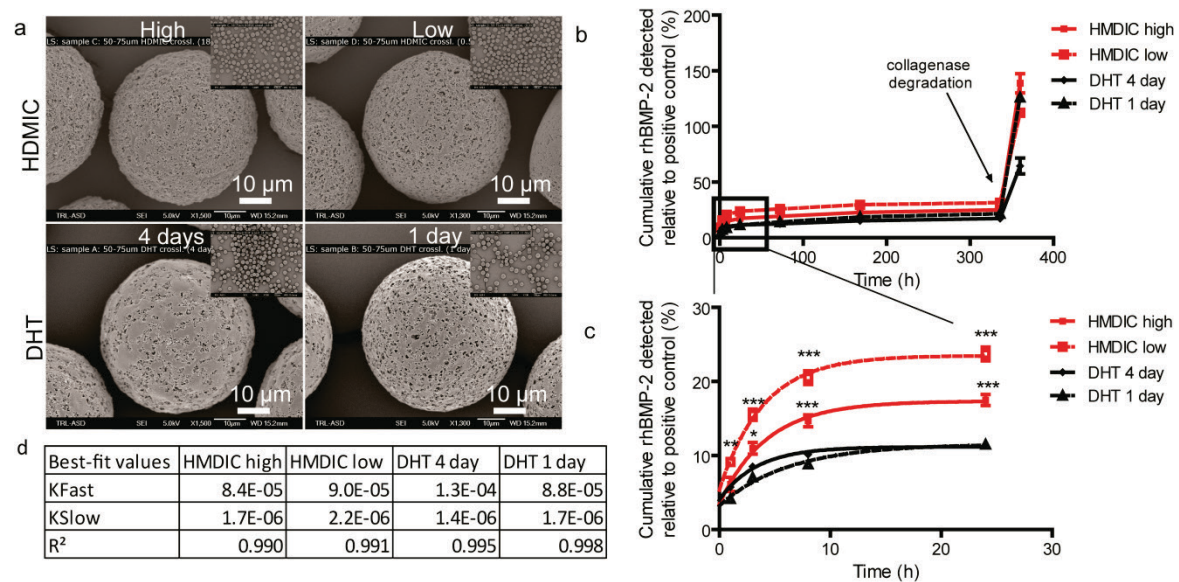| Best-fit values	600 ng BMP-2 per mg MS	60 ng BMP-2 per mg MS	6 ng BMP-2 per mg MS
K	2.8E-05	7.6E-06	9.1E-06
R²	0.91	0.97	0.97

Figure 1. Loading amount had no effect on fraction of BMP-2 released. HMDIC-high crosslinked microspheres (50-75 μm, MS#1) were loaded with different amounts of BMP-2 and cumulative release was normalized to the positive control of each concentration. Corresponding statistical table shows the results of the nonlinear regression of one phase exponential decay. Experiment was run in triplicate, mean and SD are shown for each point.

Influence of crosslinking on BMP-2 release

To study the effect of the type and intensity of crosslinking on BMP-2 release, 50-75 μm microspheres with 1 μm pores were crosslinked either chemically or thermally, employing hexamethylene diisocyanate (HMDIC) or dehydrothermal (DHT) crosslinking, respectively. As evidenced by SEM images, the spheres were spherical and their size distribution was uniform (Figure 2a). As shown in Figure 2c, the release of BMP-2 was indeed influenced by the crosslinking method. HMDIC crosslinking resulted in an increased release when compared to DHT crosslinking. In case of HMDIC, stronger crosslinking resulted in a reduced release rate and approximately 10% less BMP-2 release. For DHT, the degree of crosslinking did not significantly affect the BMP-2 release. HMDIC-high crosslinking was chosen as crosslinking method for the following experiments.

Regardless of the crosslinking method, the release of BMP-2 was rapid in the first 24 hours (Figure 2c); whereas after 1-2 days, the release rate strongly decreased (Figure 2b). The release data were extensively examined using several well-known drug release models [216]. However, none of the models such as zero-order, first order, Higuchi or Hixson models fit to data. The n exponent of the Korsmeyer-Peppas model [217] was calculated to be 0.11 which indicates that the release is not simply diffusion controlled. Interestingly, the data of the first two days of release fitted well to a single exponential decay model, whereas release curves over the full two weeks fitted better to a two-phase exponential decay ($r^2 > 0.98$), in which the initial fast release (rate 8×10^{-5}-1.2×10^{-4} (1/s)) is followed by an

attenuated release (rate: 1.3×10^{-6}-2.1×10^{-6} (1/s)). Although the exponential model is not a common drug release model, several studies employed it to describe the release [148, 218]. As can be seen from Figure 2, the majority of the BMP-2 protein was not yet released within two weeks. After two weeks, the BMP-2 loaded microspheres were degraded with collagenase and the residual amount of BMP-2 adhered to the microspheres was determined showing that more than 50% of BMP-2 initially loaded could be still be released from these spheres (Figure 2b).

Best-fit values	HMDIC high	HMDIC low	DHT 4 day	DHT 1 day
KFast	8.4E-05	9.0E-05	1.3E-04	8.8E-05
KSlow	1.7E-06	2.2E-06	1.4E-06	1.7E-06
R²	0.990	0.991	0.995	0.998

Figure 2. Crosslinking influenced BMP-2 release. (a) SEM images of microspheres crosslinked by HMDIC or DHT (MS#1-4) do not reveal sign of morphological difference. (b) BMP-2 is released from HMDIC- and DHT-crosslinked spheres for two weeks after which remaining BMP-2 was liberated by upon collagenase degradation of microspheres. (c) In first 24 hours, a significant difference between DHT- crosslinked spheres and HMDIC-crosslinked spheres, and difference between HMDIC high and HMDIC low was observed. (d) Corresponding statistical table shows nonlinear regression, two-phase decay analysis for the two weeks data. Concentration was normalized to the positive control to calculate %-release. Experiments were performed in triplicate, data are shown as mean and SD, statistical significance between means is indicated by asterisks corresponding to * = p < 0.05, ** = p < 0.01, *** = p < 0.001.

Influence of the microsphere size on BMP-2 release

To study the effect of microsphere size on BMP-2 release, microspheres of different sizes were produced (MS#1, MS#5 and MS#6). SEM analyses confirmed their comparable morphology and distinct sizes (Figure 3a). As shown in Figure 3b, the release of BMP-2 was found to be very similar for the two small-sized microsphere samples; whereas, large microspheres resulted in significantly higher release. Interestingly, large spheres exhibit 50% of burst release in the first day. The similar release rates observed for the two small sphere samples might be partially due to an overlapping sphere size of MS#1 (50.5-96.3 µm) and

MS#5 (35.0-57.7 μm); whereas the large sphere sample clearly exhibit a discrete size range (MS#6: 114.8-276.7 μm).
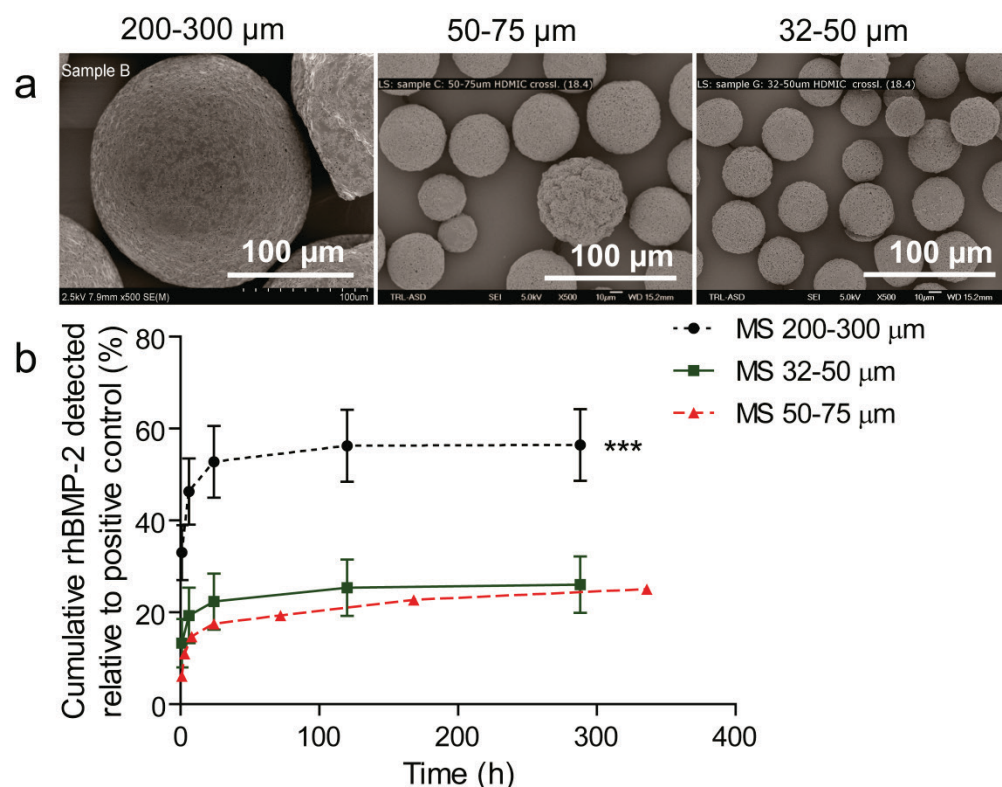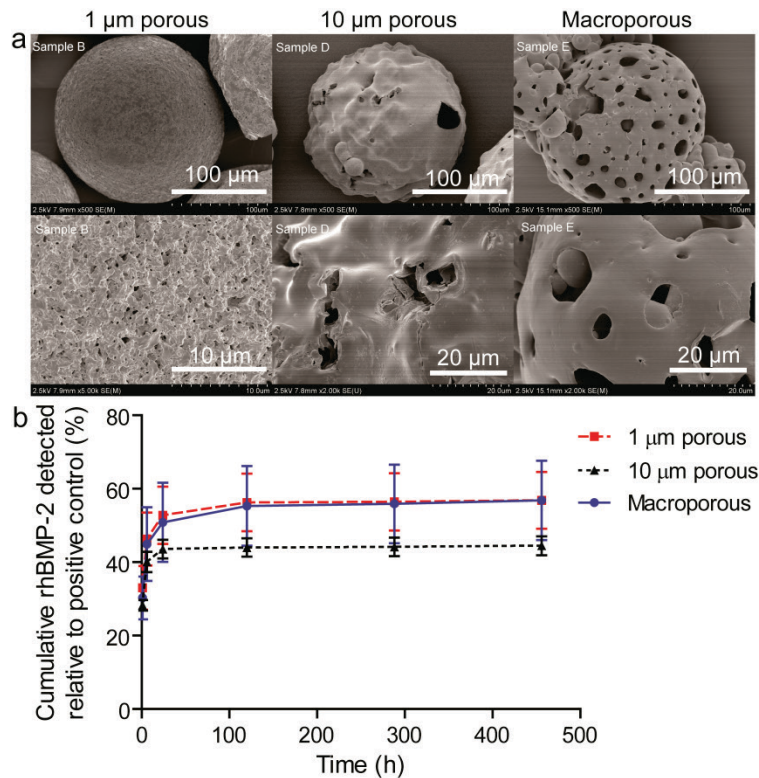

Figure 3. Microsphere size on influenced BMP-2 release. (a) SEM images of microspheres with average sizes of 50 μm, 72 μm and 207 μm (MS#1, MS#5 and MS#6). (b) A significant difference in the cumulative release of BMP-2 from large sized-spheres (207 average size) to that from small-sized spheres (50 μm and 72 μm average size) was observed. Concentration was normalized to the positive control to calculate percentage release. Experiment was run in triplicate; data are shown in mean and SD; statistical significance between means is shown with asterisks corresponding to * = $p < 0.05$, ** = $p < 0.01$, *** = $p < 0.001$.

Influence of the microsphere pore size on BMP-2 release and bioactivity of released BMP-2

To study the effect of pore size, three types of different spheres with different pore sizes were used: 1 μm porous microspheres, 10 μm porous microspheres, and macroporous spheres characterized by fully interconnected pores larger than 10 μm (Figure 4a). These spheres were produced to have large sizes between 200-270 μm (MS#6, MS#7 and MS#8), since it is not possible to produce smaller spheres with large pores (macroporous). As shown by the SEM pictures in Figure 4a, the different porous spheres provided distinct surface morphologies with varying surface roughness and completely different surface pore size. Due to the difference in porosity, the density of the spheres was different. To use the same number of spheres instead of same weight, the number of spheres per mg was determined in this experiment. The release of BMP-2 from microspheres with different pore sizes was

found to be very similar within the first 24 h (Figure 4b). Thus no effect of pore size on BMP-2 release was observed for the loading concentration used.

Figure 4. Pore size of spheres had no influence on BMP-2 release. (a) Porosity difference of microspheres having pore sizes of 1 µm, 10 µm and macropores (MS#6, MS#7 and MS#8) can be seen by SEM images. The upper images are at 500X magnification showing one microsphere, lower images are 2000X or 5000X magnification showing the surface of the spheres. (b) No significant difference in cumulative release of BMP-2 from different porous spheres was observed. Concentration was normalized to the positive control to calculate percent release. Experiment was run in triplicate, data are shown in mean and SD.

In order to investigate the bioactivity of the released BMP-2, a modified C2C12 cell line, stably transformed with a firefly luciferase gene, which is controlled by a BMP-responsive element (BRE) was used. This cell line represents a well-established read-out system for the bioactivity of various BMPs since the receptors and downstream mediators are endogenously expressed. Released protein detected by C2C12 cells shows a similar trend and same order as observed in the ELISA analysis (Supplementary Figure). Time dependent bioactivity showed that the bioactivity was in the range of 20% to 95% which was calculated by the ratio of BMP-2 detected by C2C12 cells to BMP-2 detected by ELISA for each time point (Supplementary Figure). BMP-2 released from macroporous spheres (45-71%) and 1 µm porous spheres (76%-93%) retained its bioactivity more than that from 10µm porous spheres (21-54%). Cumulative bioactive BMP-2 at Day 19 was in the range of 40-60% (Figure 5). The difference in bioactivity at Day 19 was not significant between different sphere types.
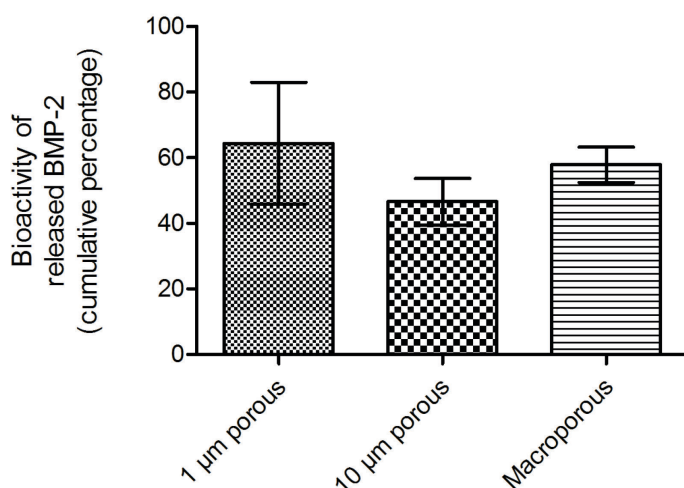
Figure 5. Released BMP-2 was found to be bioactive in the range of 40-60% depending on the sphere type. The bioactivity of released BMP-2 from the RCP spheres with various pore size ((MS#6, MS#7 and MS#8), was confirmed using a reporter cell line. BMP-2 released from the spheres was analyzed by BRE-Luc C2C12 cells by incubating supernatant with the cells and measuring the bioluminescence signal. Cumulative bioactivity in percentage at Day 19 was calculated by the ratio of the BMP-2 detected by C2C12 cells (ng) to BMP-2 detected by ELISA (ng). For each assay, the amount of BMP-2 (ng) was calculated based on serial dilutions of fresh BMP-2 solution. Experiment was run in triplicate, data are shown in mean and SD.

Binding of various BMP-2 variants to RCP using Surface plasma resonance (SPR)

Since the release experiments revealed an unexpectedly strong, long-term adsorption of BMP-2 to the RCP microspheres, we anticipated a specific interaction between BMP-2 and RCP. This interaction was further studied using SPR. It is known that the N-terminal segment of the mature part of BMP-2 contains an arrangement of two triplets of basic amino acid residues, which facilitate binding to negatively charged components of the extracellular matrix (ECM) such as heparin or heparan sulphates [104]. Therefore, we investigated whether the same motifs are involved in the strong interaction of BMP-2 with the RCP by comparing the binding capacity of wildtype BMP-2 (wtBMP-2) to RCP with two variants, which either lack (EHBMP-2) or contain a duplication of the heparin binding motif (T4BMP-2). Thus, these variants could either show an attenuated or an enhanced binding to RCP, respectively. To assess the specificity of this motif in the interaction between BMP-2 and RCP, we compared binding of these variants to RCP to the interaction of BMP-2 with the type I receptor BMPR-IA, which was shown not to be significantly affected by the presence or absence heparin binding motifs [219, 220].

As shown in Figure 6a, measurements at physiological conditions revealed strong binding of the wtBMP-2 and T4BMP-2 to both RCP and the BMPR-IA receptor (curves not shown). The wt BMP-2 binding to RCP is even faster than that of T4BMP-2. The curves were, however,

often not linear and could not be interpreted by a simple Langmuir type 1:1 interaction model. Detailed inspection of the sensograms shows that the association of the BMP-2 analyte was probably biased by so-called mass transfer limitation, which is possibly due to complementary charged segments in the BMP-2 analyte and immobilized ligand RCP. To reduce the charge interaction, measurements were also performed at higher salt concentration (500 mM, Figure 6b). Indeed at this higher salt concentration simple Langmuir type adsorption isotherms were obtained. At this high salt concentration, the binding affinity of wtBMP2 to RCP was in the same nanomolar range as its binding affinity to the BMPR-IA receptor which was in turn similar to that reported in literature [221]. Consistent with the literature [219, 220], all three BMP-2 variants bound to the extracellular domain of BMPR-IA with similar affinity (wtBMP-2: K_D=0.3 nM; EHBMP-2: K_D=0.2 nM; T4BMP-2: K_D=0.3 nM) indicating that the N-terminal segment is not involved in BMPR-IA binding (Table 2). This is in sharp contrast to the binding of the three BMP-2 variants to RCP, which was strongly affected by changes in the N-terminal segment. At 150 mM chloride, binding affinity of EHBMP-2 to RCP (K_D=63 nM) was about a ten-fold lower than binding of wtBMP-2 (K_D=6.8 nM). While at low ionic strength all 3 variants were still binding (although with a clearly different binding strength), at high ionic strength the EHBMP-2, in which the positively charged N-terminus is exchanged for a polar but less charged sequence, did no longer bind to RCP. This implies that the N-terminal region of BMP-2 containing the two basic triplet motifs is essential for the interaction with RCP. Since wildtype BMP-2 and the T4BMP-2, which harbors a doubled basic triplet motif, exhibit identical binding affinities to RCP (wtBMP-2 K_D=1.2nM vs T4BMP-2 K_D=1.9nM) and have similar binding kinetics (Table 2) it can be ruled out that the interaction between BMP-2 and RCP is based on a (non-specific) electrostatic interaction but very likely involves specific RCP binding epitopes.
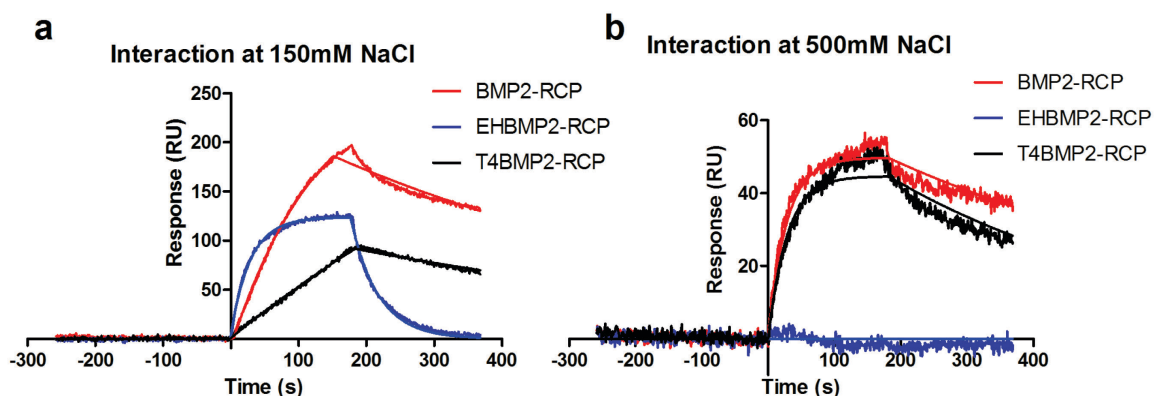
Figure 6. SPR interaction analysis of the binding of BMP-2 and variants to RCP. Binding of BMP-2 variants (wildtype BMP-2, EHBMP-2 and T4BMP-2) to RCP immobilized on the sensor surface. Five analyte concentrations ranging from 25 to 1.6nM were used, for representation only the interaction at 25nM analyte concentration is shown. (a) Due to the highly charged nature of BMP-2 and RCP, at low ionic strength the SPR data is affected by mass transfer limitation, i.e. not enough analyte is transported to the immobilized ligand on

the biosensor. This leads to an almost linear association phase (time point 0s to 200s) and results in underestimated association rate constants. (b) To overcome the mass transfer limitation, SPR measurements were performed at and 500mM sodium chloride concentration.

Table 2. Equilibrium binding constants and kinetic rate constants derived from the SPR measurements of the interaction of BMP-2 and variants with RCP

analyte	ionic strength (expr. in mM NaCl)	association rate constant k_{on} x 10^5 [M^{-1}s^{-1}]	dissociation rate constant k_{off} x 10^{-3} [s^{-1}]	equilibrium binding constant K_D [nM]
wt BMP-2		2.4	1.6	6.8
EHBMP-2	150	3.9	25	63
T4BMP-2		n.d.	n.d.	n.d.
wt BMP-2		14	1.7	1.2
EHBMP-2	500	n.b.	n.b.	n.b.
T4BMP-2		13	2.4	1.9
(ligand BMPR-IA)		k_{on} x 10^5 [M^{-1}s^{-1}]	k_{off} x 10^{-5} [s^{-1}]	K_D [nM]
wt BMP-2		3.3	8.8	0.3
EHBMP-2	500	4.5	8.9	0.2
T4BMP-2		3.2	8.8	0.3

n.d.: not-determined; n.b.: no binding

DISCUSSION

In this study, we investigated novel microspheres of collagen I-based recombinant peptide (RCP) as an injectable BMP-2 delivery system. At first, we have shown that the initial stage of the release is not affected by the loading dose in a wide range of BMP-2 loading concentrations, between 6 and 600 ng BMP-2 per mg of microspheres, implying that in this wide range of concentrations the microspheres are not saturated with BMP-2. Important factors that affect the release kinetics of BMP-2 were shown to be sphere size and

crosslinking intensity. Both the total release and the initial burst release decrease with the degree of crosslinking and increase with sphere size. Very importantly, the BMP-2 protein released from the microspheres was found to be bioactive. SPR interaction analysis suggested that a specific interaction plays a role in binding of BMP-2 to RCP (K_D: 1.2 nM). Overall, this study provided important information about the influence of the RCP sphere characteristics on BMP-2 release kinetics.

In general, we observed a two-phase exponential release from the RCP microspheres. A fast release in the first few days was followed by a very slow release that continued to decrease. After two weeks, the majority of the BMP-2 was still inside the microspheres and could be released upon enzymatic degradation of the RCP-microspheres. This surprisingly strong binding is not observed for natural gelatin particles for which a burst release followed by a linear release was reported [145]. To understand more of the unexpected strong binding of BMP-2 to RCP, an SPR study was conducted. This SPR study revealed that the basic N-terminal BMP-2 site is of major importance for the interaction with RCP. Although ionic interactions are the assumed to be the main interaction mechanism of the N-terminal basic segment found in various BMP proteins and components of the extracellular matrix, such as heparan sulfates [219], BMP-2-RCP binding is not just accomplished by simple electrostatic interaction only. This hypothesis is based on the observation that the BMP-2 variant T4 binds to RCP with similar affinity as wildtype BMP-2, although the N-terminal charged interaction epitope is present twice in this T4-BMP variant. Hence the involved binding interface appears geometrically defined and thus repetition of the motif does not provide additional surface area. Speculating on the underlying mechanism of two phase exponential release and considering the SPR data, we think there are at least two main factors involved in the binding of BMP-2 to RCP. The release kinetics suggests that there is a strongly and weakly bound fraction of BMP-2. The weakly bound part is released in the first fast phase and strongly bound part is released in the second slow phase. Also SPR data suggest there are two different kinds of interactions at physiological conditions i.e. specific and non-specific interactions. These two types of interactions can be combinations of multiple non-covalent forces such as Van der Waals, hydrophobic, electrostatic interaction that are generally involved in protein-protein binding. These results suggest there is a correlation between the molecular phenomena observed by SPR and physical phenomena observed by the release kinetics. On the other hand, the release kinetics can be affected by many other factors such as multilayer binding. As a result of the observed complex interaction it is not possible to model the release by employing simple non-interacting drug release mathematical models (see also [222]). We have studied the release of BMP-2 variants from the RCP microspheres to compare the order of binding of the variants found in the SPR experiment to the order of release from spheres (Figure 7). In contrast to the SPR data we have seen that the release of both EHBMP-2 and T4BMP-2 is faster than wtBMP-2. A possible explanation for the difference is that the molecular conformation of RCP immobilized on the SPR chip surface is different than that of the microsphere surface.

Crosslinking the microspheres might have prevented binding of T4 variant by steric hindrance. Taken together, the results show that BMP-2 binding to RCP is also affected by the structure or treatment method of RCP.
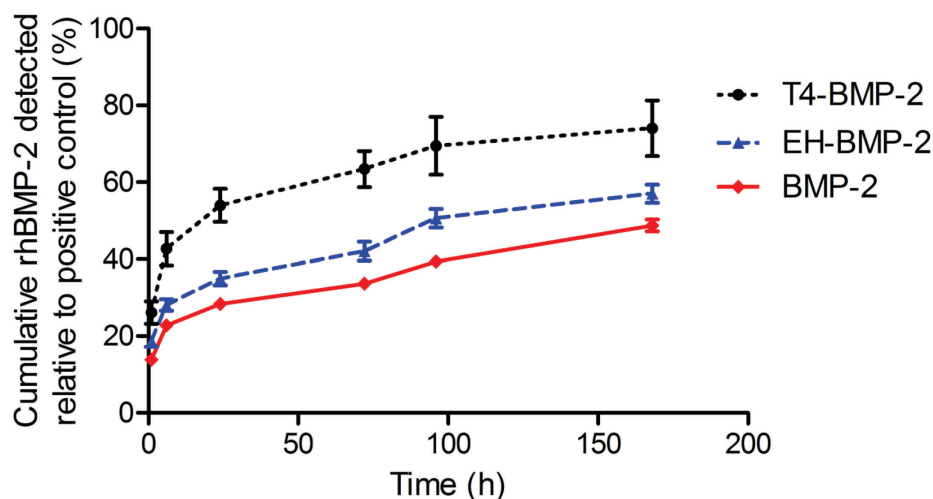
Figure 7. The release of BMP-2 variants from RCP microspheres (MS#1). Concentration was normalized to the positive control to calculate percent release. Experiment was run in triplicate, data are shown in mean and SD.

The strong binding of BMP-2 to RCP did not impair its bioactivity upon release. Using a BMP-2 responsive cell-based bioactivity assay the released BMP-2 was found to be bioactive almost to the same level as measured by ELISA. These data suggest that adsorption of BMP-2 to the scaffold does not abolish its bioactivity due to unfolding or facilitated degradation. Unfortunately, it was not possible to confirm the bioactivity of the strongly bound fraction since the enzymatic treatment required to destroy the RCP microspheres was not compatible with the cell-assay.

Important factors that affect the release kinetics of BMP-2 from the RCP microspheres were shown to be sphere size and crosslinking intensity. Both the total release and the initial burst release decrease with the degree of crosslinking and increase with sphere size. In agreement with data published for gelatine microspheres [201], we observed the influence of the crosslinking degree on BMP-2 release. For example, a higher crosslinking degree as induced by HMDIC resulted in less burst and a slower release. The ratio between hydrophobicity and charge can change as a result of crosslinking of charged groups and thus it may influence the binding of BMP-2. As shown above, there is also an effect of sphere size on release. Small spheres with a mean diameter of 50 μm and 72 μm had a similar release pattern, whereas much larger microspheres with a mean size of 207 μm released significantly more BMP-2 compared to the smaller spheres mainly due to an enhanced initial burst release. For pure diffusion controlled release, a faster release from smaller spheres is expected as a result of the shorter diffusion distances and larger total surface area [223].

However, as mentioned above, the current release system is not diffusion controlled due to the complex interaction between BMP-2 and RCP. The reason why, in our case, large spheres release more BMP-2 is rather speculative. For instance, different crosslinking density of the spheres can play a role. Although the spheres were crosslinked with the same amount of crosslinker, the crosslinking might be denser at the surface of large spheres than that of inside. This difference would also change the swelling characteristics and swelling time of the spheres. These factors might have influenced the ratio of strong/weak binding of BMP-2 to the microspheres, and thus the release profile. Similar to this study, it has been shown that increasing the chitosan sphere size increased the release of bovine serum albumin (BSA) [224].

In literature, optimal release profile for BMP-2 is generally described as a small initial burst release followed by sustained release over a couple of weeks, especially for ectopic bone formation [225]. Although the initial burst release of BMP-2 can be considered as a drawback, it may be necessary to trigger the initial healing process promoting migration of stem cells towards the site of implantation [226]. Absence of a burst release might impair the bone formation ability of BMP-2 loaded material [227]. A small burst release in the nanogram range followed by a sustained release has been shown to be more effective in bone formation for implants loaded with 2 µg BMP-2 [227]. On the other hand, burst release delivering high doses in the high microgram to milligram range could cause undesired side effects such as the formation of ectopic bone in the surrounding soft tissue, as it is the case for absorbable collagen sponge [62]. Thus, when considering burst release, it is important to distinguish between nanogram and microgram/miligram amounts of release. Here, we present that HMDIC crosslinked small spheres release 15-20% of BMP-2 loaded in the first day; DHT-spheres release 10% of BMP-2 showing that burst release can be modulated by crosslinking degree and 10% burst release is minimal compared to the BMP-2 release from collagen sponge which is more than 50% in the first day [228, 229]. Therefore, small sized spheres are expected to function better *in vivo* due to a small initial burst release and more sustained release profile. The design of the different RCP microspheres presented in this manuscript provides important information about the influence of the sphere characteristic on BMP-2 release and allows the generation of tuneable BMP-2 delivery systems for a broad variety of therapeutic applications for bone regeneration. We have also laid the groundwork for future *in vivo* studies by narrowing down potential system design parameters. In these in vivo studies also the degradation of the RCP microspheres can be further examined.

CONCLUSION

We have developed a novel BMP-2 delivery system based on tuneable RCP microspheres. This *in vitro* study provided important information about the influence of the RCP microsphere characteristics on BMP-2 release kinetics and demonstrated the potential of RCP microspheres as BMP-2 delivery material. BMP-2 was found to bind to RCP with high

affinity (K_D: 1.2 nM) suggesting a specific interaction between two proteins. Among different spheres studied, small sized RCP spheres crosslinked by HMDIC or DHT are most promising delivery materials for BMP-2 showing a small burst release (10%-20%) in the first day succeeded by a sustained release.

ACKNOWLEDGEMENT

DISCLOSURE STATEMENT

Didem Mumcuoglu and Laura de Miguel obtained fellowships from the above mentioned programme and performed major part of their research at Fujifilm Manufacturing Europe in cooperation with the Erasmus Medical Centre in Rotterdam, The Netherlands. Sebastiaan Kluijtmans is employed by Fujifilm Manufacturing Europe.

SUPPLEMENTARY INFORMATION
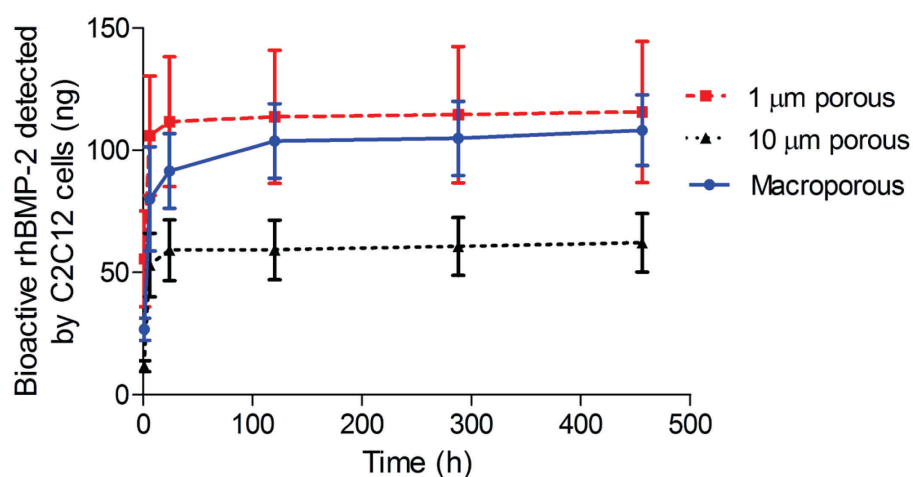
Time (h)	Bioactivity percentage (ng detected by C2C12 cells/ng detected by ELISA x 100)					
	1	**6**	**24**	**120**	**288**	**456**
1 µm porous	85	94	76	68	69	69
10 µm porous	21	54	51	50	51	52
Macroporous	45	71	64	62	61	62

Supplementary Figure 1. Bioactivity of released BMP-2 over 19 days. BRE-Luc C2C12 cells incubated with BMP-2 released from porous microspheres (MS#6, MS#7 and MS#8), and cumulative released bioactive BMP-2 was calculated based on BMP-2 standard calibration curve. Corresponding table shows the bioactivity in percentage at each time point calculated by the ratio of the BMP-2 detected by C2C12 cells (ng) to BMP-2 detected by ELISA (ng). For each assay, the amount of BMP-2 (ng) was calculated based on serial dilutions of fresh BMP-2 solution.
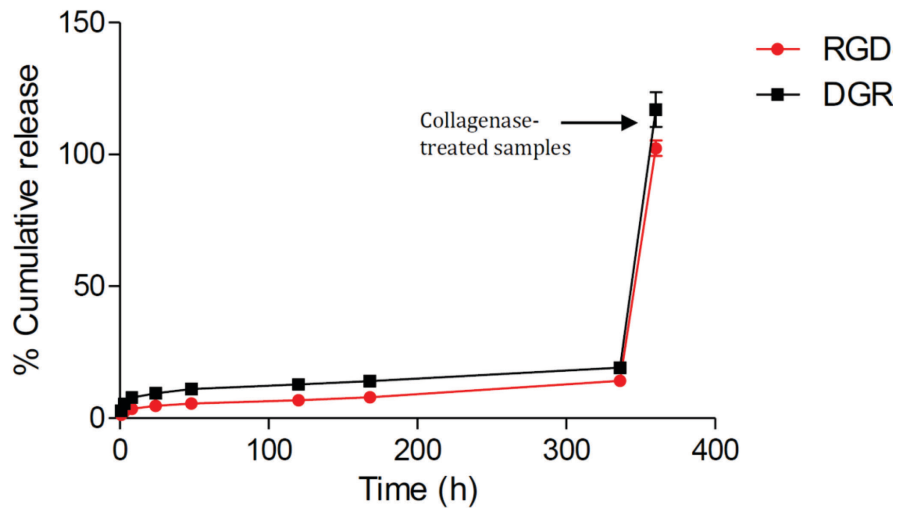
Supplementary Figure 2. BMP-2 release from spheres comprised of RGD and DGR containing RCP. RGD microspheres correspond to HMDIC-high crosslinked microspheres (50-75 μm, MS#1). Arginine-glycine-aspartic acid (RGD) sequence in RCP was replaced with aspartic acid-glycine-arginine (DGR) and DGR spheres were produced using the same method of RGD particles. BMP-2 is released from these spheres for two weeks after which remaining BMP-2 was liberated by upon collagenase degradation of microspheres. The percentage of released BMP-2 was calculated relative to the positive control, which is BMP-2 solution at the same concentration (900 ng/mL) without microspheres. Experiment was performed in triplicate, data are shown as mean and SD.

Chapter 3a

CHAPTER 3B

BMP-2 LOADED COLLAGEN I DERIVED RECOMBINANT PROTEIN MICROSPHERES INDUCED ECTOPIC BONE FORMATION IN RATS

Didem Mumcuoglu[1,2], Claudia Siverino[3,4], Shorouk Fahmy-Garcia[2,5], Sebastiaan G.J.M. Kluijtmans[1], Gerjo J.V.M. van Osch[2,6], Joachim Nickel[3,4], Eric Farrell[7]

1 Fujifilm Manufacturing Europe B.V., The Netherlands,
2 Department of Orthopaedics, Erasmus MC, University Medical Center Rotterdam, The Netherlands
3 Department for Tissue Engineering and Regenerative Medicine, University Hospital Wuerzburg, Germany,
4 Fraunhofer ISC, Translational Center Wuerzburg, Germany
5 Department of Internal Medicine, Erasmus MC, University Medical Center Rotterdam, The Netherlands
6 Department of Otorhinolaryngology, Head and Neck Surgery, Erasmus MC, University Medical Center Rotterdam, The Netherlands
7 Department of Oral and Maxillofacial Surgery, Special Dental Care and Orthodontics, Erasmus MC, University Medical Center Rotterdam, The Netherlands

ABSTRACT

There is a need for development of an effective delivery system for BMP-2. In this report, we aimed to control the release of BMP-2 by using RCP microspheres for which a strong binding of BMP-2 was observed previously. Microspheres loaded with 83 µg/mL, 8.3 µg/mL and 0.83 µg/mL BMP-2 were injected subcutaneously in rats to compare the ectopic bone formation capacity of these concentrations. Bone formation was imaged by micro-CT for 12 weeks and finally confirmed by histology. Only microspheres comprising 83 µg/mL BMP-2 induced ectopic bone formation, as confirmed by micro-CT and histological examination, and we have observed microspheres in these samples at the end of the experiment. On the other hand, 8.3 µg/mL, 0.83 µg/mL and the negative control did not form any bone and could not be retrieved at the end of the experiment, as a result of degradation of microspheres. Time course analysis of bone formation revealed that bone volume increased between 2 – 6 weeks after injection. Bone density continued to increase from week 2 until the end of the experiment. Overall, this study showed that a BMP-2 concentration of 83 µg/mL is necessary to induce ectopic bone formation with the RCP microsphere paste, and even with this concentration bone formation was minimal showing that the RCP microsphere delivery system can be further developed for a better control of BMP-2 release over time and to induce higher ectopic bone volume.

INTRODUCTION

There is a need for the development of an effective biomaterial for bone regeneration therapies [230]. This biomaterial should be osteoinductive and osteoconductive [231]. Often use of growth factors such as bone morphogenetic protein rendered osteoinductivity of the biomaterial. Among other growth factors, bone morphogenetic protein-2 (BMP-2) has been widely used in this field and FDA approved for spinal fusion, tibial non-unions and oral maxillofacial reconstructions [57, 58, 232]. However, use of BMP-2 has been associated with many adverse events as reported previously [66, 142, 195]. These adverse events are related to the burst release of BMP-2 from the collagen sponge and to the high loading dose [66, 233]. This high dose (1.5 mg/mL), often described as supraphysiological dose, was necessary to achieve effective bone formation when delivered on a collagen sponge. To overcome this limitation, an effective delivery system that will change the release profile of BMP-2 should be designed [64]. Other biomaterials tested in ectopic models used varying doses [234]. Some of the successful low-dose examples are with β-tricalcium phosphate (9 mm^3) containing 5 µg BMP-2 induced 32.5% bone formation [235]. A type of collagen sponge (6 mm diameter) with 5 µg BMP-2 induced max. 5 mm^3 bone [236], and silk-fibroin particles (10 mg) with 5 µg BMP-2 induced 2 mm^3 bone [237]. In another study, a low dose BMP-2 (<1 µg per specimen) delivered on a collagen sponge or with brushite calcium-phosphate particles did not form bone at all [238]. A fibrous glass membrane with 8.7 µg BMP-2 was effective in controlling BMP-2 release but resulted in slow bone regeneration [239]. Collagen and hydroxyapatite scaffold with 10 µg BMP-2 formed ectopic bone in rats [240]. Hydroxyapatite/collagen/alginate composite with 4 µg, 20 µg and 100 µg BMP-2 was tested and only the highest dose yielded bone, calcifying half of the volume of the implant [241].

We have previously shown *in vitro* that RCP microspheres are potential slow-release systems for BMP-2 (Chapter 3a). In the current study, we have investigated the potential use of these BMP-2 loaded RCP microspheres in ectopic bone formation *in vivo*. For that purpose, we have injected BMP-2 containing microspheres in form of a paste, subcutaneously into rats and followed bone formation by microCT. We used a BMP-2 concentration of 83 µg/mL (8.3 µg per implant) that we expect to induce bone formation based on literature and we selected two lower doses (8.3 µg/mL and 0.83 µg/mL) with a goal to reduce the dose of BMP-2.

MATERIALS AND METHODS

Preparation of microspheres

Microspheres were prepared by emulsification as described elsewhere (Chapter 3a). Small-sized (50-75 µm) dehydrothermal treatment (DHT) crosslinked spheres were chosen in this study because this type of spheres resulted in only 10 % initial burst release of BMP-2. Dehydrothermal treatment (DHT) to crosslink the particles was performed for 4 days at 160

°C in vacuum (~5x10^{-3} mbar). After crosslinking, the CaCO$_3$ porogen was removed by suspending the microspheres in 0.23 N HCl for 30 min until the formation of carbon dioxide stopped. The microspheres were washed repeatedly with water until a neutral pH was achieved. Size, morphology and crosslinking density of the spheres were characterized as previously described.

Adsorbed BMP-2

Wild-type rhBMP-2 was produced as described elsewhere [209]. BMP-2 was adsorbed to the microspheres by incubation of 5 μL of 0.2 μg/μL BMP-2 solution per mg of spheres overnight at 4 °C.

Preparation of the paste

To obtain the high dose (83 μg/mL final concentration of BMP-2), 100 mg BMP-2 loaded microspheres were mixed with 230 mg of empty microspheres. 10 mg loaded microspheres were mixed with 320 mg empty microspheres to obtain the middle dose (8.3 μg/mL final concentration of BMP-2) and 1 mg loaded microspheres were mixed with 329 mg empty microspheres to obtain the low dose (0.83 μg/mL). Empty microspheres of 330 mg were used as a control. The microsphere mixtures were subsequently mixed with 1.2 mL saline (0.9 % NaCl) for at least 10 min with a spoon. Then, freshly prepared paste was loaded to 1 mL syringes and 100 μL of paste was injected subcutaneously in the animals using a 19 G needle.

Study design and ethics

All animal experiments were performed with prior approval of the ethics committee for laboratory animal use (protocol number EMC 15-114-05). 9 weeks old Male Sprague Dawley (SD) rats (Charles River) were used in this study to evaluate ectopic bone formation. The animals were randomly assigned and housed in pairs in specific pathogen free (SPF) environment and allowed to adapt to the conditions 7 days before implantation. The animals were maintained at 22 ± 5°C on a 12 h dark/light cycle with ad libitum access to standard rat chow and water. At 12 weeks after implantation, animals were euthanized with CO$_2$ and the specimens were harvested for micro-CT analysis and histology.

Subcutaneous injection of paste to study ectopic bone formation

To evaluate the effect of different doses of BMP-2 on ectopic bone formation, BMP-2 was delivered with microspheres in the form of a paste and subcutaneously injected (total volume 100 μl per injection) in the dorsum of the animals. Each animal received 4 or 5 randomly assigned injections. All injections were performed on animals under isoflurane inhalation. To study BMP-2-dose effect on bone formation, three different BMP-2 concentration were used (83 μg/mL, 8.3 μg/mL, 0.83 μg/mL BMP-2) (n=7 per group). As a control, microspheres without BMP-2 were injected (n=7).

Micro-CT imaging

Micro CT (Quantum FX, Perkin Elmer, Waltham, MA, USA) was used to image animals biweekly until the end of the experiment and also to image the implants retrieved at 12 weeks. To image the ectopic bone *in vivo* the following parameters were used: Field of view: 73 mm, Voltage: 90 kV, Current: 160 µA, Scan Time: 120 sec. To image the implants a field of view of 20 mm was used. Trabecular and cortical bone mineral density (BMD) was measured on the basis of calibration scanning, using two phantoms with known density (0.25 g/cm^3 and 0.75 g/cm^3 ; Bruker MicroCT) under identical conditions. For image processing, Analyze software was used (Mayoclinic, Rochester, MN, USA), threshold levels were set to 0.1 g/cm^3.

Histology

For histological examination, specimens were fixed in 4% formalin solution and decalcified with 10 % EDTA for 2-4 weeks. Implants were dehydrated and embedded in paraffin. Sections of 6 µm thickness were prepared using a microtome (Leica Biosystems, Nussloch, Germany) and mounted on subbed glass slides (Thermofisher Scientific, Waltham, MA, USA). One of each five consecutive sections was de-paraffinized and rinsed with distilled water to be stained with hematoxylin and eosin (H&E) as described elsewhere [242]. The sections were imaged by Keyence BZ-9000 BIOREVO (KEYENCE Deutschland GmbH, Neu-Isenburg, Germany).

RESULTS

To compare the bone forming ability, 100 µL paste of microspheres containing 83 µg/mL, 8.3 µg/mL, or 0.83 µg/mL of adsorbed BMP-2 was injected subcutaneously to rats and samples were retrieved at 12 weeks. However, only 83 µg/mL BMP-2 induced bone formation whereas 8.3 µg/mL or 0.83 µg/mL failed to form bone, as shown by the representative micro-CT image in Figure 1. In these two low dose groups and in the negative control group, the paste was disappeared and implants could not be retrieved. In the 83 µg/mL BMP-2 group, 4 out of 7 injections resulted in bone with a minimum bone volume of 2.2 mm^3 and maximum of 7.3 mm^3 (Figure 1a). Strikingly, the bone volume was much lower than the injected paste volume of 100 µL (100 mm^3). The density of the ectopic bone for the four bone-positive implants (formed by 83 µg/mL BMP-2) was between 0.54 and 0.61 g/cm^3 (Figure 1b.).

Histology confirmed the presence of ectopic bone in 4 out of 7 samples in the 83 µg/mL BMP-2 group. In the other groups, for which the implants could not be retrieved histological examination was not performed. Figure 1d shows the histology of a 83 µg/mL BMP-2 sample and confirms the ectopic bone formation.
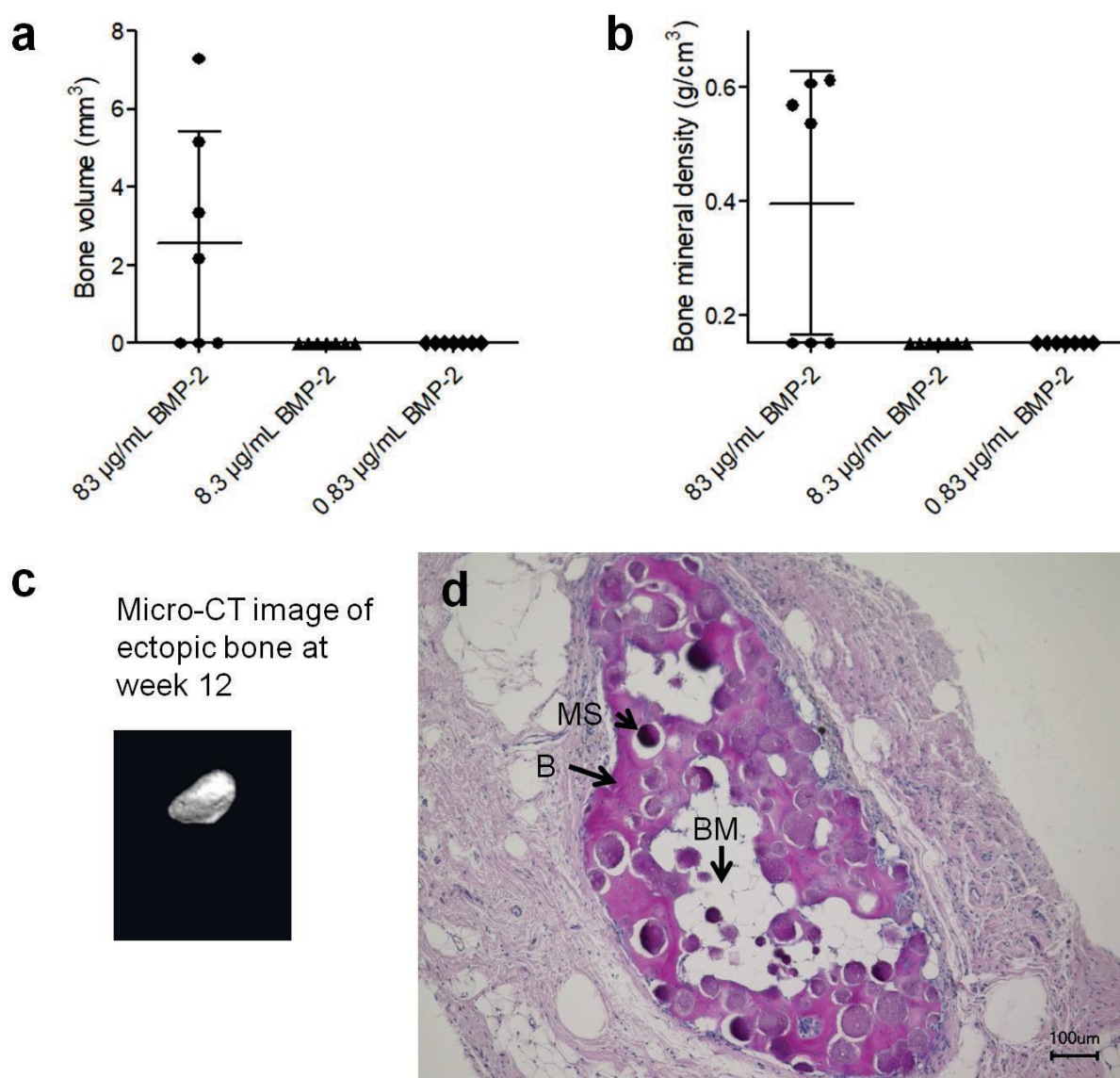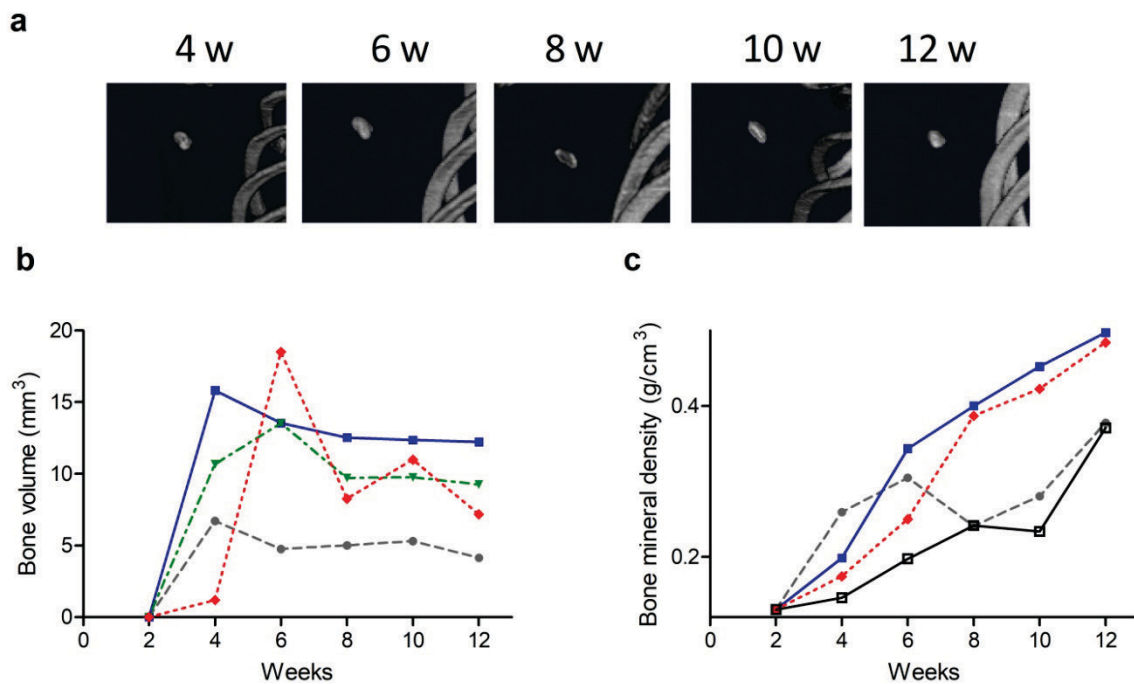
Figure 1. a. Bone volume (mm³) at 12 weeks. b. Bone density (g/cm³) at 12 weeks. A threshold of 0.1 g/cm³ was used for density calculation. Data is shown as dots representing each implant and mean ± SD, n=7 for each group. c. Representative CT-image of bone formation induced by 83 µg/mL BMP-2 at 12 weeks. d. Histology of an implant retrieved at week 12, showing the microspheres (MS), bone (B), bone marrow-like structure (BM).

The time-dependent bone formation was studied by microCT. Representative microCT images are shown in Figure 2a. The bone volume over time for the implanted materials giving bone (4 out of 7 for the 83 µg/mL BMP-2 group) is shown in Figure 2b. The bone volume increased between 2 and 6 weeks (Figure 2b). Between week 6 and week 8 there is a slight decrease in volume and after 8 weeks bone volume remained constant until the end of the experiment. It is important to note that, probably as a result of imaging *in vivo* with

less resolution, there is a slight difference between *ex vivo* and *in vivo* bone volumes. Bone densities (Figure 2c) increased from 2 weeks until the end of the experiment at 12 weeks.

Figure 2. a. Representative images of ectopic bone formation *in vivo* induced by an RCP paste comprising 83 µg/mL BMP-2 followed over a time course of 12 weeks. b. Bone volume of 83 µg/mL BMP-2 over time course of 12 weeks. c. Bone density of 83 µg/mL BMP-2 over time course of 12 weeks. Threshold of 0.1 g/cm^3 was used for density calculation. Data is shown as lines representing each implant, n=4 implants showed bone.

DISCUSSION

We have studied the potential use of a paste of BMP-2 loaded RCP microspheres in bone formation using an ectopic *in vivo* model. Our results showed that 4 out of 7 injections of the highest dose used of 83 µg/mL BMP-2 induced bone formation, while the lower doses, 8.3 µg/mL or 0.83 µg/mL BMP-2, did not result in any ectopic bone. The highly variable outcome for the high dose stresses the need for a better design of the delivery system.

The high dose of 83 µg/mL BMP-2 (8.3 µg per implant) used in our study was expected to induce ectopic bone formation based on previous findings. β-tricalcium phosphate [235], a type of collagen sponge [236] and silk-fibroin particles [237] all loaded with 5 µg BMP-2 yielded ectopic bone with a bone volume in the range of 2 mm^3 - 5 mm^3. Indeed, the paste loaded with 83 µg/mL BMP-2 did give ectopic bone but the results were highly variable: 3 out of 7 injections failed to induce bone formation. In addition, large variations in bone volume indicate that bone formation is not uniform. This might be explained by the rapid degradation of the DHT crosslinked microspheres, resulting in premature release of BMP-2.

Although the degradation rate of RCP microspheres *in vivo* was not investigated in this study, the same type of RCP microsphere injected subcutaneously was shown to be mostly degraded at week 4 [243]. Interestingly, microspheres were still detected at the 12 weeks histological end point examination of the bone-positive 83 µg/mL BMP-2 samples, whereas at lower BMP-2 concentration samples could not even be retrieved, most probably due to degradation of microspheres. This could indicate that bone formation partially prevented microsphere degradation. This phenomenon can be explained by the bone forming cells depositing matrix. This matrix deposition and calcification, might have prevented infiltration of other cells such as macrophages to degrade the microspheres.

Our results indicate that the BMP-loaded RCP microsphere slow release system might be further improved by several strategies focussed to decrease the degradation rate of the RCP microspheres. For example, the effect of crosslinking can be studied. It has been shown earlier that hexamethylene diisocyanate (HMDIC) crosslinked RCP particles are slightly more persistent against degradation than dehydrothermal (DHT) crosslinked particles *in vivo* [243]. Secondly, a composite material can be used to protect the microspheres and increase their degradation time. A hydrogel, for example, with a higher degradation time can increase the effectiveness of this system by increasing the degradation time and by protecting the RCP material from cell infiltration. In addition, the release of BMP-2 should also be studied *in vivo* to be able to assess its retention time and its relation to crosslinking and degradation rate of the carrier material.

In conclusion, BMP-2 loaded RCP microspheres were able to partially form bone at a concentration of 83 µg/mL. As a future prospect, the BMP-2 concentration can be further increased to achieve reproducible bone formation. Another alternative is to change the design of system for a better temporal control of the BMP-2 delivery resulting in successful bone formation with a lower dose of BMP-2.

ACKNOWLEDGEMENT

CHAPTER 4

NOVEL *IN SITU* GELLING HYDROGELS LOADED WITH RECOMBINANT COLLAGEN PEPTIDE MICROSPHERES AS A SLOW RELEASE SYSTEM INDUCE ECTOPIC BONE FORMATION

S. Fahmy-Garcia[1,2§]; D. Mumcuoglu [1,3§]; L. de Miguel [3]; V. D. Dieleman [4]; J. Witte-Bouma [4]; B.C.J. van der Eerden [2]; M. van Driel [2]; D. Eglin [5]; J. A. N. Verhaar [1]; S.G.J.M. Kluijtmans [3]; G.J.V.M van Osch [1,6] and E. Farrell [4]

1 Department of Orthopedics, Erasmus MC, University Medical Center, Rotterdam, The Netherlands
2 Department of Internal Medicine, Erasmus MC, University Medical Center, Rotterdam, The Netherlands
3 Fujifilm Manufacturing Europe B.V, Tilburg, The Netherlands
4 Department of Oral and Maxillofacial Surgery, Special Dental Care and Orthodontics, Erasmus MC, University Medical Center, Rotterdam, The Netherlands
5 AO Research Institute Davos, Davos Platz, Switzerland
6 Department of Otorhinolaryngology, Head and Neck Surgery, Erasmus MC, University Medical Center, Rotterdam, The Netherlands
§ S. Fahmy-Garcia and D.Mumcuoglu contributed equally to this work.

ABSTRACT

There is still the need for optimized *in-situ* gelling BMP-2 releasing formulations to fill and repair bone defects. Collagen-I based Recombinant Peptide (RCP) microspheres (MS) were used as a carrier for BMP-2. The MS were dispersed in hydrogels obtained from high mannuronate (SLM) alginate, high guluronate (SLG) alginate and thermoresponsive hyaluronan derivative (HApN). SLM+MS, SLG+MS and HApN+MS formulations showed sustained release of BMP-2. These formulations were injected subcutaneously in immune competent rats. SLM+MS, SLG+MS loaded with BMP-2 induced ectopic bone formation in the rats as revealed by X-ray tomography and histology at 4 and 10 weeks, whereas HApN+MS did not. Vascularization occurred within all the formulations studied and was significantly higher in SLG+MS and HApN+MS than in SLM+MS. CD68, iNOS and CD206 markers were used to assess the presence of inflammatory cells at 1, 4 and 10 weeks after implantation. Inflammation decreased over time in alginate groups, but increased in the HApN+MS groups suggesting that a chronic inflammatory milieu to be detrimental to bone induction. This study highlights the interplay of the BMP-2 and the delivery matrix material on the local induction of bone.

KEYWORDS: Injectable, alginate, hyaluronan, microspheres, BMP-2 (bone morphogenetic protein-2), bone regeneration

INTRODUCTION

Bone is a tissue with high self-regeneration capacity. However, in cases of trauma or certain diseases bone does not heal properly and therefore surgical intervention using autografts or allografts is necessary. Currently, autografts are the gold standard; however, they are associated with donor site morbidity, increased pain, high cost and long patient recovery time. The alternative is to use allografts, but they carry the risk of immunogenicity, infectious agents and lack the osteoinductive capacity of autografts [231]. To overcome these limitations there has been a vast effort to develop new biomaterials to aid large bone defect repair. Among these materials, natural biomaterials have been widely studied due to their advantages such as biodegradability, biocompatibility and the ability to interact with the extracellular matrix and cells [244]. Injectable formulations are preferred over implants for the treatment of defects that do not require operational fixation since the application is easier and the patient will not suffer from surgery and consequently, achieve a faster recovery. Moreover, in the case of irregular bone defects, injectable scaffolds might be advantageous because they can adapt to the defect shape better [245]. Alginate, hyaluronic acid (HA) and collagen derived materials have been investigated as scaffolds, particles and *in situ* gelling hydrogels [246].

Materials can be combined with bone forming proteins such as bone morphogenetic protein 2 (BMP-2) to stimulate bone formation. BMP-2 is considered to be one of the most powerful osteoinductive factors and is the only bone morphogenetic protein (loaded in a collagen sponge) approved and currently used as a bone graft substitute [194, 247]. However, large doses of BMP-2 are needed to produce a significant osteogenic effect [248]. The major reason for this is the burst-release of the protein from the collagen sponge. Half of the BMP-2 was released in the first two days *in vivo* in a rabbit ulna osteotomy model [65]. This often results in undesired ectopic bone formation, soft tissue swelling and bone resorption [249]. Therefore, a biomaterial that can provide a slower protein release may perform better in clinics, eliminating adverse effects. There are several challenges for developing a suitable protein carrier material [234]. It should promote the recruitment of skeletal and endothelial progenitor cells and trigger their differentiation to mature osteoblasts and endothelial cells with a minimum amount of loaded protein.

In this study, we aim to develop *in situ* gelling alginate and HA formulations to retain BMP-2 releasing microspheres, resulting in slow localized growth factor release. We have previously reported the use of recombinant collagen-like peptide microspheres for slow release of BMP-2 [250] (Chapter 3). The recombinant collagen-like peptide does not only facilitate the cell attachment by its arginylglycylaspartic acid (RGD) rich peptide sequence [204] but also can be expected to decrease the risk of immune reaction due to its animal

free origin. This cell attachment stimulation is very important when in combination with materials such as alginates and HA cell attachment is suboptimal.

Alginate is a polysaccharide composed of β-D-mannuronic acid (M-block) and α-L-guluronic acid (G-block) monomers. Several studies have demonstrated the potential of this hydrogel for bone tissue engineering [251]. Alginate *in situ* gelling formulations have been developed in combination with particles and *in vitro* experiments showed the potential of the formulations for drug delivery [252]. Previously, alginate hydrogel with gelatin microspheres loaded with BMP-2 was used to study osteogenesis *in vivo*. However, the formulations could not induce bone formation probably due to fast degradation of material; and only after addition of biphasic calcium phosphate granules, was the bone formation achieved [213]. There are various types of alginate where the ratio of monomer units and molecular weight of the polymer chains change. These parameters affect the degradation behavior of the hydrogels [253]; therefore, in this study we chose to use two different types of alginates, sterile lyophilized high mannuronate (SLM) alginate and sterile lyophilized high guluronate (SLG) alginate. *In situ* gelling formulations of alginates were developed via calcium complexation. Hyaluronic acid (HA) is another linear polysaccharide consisting of repeating units of D-glucuronic acid and N-acetyl-D-glucosamine and is an abundant glycosaminoglycan in extracellular matrices. Therefore, injectable HA hydrogels have been used for bone regeneration with BMP-2 [254]. However, to induce subcutaneous bone formation with HA, a very high dose of BMP-2 (150 µg/mL) was used [255]. HA gels are often functionalized to engineer better delivery systems. Investigators have recently shown that HA gels functionalized with fibronectin formed more ectopic bone than its non-functionalized counterpart [256]. However, functionalizing HA did not always induce more bone formation. For example, heparin functionalization of HA led to less ectopic bone formation than its non-functionalized counterpart formation when implanted intramuscularly [225]. In another study, HA failed to induce bone formation either in the presence or absence of BMP-2 [257]. These studies showed that HA and alginates have potential for use in bone regeneration. However, choosing the right formulations of engineered materials with a right dose of BMP-2 is challenging. Additionally, a huge demand in bone regeneration field is the development of *in situ* gelling materials that enable slow protein release, support cell attachment, vascularization and thus induction of bone formation. In this study, we have used Poly(N-isopropylacrylamide) functionalized hyaluronic acid (HApN) that shows thermoresponsive behavior.

We aimed to develop *in situ* gelling formulations with natural polymers for the RCP microspheres that can provide slow BMP-2 release and increase cell attachment. We also wanted to assess how the hydrogel matrices influence the *in vitro* release of BMP-2 from the microspheres and the bone induction *in vivo.* For that purpose, we have developed three different hydrogel-microsphere systems: two different thixotropic alginate formulations and a thermoresponsive (gelling above 32˚C) HApN. The function of these gels is to be injectable, *in situ* gelling, supportive of cell attachment, provide a sustained release

of BMP-2 and ultimately induce *de novo* bone formation. The mechanical properties of these gels and BMP-2 release characteristics *in vitro* were evaluated. The bone formation ability of these materials was studied in an ectopic bone formation model *in vivo*. The volume and morphology of the ectopic bone, vascularization, cellular infiltration and inflammation were evaluated.

MATERIALS AND METHODS

Materials

Human collagen type I based recombinant peptide (RCP) is a product of Fujifilm commercially available as Cellnest™. It is produced in a fermentation process by genetically modified yeast *Pichia pastoris* as described elsewhere [203, 204]. RCP is composed of 571 amino acids; it has an isoelectric point (pI) of 10.02 and a molecular weight of 51.2 kDa. BMP-2 was produced as described previously [209] and it was kindly provided by Dr. Joachim Nickel (Fraunhofer IGB, Germany). Pronova SLM20 (sterile alginate where over 50% of the monomer units are mannuronate) and Pronova SLG20 (sterile alginate where over 60% of the monomer units are guluronate) were ordered from Novamatrix (Sandvika, Norway). Thermoresponsive HApN consisting of HA grafted with poly (N-isopropylacrylamide) (PNIPAM) was prepared as described in D'Este *et al* [258].

Hexamethylene diisocyanide (HMDIC), corn oil, sodium chloride, calcium carbonate ($CaCO_3$) and glucono delta-lactone (GDL) were purchased from Sigma-Aldrich (St. Louis, MO, USA). Ethanol, acetone and hydrochloric acid were purchased from Millipore (Billerica, MA, USA). ELISA development kit and reagents for BMP-2 determination were ordered from Peprotech (Rocky Hill, NJ, USA). Dulbecco's Modified Eagle's Medium (DMEM), fetal bovine serum (FBS), phosphate-buffered saline (PBS) and penicillin-streptomycin (P/S) were ordered from Thermofisher Scientific (Waltham, MA, USA).

RCP microsphere preparation

RCP microspheres were produced by emulsification using calcium carbonate ($CaCO_3$). Briefly, a 20% aqueous RCP solution was prepared and mixed with $CaCO_3$ fine powder (with a size of <1 μm) in a 1:1 (w/w) ratio of RCP to $CaCO_3$. This suspension was emulsified in corn oil at 50 °C. After cooling, the emulsified microspheres were precipitated and washed three times with acetone, and subsequently dried overnight at 60 °C. The microspheres were sieved to 50-72 μm size (Retsch GmbH, Germany). Particles were then crosslinked by HMDIC by mixing 1 g of spheres and 1mL of HMDIC in 100 mL ethanol for 1 day while stirring. Excess crosslinker was removed by washing several times with ethanol after which the particles were dried at 60 °C. The particles used for the alginate and HApN formulations were prepared in identical way except that, for the HApN formulation, $CaCO_3$ was removed after the crosslinking step. For the alginate formulations the $CaCO_3$ was left in as the Ca^{2+} also serves to crosslink the alginate into a hydrogel. For the HApN formulation $CaCO_3$ was

removed by suspension of MS in 0.23 M hydrochloric acid for 30 min, followed by repeated washing with water until a neutral pH was achieved, and the MS were dried at 60 °C. Complete removal of the calcium was confirmed by EDX mapping (Supplementary Figure S2). The morphology of $CaCO_3$ containing and $CaCO_3$ free microspheres was analyzed by scanning electron microscope (SEM) (Supplementary Figure S1). $CaCO_3$ crystals clearly can be observed on the surface of the $CaCO_3$ comprising microspheres (Supplementary Figure S1). Particles were gamma sterilized at 25 kGray (Synergy Health, The Netherlands) prior to use *in vitro* and *in vivo*.

Preparation of the hydrogel formulations

Preliminary tests with different ratio of alginate/microspheres revealed a narrow range of ratio to obtain thixotropic behavior of the hydrogel. To prepare the formulations with SLM20 and SLG20 alginates, alginates were dissolved in 0.9 % sterile sodium chloride to create 2% w/v solution. 68 mg of calcium comprising microspheres were incubated overnight at 4 °C with 170 µL of 122.5 µg/mL BMP-2. The following day, the swollen particles were mixed with 1014 µL of SLM or SLG solution. To the SLG formulation, 106 µL of 0.06 M freshly-prepared GDL solution was added and mixed immediately. GDL was used to dissolve minute amounts of $CaCO_3$ so that alginate can be crosslinked and increase the mechanical properties of the formulation. In parallel, 106 µL of 0.9 % sodium chloride was added to the SLM formulation for which it was not necessary to add GDL as shown by rheology. The formulations were thoroughly mixed passing through a 19 G needle immediately and incubated overnight at 4 °C to equilibrate. One day later, prepared formulations were mixed again prior to injection *in vivo* or to use for *in vitro* experiments. For both *in vivo* and *in vitro* experiments 200 µL of the prepared formulations were used. The final amount of BMP-2 was 3.3 µg in each 200 µL hydrogel+MS formulation (Table 1). Solubilized Ca^{2+} ion as shown in µM and % in Table 1 was detected by calcium colorimetric assay following the manufacturer's instructions (Sigma-Aldrich).

The ratio of HApN/MS was selected based on their mechanical properties and injectability, and the following formulations were used for *in vitro* and *in vivo* experiments. First, a 15 % w/w solution of HApN was prepared in PBS. On the same day, 170 µL BMP-2 at 122.5 µg/mL concentration was added to 34 mg of MS (without $CaCO_3$) and particles were incubated at 4 °C overnight. Next day, 850 µL HApN (15% w/w) and 270 µL PBS were added to the swollen particles and the formulation was mixed with a 1 mL syringe and 19 G needle. The composition of the final formulations is shown in Table 1. In order to keep the amount of RCP the same in all different formulations, half of the microspheres were used in HApN condition compared to SLM+MS or SLG+MS formulations that contained 50 % $CaCO_3$ and 50% RCP in the microspheres. The prepared formulations were mixed and incubated overnight at 4 °C to equilibrate. All formulations were prepared under sterile conditions.

Table 1. Composition of the formulations used for the in vitro BMP-2 release study and for the in vivo experiment.

Formulation	SLM or SLG (%)	HA (%)	MS with CaCO$_3$ (mg/mL)	MS without CaCO$_3$ (mg/mL)	CaCO$_3$ (mg/mL)	RCP (mg/mL)	GDL (mM)	Ca^{2+} soluble (µM)	Ca^{2+} soluble (%)	BMP-2 (µg/mL)
SLM with MS	1.5	-	54	-	27	27	-	-	-	16.1
SLG with MS	1.5	-	54	-	27	27	5	3.18	0.93	16.1
HA with MS	-	10	-	27	-	27	-	-	-	16.1

Rheology

The mechanical properties of prepared hydrogels containing BMP-2 loaded microspheres were measured by a rheometer (Anton Paar MCR301, Austria). A 20 mm diameter parallel plate measuring system was used. After sample addition to the plate, silicon oil was applied to the edges to prevent evaporation. All measurements were performed with a normal force of 0.1 N. As a pre-characterization, the storage (or elastic) modulus (G') and loss (or viscous) modulus (G'') were measured at different strains to determine the linear viscoelastic region. To determine the linear viscoelastic region in alginate formulations (shown in supplementary table S1) four different formulations were prepared. SLG alginate (1.5 %, w/v); SLG alginate (1.5 %, w/v) with microspheres (8 %, w/v); SLG alginate (1.5 %, w/v) with microspheres (8 %, w/v) and GDL (5mM); and SLG alginate with CaCO$_3$ (4%, w/v) and GDL (5mM) were prepared. After pre-characterization, thermosensitive HApN+MS formulation was measured at 2% strain, at 1 Hz while heating from 15 °C to 40 °C followed by cooling from 40 °C to 15 °C.

Alginate formulations were measured by a two-step repeating cycle. At the first step of the cycle, storage and loss moduli were measured at 1 % strain, at 1 Hz, at 37 °C. At the second step, 500 % strain, 1 Hz frequency, 37 °C temperature was applied. The cycle repeated four times to characterize thixotropic behavior.

Release of BMP-2 from hydrogel formulations

The formulations containing hydrogels and BMP-2 loaded microspheres were prepared as described above. 200 µL of hydrogel formulations was added to 24 well plate inserts with 0.4 µm pore size. 1 mL DMEM with 10% FBS and 1 % P/S per well was added to the reservoir plate. The plates were incubated at 37 °C under constant agitation at 300 rpm. When removed from the incubator, the plates were put on a hot plate at 37 °C to prevent the gel-sol transition of HApN hydrogels. At each time point 1 mL medium was collected and changed with fresh medium. The collected release media were analyzed by rhBMP-2 ELISA

development kit (Peprotech) according to manufacturer's protocol. As a positive control, 200 µL of 16.5 µg/mL BMP-2 solution was added to the inserts and 1 mL medium was added to bottom wells of the transwell plate. At each time point 1 mL medium was collected and changed with fresh medium.

Conditions for animal experiment

All animal experiments were performed with prior approval of the ethics committee for laboratory animal use (protocol #EMC 116-15-01). 34 male Sprague Dawley (SD) rats at 12 weeks old were used in this study to evaluate bone formation. The animals were randomly assigned and housed in pairs in a specific pathogen-free environment and allowed to adapt to the conditions of the animal house for 7 days before starting the study. The animals were maintained at 20-26 °C on a 12 h dark/light cycle with ad libitum access to standard rat chow and water. To evaluate the effect of BMP-2 loaded in the different formulations, RCP microspheres with a constant concentration of rhBMP-2 (3 µg per injection) and incorporated in SLG, SLM or HApN hydrogels were subcutaneously injected (total volume 200 µl per injection) in the dorsum of the animals. As controls, SLM+MS, SLG+MS and HApN+MS were implanted without BMP-2 addition. N=6 replicates were used for each condition and each animal received 6 randomly assigned injections. All injections were performed using a 19 gauge needle on animals under isoflurane inhalation. At 1, 4 and 10 weeks after implantation, animals were euthanized with CO_2 and the specimens were harvested for further analysis. To reduce the number of animals used in this study, controls were harvested at 1 and 10 weeks after implantation.

Micro-CT analysis

When animals were euthanized at 4 and 10 weeks following transplantation, retrieved implants were immediately scanned at a resolution of 9 µm, using a SkyScan 1172 system (Bruker, Belgium). The following settings were used: X-ray power and tube current were 40 kV and 0.25 mA, respectively. Exposure time was 5.9 s and an average of three pictures was taken at each angle (0.9°) to generate final images. These images were further reconstructed by SkyScan NRecon software (Bruker) using a range of 0-0.1 on the histogram scale, 20% beam-hardening correction and ring artefact reduction with a value of 5. For image processing SkyScan CTAnalyser software (Bruker) was used. Threshold levels of 120 (lower) and 255 (higher) were set to extract the amount of mineral volume from the tissue volume (BV/TV).

Histology

For histological examination, specimens were fixed in 4% formalin solution for 48 h and decalcified with 10% w/v EDTA for 2-4 weeks. Implants were dehydrated and embedded in paraffin. Sections of 6 µm thickness were prepared using a microtome and mounted on subbed glass slides (StarFrost, Knittel Glass, Germany). Three selected cross sections from

each implant, with a minimum distance of 120 µm apart were deparaffinised and rinsed with distilled water to be stained with hematoxylin and eosin (H&E). The sections were imaged by NanoZoomer-XR (Hamamatsu, Japan). A square grid (400-800 µm) overlay was used to quantify newly formed blood vessels, which were identified based on the presence of erythrocytes within a tubular-like structure. The number of blood vessels was counted within the implants in a blinded fashion by two examiners and averaged.

CD68 marker was used to distinguish cells of the macrophage lineage, iNOS and CD206 markers were used for detection of M1 and M2 macrophage subsets. For detection of CD68, iNOS and CD206 positive cells, sections were deparaffinised and washed. In the case of CD68 and CD206, antigen retrieval was performed using a citrate buffer (10 mM, pH 6.0) at 90 ºC for 20 min. For iNOS, 10mM Tris, pH 9.0, 1 mM EDTA Solution, 0.05% v/v Tween 20 buffer was used. To avoid non-specific binding, slides were pre-incubated 30 min with 10% v/v normal goat serum (NGS) (Southern Biotech, USA) in PBS/1%BSA w/v and 2% w/v milk powder to block non-specific binding followed by 1 h incubation with either primary CD68 antibody (Acris, Germany) diluted to 0.5 µg/ml, primary CD206 antibody (Abcam, UK) diluted to 2.5 µg/ml or primary iNOS antibody (Abcam) diluted to 2 µg/ml. CD68 stained samples where then incubated for 30 min with biotinylated secondary goat anti-mouse antibody diluted 1:100 in PBS + 1% w/v BSA + 5% v/v rat serum (Jackson, PA, USA). For CD206 and iNOS staining, secondary biotin labeled goat anti-rabbit antibody (Biogenex, UK) diluted 1:50 in PBS+ 1% w/v BSA + 5 % v/vrat serum was used. Finally, slides were incubated with label streptavidin-AP (Biogenex) diluted at 1:100, rinsed with 0.2 M Tris-HCl pH 8,5 and stained with substrate. Substrate consisted in 0,1 mg/ml New Fuchsin (Sigma-Aldrich), 0,3mg/ml naphtol AS-MX phosphate (Sigma-Aldrich), 0,0025% w/v $NaNO_2$ (Sigma-Aldrich), 3% v/v di-methylformamide (Sigma-Aldrich) and 0,25 mg/ml levamisole (Sigma-Aldrich) dissolved in 0.2 M Tris-HCl (pH 8.5). Slides were counterstained with haematoxylin (Sigma-Aldrich) and analyzed using confocal microscope. Mouse IgG1 antibody (Dako Cytomation, Denmark) and rabbit IgG1 (Dako Cytomation) were used as negative controls.

Type II collagen occurs exclusively in cartilage, therefore, to investigate the presence of cartilaginous tissue within the formulations, collagen II staining was performed on the samples as previously described [259].

After Nanozoomer-XR imaging Hamamatsu Photonics, all the retrieved implants were ranked for CD68, iNOS and CD206-positive cells in terms of both staining intensity and number of cells stained by two observers who scored all stainings and were blinded with regard to treatment. The results obtained by the two observers were averaged and rated on ordinal scale (lowest number= no/minor to highest number=moderate/heavy).

Statistical analysis

To investigate whether there were differences in the number of blood vessels and CD68, iNOS and CD206 positive cells between conditions, a Kruskal-Wallis test was applied and Dunn's post-hoc was used for analysis. Micro-CT quantitative data and BMP-2 release data were analyzed using one-way analysis of variance and Bonferroni's post-hoc multiple comparison test was applied to the obtained results. A value of P < 0.05 was considered to be statistically significant.

Quantitative data are presented as bars, indicating the mean ± SD, while qualitative data are presented as box plots, indicating median, and the interquartile distance with the whiskers showing the largest and smallest values.

RESULTS

RCP microsphere-alginate in situ gelling hydrogels have shear-thinning behavior

Strain-dependent oscillatory rheology of RCP microsphere-alginate hydrogels showed an extremely broad linear viscoelastic region in addition to network rupture at high strains for the alginates containing 8% microspheres (Supplementary Table S1 and Supplementary Figure S3). The SLG alginate with microspheres (SLG + 8 % microspheres) broke at 150 % strain whereas the formulation containing GDL (SLG + 8 % microspheres+ GDL) was not broken at the maximum strain measured, 167% (Supplementary Table S1). This demonstrates that addition of GDL to the formulation, releasing 3.18 µM Ca^{2+} ions (Table 1), improved the mechanical properties of the SLG gel. The viscoelastic region was much smaller for the control consisting of alginate, $CaCO_3$ particles (1 µm) and GDL. This formulation was broken at 40% strain showing the reinforcing effect of the microspheres in the formulation.

Interestingly, the optimized formulations of SLM+MS and SLG+MS were thixotropic. When 500% strain was applied, a decrease in both loss and storage moduli was observed and the hydrogel structure was broken showing the shear-thinning effect (Figure 1A). When the stress was removed, the hydrogel recovered almost instantaneously indicating that the gel can be formed *in situ* directly after injection *in vivo*. This cycle can be repeated several times without loss of function. Both of the alginates were injectable due to this shear thinning behavior. The formed hydrogels had storage (elastic) moduli between 1-2 kPa for both alginate gel formulations.
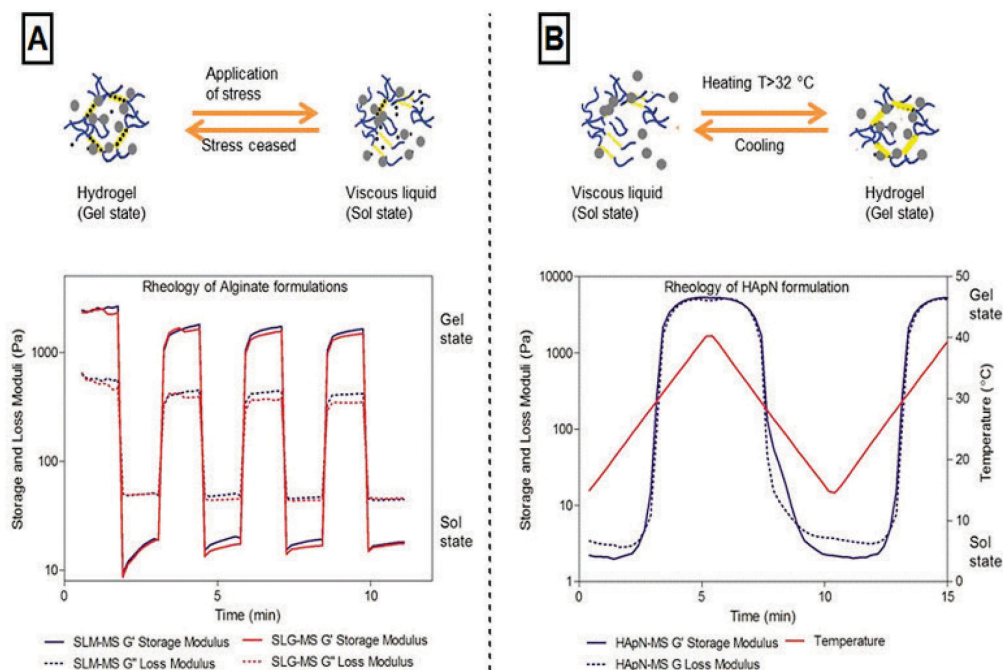
Figure 1. Mechanical properties of the SLM+MS, SLG+MS and HApN+MS composites. A. Thixotropic behaviour of the alginate hydrogel formulations containing SLM or SLG alginate and microspheres is shown by rheology. Gel is disrupted under shear stress and hydrogels recuperate when stress is removed within 30 sec. B. The thermo-responsiveness of the HApN hydrogel with microspheres is shown by rheology. Gel is formed when suspension is heated to 40 °C and the viscous liquid state forms when the gel is cooled to 15 °C.

HApN-microsphere formulation have thermoresponsive behavior

HApN hydrogel grafted with PNIPAM has an intrinsic property of thermo-inducible gel formation as shown earlier by D'Este *et al.* [258]. In combination with microspheres the thermoresponsive behavior was retained, which can be seen by the mechanical characterization of the hydrogel at increasing and decreasing temperatures between 15 °C and 40 °C (Figure 1B). In the cooling phase, there was a change from the gel state to the liquid state whereas in the heating phase, liquid to gel transition occurs. Both the storage modulus and loss modulus of the formed gel increased to 5 kPa at 37 ° C.

BMP-2 release from HApN-MS hydrogel was lower than alginate-MS hydrogels

Apart from the injectability of the hydrogel, the ability of the hydrogels to provide sustained BMP-2 release is important for bone formation. Therefore, the release of BMP-2 from these formulations was studied compared to hydrogel or microsphere only conditions. Both alginate hydrogels with microspheres released BMP-2 slower than alginate without microspheres, showing the synergistic effect of microspheres and hydrogels to control the release (Figure 2A). During the time-course study of two weeks, 202 ± 42 ng (mean ± SD) of BMP-2 was released from SLG+MS formulation and 46 ± 23 ng (mean ± SD) was released

from SLM+MS formulation. At the end of the experiment (Day 14), 2.3 µg ± 0.1 µg (mean ± SD, n=3) cumulative release was detected from the positive control which was 3.3 µg BMP-2 initially added to the inserts of the transwells. The numbers indicated that the majority of BMP-2 was retained in the alginate-MS formulations.
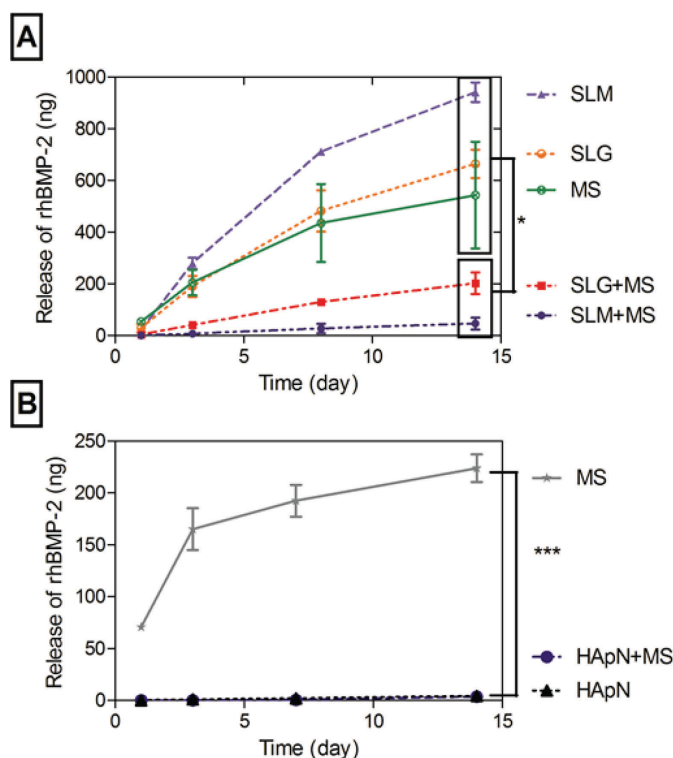

Figure 2. In vitro BMP-2 release from the A. SLM alginate, SLG alginate formulations and microspheres (MS) containing CaCO$_3$ and B. from hyaluronic acid-pN (HApN) formulations and microspheres without CaCO$_3$. The cumulative release of BMP-2 in DMEM with 10% FBS and 1 % P/S detected by ELISA is demonstrated over time. BMP-2 release from A. SLM alginate only (SLM), SLG alginate only (SLG), microspheres containing CaCO$_3$ (MS), SLG alginate with microspheres (SLG+MS), SLM alginate with microspheres (SLM+MS); B. only microspheres without CaCO$_3$ (MS), hyaluronic acid-pN with microspheres (HApN+MS) and hyaluronic acid-pN (HApN) are compared. Statistical difference at 14 days of cumulative release analyzed by one-way ANOVA, *p<0.05, *** p<0.001.

Interestingly, the release from the HApN+MS and from HApN hydrogel only was limited (Figure 2B). The total release was 3.7 ± 0.4 ng and 4.2 ± 0.2 ng, a fraction of the 3.3 µg loaded into the gels. To confirm that the unreleased BMP-2 was still inside the hydrogel after 2 weeks, ten times diluted samples were loaded on a SDS-PAGE gel (Supplementary Figure S4). We could detect a band of BMP-2 after 2 weeks of release, which confirmed that HApN hydrogel prevented BMP-2 release.

Injectable BMP-2 loaded hydrogel formulations induced ectopic bone formation

BMP-2 loaded in RCP microspheres were injected subcutaneously after encapsulation in the three hydrogel formulations tested; alginate SLM+MS, alginate SLG+MS and thermo-responsive HApN+MS. Identical formulations without addition of BMP-2 were used as controls. 1 week post injection histology revealed noticeable differences in terms of composite integrity between formulations (Figure 3A). In the alginate formulations, both the microspheres and the alginate layer were mostly intact, with some cellular infiltration in the fissures that appeared in the gel. However, in the HApN formulation, much of the hydrogel had disappeared, many of the microspheres were being degraded and numerous cells could be observed within the implants (Figure 3A). After 4 weeks, bone formation was observed in one third of the alginate harvested formulations (Figure 3A).

Bone formation was analyzed at 4 and 10 weeks by micro-CT, showing a similar amount of calcified tissue in all three hydrogel formulations tested at 4 weeks (Figure 3B). Interestingly, in the alginate formulations cartilaginous regions were found at that time point, suggesting that endochondral ossification process was occurring near by the MS (Supplementary Figure S5). At 10 weeks, micro-CT confirmed the greatest amount of bone formation when alginate SLG was used as a carrier, showing a more than three-fold increase compared to the 4 weeks scan (mean ± SD, from $4.4 ± 5.4$ mm^3 mineral volume at 4 weeks to $22.3 ± 11$ mm^3 at 10 weeks). When alginate SLM +MS or thermo-responsive HApN+MS were used, the amount of calcified tissue found within the implants did not change significantly over time (Figure 3B). Moreover, the alginate SLG+MS composite significantly increased the amount of mineral volume formed at 10 weeks compared to alginate SLM ($22.3 ± 11$ mm^3 vs. $4.24 ± 3$ mm^3)(Figure 3B). As we expected, when alginate formulations were implanted without BMP-2, mineral tissue was barely found (Figure 3C). Interestingly, the thermo-responsive HApN+MS formulation showed calcified tissue on micro- CT, even without the addition of BMP-2 (Figure 3C), but histological analysis did not show bone formation and the composite structure was almost degraded with or without BMP-2 addition at the end of the experiment (Figure 3A).
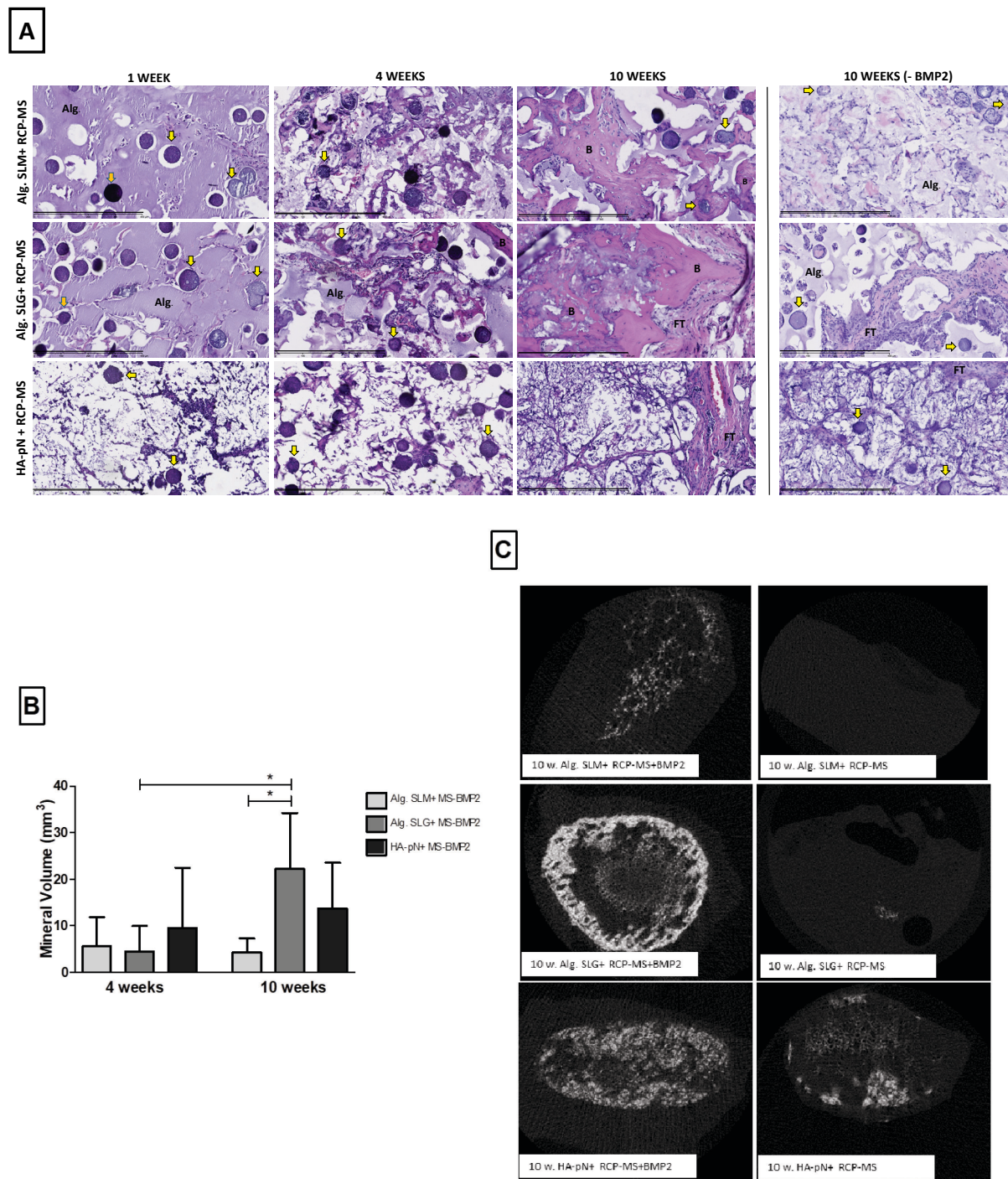
Figure 3. Alginate hydrogel formulations loaded with BMP-2 induced ectopic bone formation. A. H&E sections at 1, 4 and 10 weeks after implantation showing the alginate scaffolds (alg), microspheres (indicated by yellow arrows), formed bone (B) and fibrous tissue (FT). Controls (empty composites) are shown at 10 weeks. Images are shown at high magnification (scale bar is 400 µm). B. Comparison of the mineral volume obtained in the different composites with the addition of BMP-2 at 4 and 10 weeks-period. The bars represent the mean ± SD (* p < 0.05). C. Reconstructed micro-CT images 10 weeks after

subcutaneous injection of alginate SLM+ MS, alginate SLM+ MS and HA+ MS with and without BMP-2.

Inflammatory cell infiltration decreased over time in alginate in comparison to hyaluronan formulations

To investigate the role of inflammation in the bone formation process, we used CD68 as a general marker to identify cells of the macrophage lineage. We observed a significant time dependent decrease in staining in the alginate SLG (median ± 95% CI, 39 ± 8.3 at 1 week vs. 7 ± 7.5 at 10 weeks, $p < 0.05$) (Figure 4A-B). In the alginate SLM formulation CD68-positive staining was less pronounced than in SLG alginate at week 1, increased at week 4 and then significantly dropped again at week 10 (mean ± 95% CI, 14 ± 3.9 at 1 week and 33.5 ± 7.3 vs. 10 ± 11 for 4 and 10 week rank, respectively). In the HApN formulation macrophage recruitment was slower than in alginate SLG formulation and had the highest CD68-positive staining at 10 weeks (median ± 95% CI, from 23.5 ± 6.3 at week 1 to 48.5 ± 5.5 at the end of the experiment, $p < 0.01$) (Figure 4A-B). Furthermore, when we compared the formulations to each other at 1, 4 and 10 weeks post implantation, the SLG formulation showed more pronounced infiltration of CD68-positive cells at 1 week than SLM (39 ± 8.3 vs. 14 ± 3.9, $p < 0.01$) and CD68-positive staining at 10 weeks in the HApN formulation was significantly higher than in both, alginate SLM and alginate SLG (10 ± 11 for SLM, 7 ± 7.5 for SLG vs 48.5 ± 5.5 for HApN, $p < 0.05$).

To further investigate whether the different formulations promoted the activation of distinct macrophage phenotypes, pro-inflammatory (M1) and anti-inflammatory (M2) macrophage subsets were identified. To achieve this, iNOS and CD206 markers were used. iNOS, was used as marker for M1 macrophages. The HApN formulation had significantly more iNOS-positive staining compared to the alginate SLG formulation at 10 weeks (median ± 95% CI , 41.25 ± 9.6 vs. 7 ± 8.8, $p < 0.05$) (Figure 4C).

CD206-positive staining to identify M2 macrophages did not show any difference between formulations at week 1. At 4 weeks, CD206-positive staining was significantly higher in SLM than in HApN formulations (28.2 ± 4 vs. 10.5 ± 4.2). At week 10 no significant differences were found between them (Figure 4D).

Injectable formulations loaded with BMP-2 promoted blood vessel growth

Vascularization is a prerequisite for ossification. In all three formulations blood vessel density increased over time (Figure 5A). Interestingly the quantity of blood vessels found within the implants differed markedly between formulations, showing more than five-fold more vessels in the HApN formulation – mean ± SD; 395 ± 82 counted at 10 weeks– compared to the SLM alginate –with 144 ± 79 at 10 week ($p < 0.001$) (Figure 5A-B). In addition, in alginate SLG and HApN the quantity of blood vessels was significantly higher at 10 weeks than at 1 week (mean ± SD; 144 ± 79 vs. 13 ± 16 in alginate SLG, and 395 ± 82 vs.

38 ± 27 in HApN) (Figure 5A). Without BMP-2 no significant increase in the number of blood vessels were observed between 1 and 10 weeks in any of the formulations (data not shown).
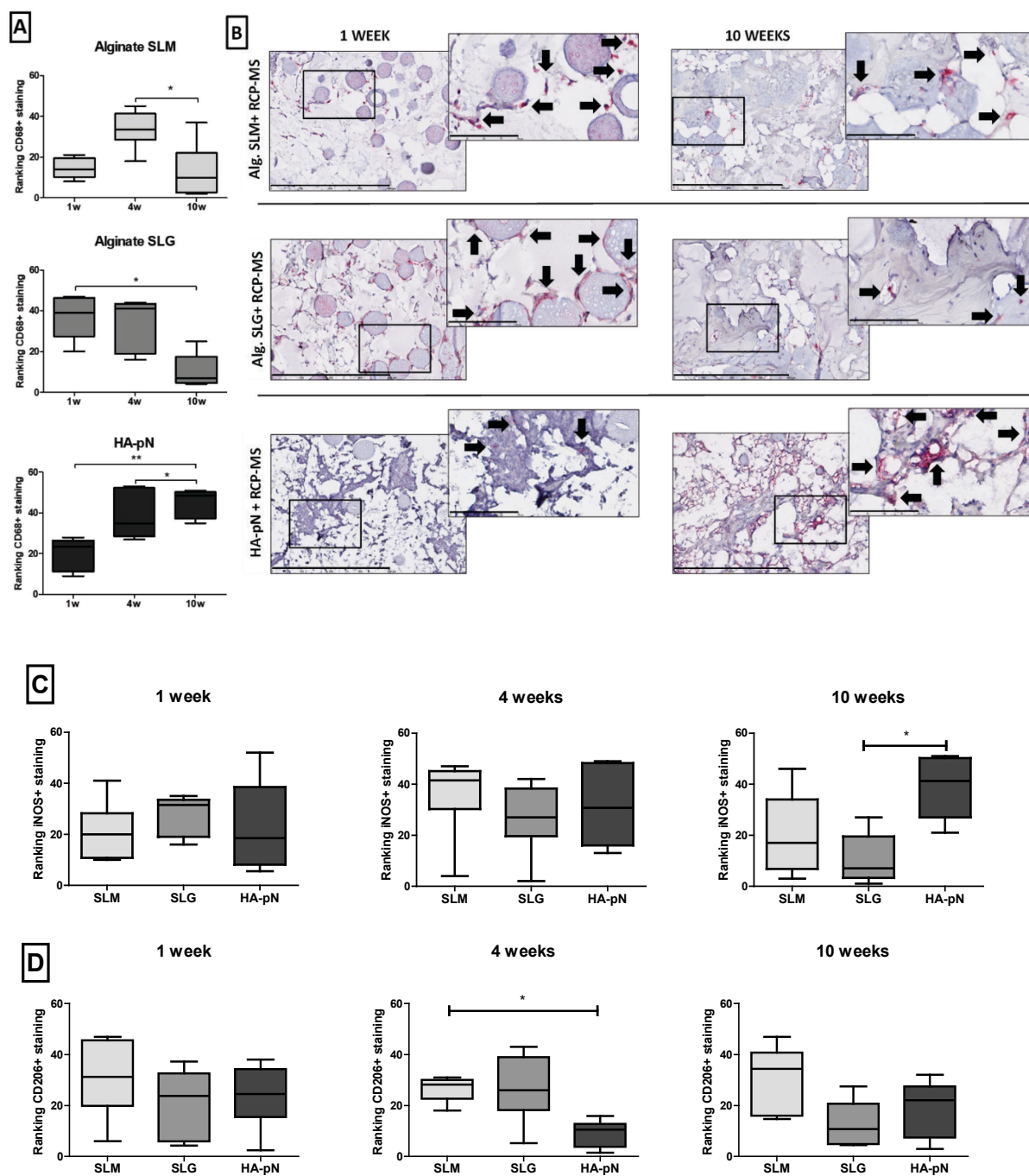
Figure 4. CD68, iNOS and CD206 positive staining differed between hydrogel formulations. A. Two blind observers ranked the implants according to the CD68 positive staining found in the composites at 1, 4 and 10 weeks. B. CD68 staining of a representative sample of each implant formulation at 1 and 10 weeks (scale bar is 400 µm). The square grid shows the

selected magnified area for each composite. CD68-positive cells are indicated by black arrows (scale bar is 100 µm). C. Ranked implants by two blind observers according to the iNOS positive staining found in the composites at 1, 4 and 10 weeks. D. Ranked implants by two blind observers according to the CD206 positive staining found in the composites at 1, 4 and 10 weeks. The line in the middle of the box is plotted at the median. The box extends from the 25th to 75th percentiles and the whiskers are drawn down to the 5th percentile and up to the 95th, (* p < 0.05, ** p < 0.01).

DISCUSSION

In this study, we have tested *in situ* gelling HApN formulation with thermo-responsive behavior and alginate formulations with shear-thinning behavior as slow-release systems for the induction of *de novo* bone formation. We have found differences in the BMP-2 release pattern when loaded in HApN vs. alginate hydrogels. Also, a further decrease in release rate was observed when BMP-2 was absorbed to recombinant collagen peptide (RCP) microspheres and then combined with alginate hydrogels. Furthermore, we have shown that the slow-release gel-microsphere system comprised of SLG alginate supported the essential processes needed for bone formation, such as inflammatory cell infiltration, vascularization and osteogenesis *in vivo* and was superior to the SLM alginate and HApN formulations. Through analysis of the phenotype of the infiltrating cells and kinetics of blood vessel invasion we shed some light on the possible reasons for the differences observed between formulations.

Injectable matrices have been the subject of much research in the fields of drug delivery and tissue engineering due to the minimally invasive nature with which they can be delivered [245]. We selected alginate and HApN formulations as carriers of microspheres for two reasons. First, they are both natural-origin polymers that are commonly used for bone regeneration; second, they can form *in situ* gelling systems. The *in situ* hydrogel forming ability of PNIPAM functionalized HA and alginate has already been shown [258, 260]. However, the formulations with microspheres are novel and were developed specifically for this study. One advantage of the system with alginate is that it can form a reversible hydrogel (thixotropic) which has not been observed in other *in situ* gelling alginates [25].

This reversible behavior of the gel makes handling much easier since the hydrogel can be prepared in advance and stored prior to application. Another advantage of both types of alginate formulations used in this study was the gelation time, which was so quick that the formed gel stayed in the injection site. In addition, the relatively slow degradation time of the alginates matched the time required for bone formation. The alginates showed some signs of initial degradation on histology by the first week, but after 10 weeks hydrogel was still present, which kept the microspheres and protein at the site, supported the formation of new bone and delayed the release of BMP-2.
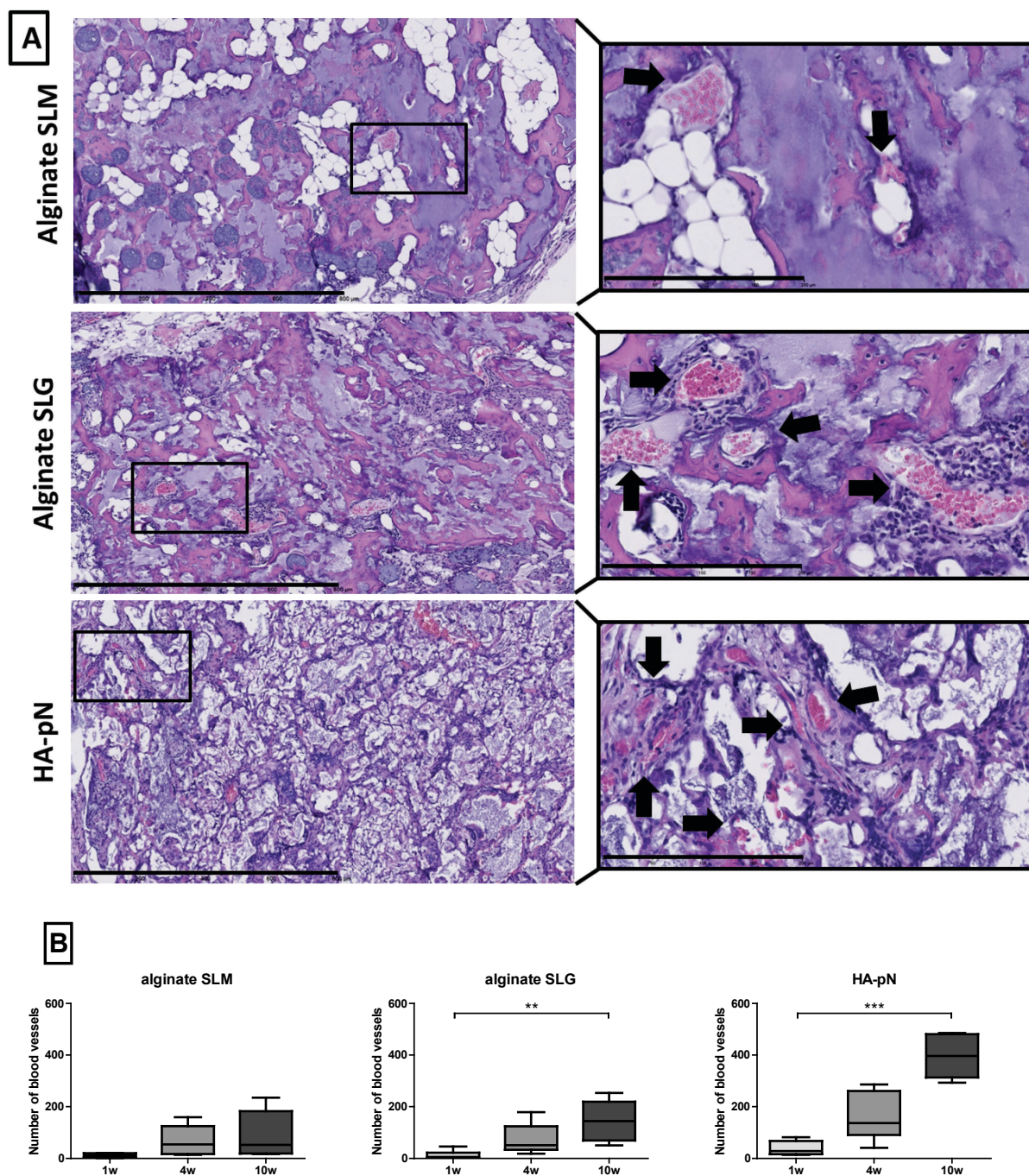
Figure 5. Alginate SLG and hyaluronic acid loaded with BMP-2 significantly promoted blood vessel ingrowth. A. Representative pictures of each implant formulation at 10 weeks (scale bar is 800 μm). The square grid shows the selected magnified area for each composite (scale bar is 200 μm). B. In each section, blood vessels were counted. The graphs show the absolute number of blood vessels counted per composite formulation at 1, 4 and 10 weeks. The line in the middle of the box is plotted at the median. The box extends from the 25th to 75th percentiles and the whiskers are drawn down to the 5th percentile and up to the 95th, (* $p < 0.05$, ** $p < 0.01$, *** $p < 0.001$).

Regarding protein release, the type of the hydrogel was found to be important. We observed that the combination of alginate and microspheres considerably slowed down the release of BMP-2. SLG+MS lead to more BMP-2 release than SLM+MS resulting in more bone formation. However, when HApN was used as a hydrogel, with or without the addition of RCP-MS, most of it was retained. These data suggest a strong interaction between thermo-responsive HApN hydrogel and BMP-2 resulting in the retention of the protein. This has been observed previously for HA. In one study, HA-based powder gel composite showed slow release of less than 20 % of the total amount of rhBMP-2 [261]. Most likely this lack of release prevented the attraction of the necessary cells at the early stages and by the time it had been released the material was too degraded to modulate the release rate or structurally support bone formation. Whether this affinity for BMP-2 is specific to PNIPAM functionalized HA or is a more general phenomenon requires further investigation.

The mechanical properties of the alginates showed that the storage (elastic) moduli are in the range of elastic moduli of endothelial tissue and stromal tissue [262]. However, the elastic modulus of HApN with microspheres is higher than that of alginates and comparable to elastic modulus of a smooth muscle [262]. These mechanical properties indicate that the gels can retain the microspheres *in situ*, fill a defect and provide initial support during the formation of bone. The mechanical properties of these thixotropic alginate hydrogels (1-2 kPa) are similar to non-*in situ* gelling alginates [263]. According to Banerjee *et al.*, gels with very high elastic moduli are undesirable and thixotropic gels with moderate elastic moduli (which were what we used in this study) should be suitable for bone regeneration [264]. With regard to HA, 50% cross-linked HA had an elastic modulus of 30 Pa [265], which is far lower than the PNIPAM functionalized hydrogel presented in this study (5 kPa). After bone fracture, following the initial inflammation a callus forms. The mechanical properties of fracture callus have been measured and found to depend on multiple tissue types: the range of the indentation moduli was 0.61–1.27 MPa (median = 0.99 MPa) for granulation tissue, 1.39–4.42 MPa (median = 2.89 MPa) for chondroid tissue and 26.92–1010.00 MPa (median = 132.00 MPa) for woven bone [266]. We therefore concluded that an elastic modulus in the range of 1-10 MPa is suitable for supporting the regenerative tissue. Given the mechanical properties of these hydrogels, it could be feasible to apply them directly to repair non-load bearing bone defects. For fractures or defects in the load bearing-bones, the application would still require some other kind of mechanical stabilization, be that a traditional cast, internal fixation or combination with other stronger biomaterials.

HA is a commonly used material for cartilage regeneration. Eglin *et al.* found that thermo-responsive HApN can be used to support hMSCs for the treatment of degenerated intervertebral disc and therefore HA hydrogels were developed as a bone-cartilage interface [267]. Injectable HA has been shown to be successful in a rabbit osteochondral defect model [268]. Interestingly, one study suggested that HA might impede bone formation by inhibiting osteoblast differentiation [269]. Maus *et al.* used combinations of commercially available injectable HA with and without 200 µg BMP-2 in a sheep femoral defect. However, none of

the conditions resulted in significant bone formation [257]. Bakhta *et al.* used hyaluronan-based hydrogels loaded with 5 µg BMP-2 ectopically and observed significant bone formation within the formulations and a mineral volume of 4.4 ± 0.5 mm^3 after 8 weeks [270]. However, prior to our study, *in situ* gelling HA had never been used in combination with particles to enhance cell adhesion and to promote bone tissue formation. We used microspheres rich in RGD motifs as BMP-2 carrier and failed to show bone formation after 10 weeks. Unlike Bakhta *et al.*, who implanted the composites intramuscularly, which is more conducive to supporting *de novo* bone formation, we injected our composite subcutaneously and this might account for the discrepancy observed.

How to modulate inflammation has become a hot topic in bone repair in the past decade [271-274]. Several groups have studied both the influence of different biomaterials upon macrophage polarization *in vitro* [275-279] and the positive dose-dependent relationship between the dosage of BMP-2 and the inflammatory volume [62, 196, 233, 280, 281]. Most *in vivo* bone formation studies have investigated the inflammatory response involved by using a single marker to identify monocyte-macrophage-osteoclast cells such as TRAP or have relied on generic histology (e.g. H&E) to assess inflammation [233, 280, 282, 283]. In our study, we used CD68, iNOS and CD206 as markers to identify macrophage presence and to indicate their phenotype within our tested composites. The BMP-2 dose used in this study was low, to prevent potential side-effects associated with higher doses (such as inflammation), to allow us to better investigate the effects of the materials. We observed a late CD68+ cell infiltration in the HApN composites, which increased over time. It has been reported that macrophages can specifically recognize HA through receptors such as CD44 or the hyaluronan receptor for endocytosis, HARE [284] and that the HA–CD44 interaction is involved in multiple cellular functions such as inflammation [285]. This might explain the high levels of inflammatory cell infiltrate observed at the later time points in the HApN+MS group. In contrast, in alginate formulations, CD68+ staining was lower at 10 weeks than at 1 week, and bone formation was successfully achieved. It is known that alginates from wound dressings interact with wound macrophages [286] and alginate-collagen composites have been shown to locally integrate with host tissue in an abdominal wall defect model [287]. In our study, at 4 weeks, there was more CD206+ staining in the alginate composites than in the HApN+MS formulation, suggesting a possible polarization of the monocytes towards the anti-inflammatory/tissue remodeling M2 phenotype. Moreover, there were significantly more iNOS+ cells in the HApN+MS formulation than in the alginate formulations at 10 weeks, which is more indicative of a pro-inflammatory situation. Taken together the results suggest that within alginate formulations there was an initial inflammatory phase that resolved over time, leading to bone formation. In contrast, in the HApN+MS formulation the presence of pro-inflammatory cells increased over time and there were with significantly fewer anti-inflammatory CD206 positive cells. This likely also negatively influenced the bone formation process in the HApN+MS gels.

Vascularization is another critical factor for successful bone formation. It has been demonstrated that HA-based scaffolds promote angiogenesis when used in a wide variety of applications, such as abdominal wall defect repair, brain injury or heart disease models [288-290]. Moreover, Cui *et al.* demonstrated the ability of HA-RGD scaffolds to support angiogenesis in the cortex of the brain [291]. Similarly, alginate-based beads loaded with VEGF had been used subcutaneously for bone tissue engineering, promoting angiogenesis [292]. Furthermore, a study in which alginate and alginate-RGD hydrogel were injected into the infarct area of rats showed that both increased arteriole density but that the greatest angiogenic response was in the alginate-RGD hydrogel condition [293]. Our findings agree with the results obtained in previous studies and we have demonstrated that both thermoresponsive HA and alginate enriched with RGD microspheres are able to promote vasculature formation ectopically when loaded with BMP-2. It is, however, clear that in this case more does not necessarily mean better: although significantly more vessels were present in the HA implants than in the alginates, this did not lead to the formation of any bony tissue.

CONCLUSIONS

In situ gelling hydrogels encapsulating BMP-2 loaded RCP microspheres represent an injectable slow-release protein delivery system. Alginate formulations effectively promoted bone formation in an ectopic model. While there was successful infiltration of cells into all three formulations, differences between materials were observed in the macrophage phenotype and invasion kinetics. Also, while there was ample vascularization in all three materials there were clear differences in the total number of blood vessels with the higher number present in the HA formulation not increasing the success of *de novo* bone formation. Thus, alginate SLG combined with RCP-MS and loaded with low dose BMP-2 displayed optimal protein release rate, cellular invasion, material degradation rate and vascularization kinetics to support bone formation. This study presents a novel cell-free injectable slow-release system that has potential as a void-filling material for the induction of new bone formation.
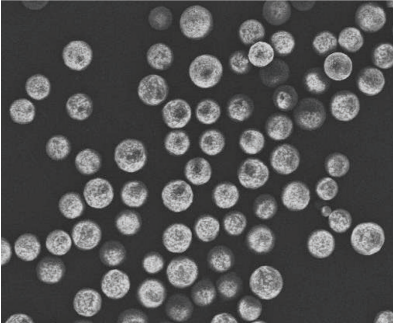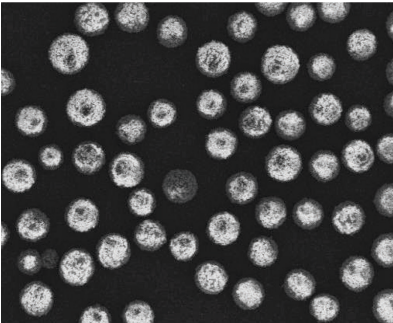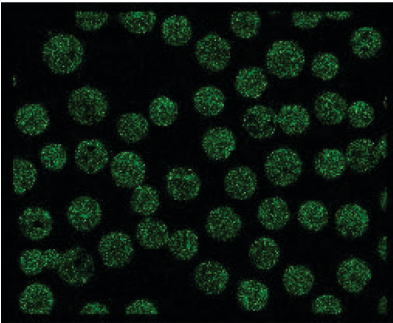
ACKNOWLEDGEMENTS

SUPPLEMENTARY INFORMATION
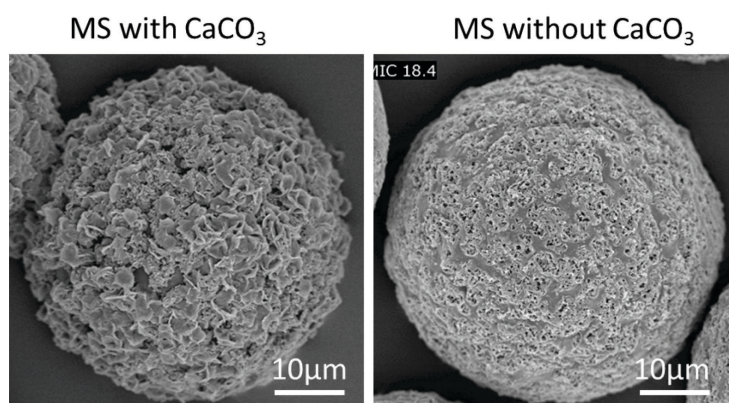
Supplementary Figure S1. Morphology of microspheres shown by scanning electron microscopy (SEM). The $CaCO_3$ crystals are visible on the microspheres on the left.

SEM: CaCO3 removed MS	Calcium (Ca)
	Not detected
SEM: CaCO3 containing MS	Calcium (Ca)

Supplementary Figure S2. Energy-dispersive X-ray spectroscopy mapping of microspheres before and after $CaCO_3$ removal.

Supplementary Table 1. Table showing the strain % at which the structure breaks, as shown by the amplitude sweeping test analyzed by rheology.

| Type of structure	Strain % at which the structure breaks
Alginate only	12
Alginate (SLG-20) + 8 % microspheres	150
Alginate (SLG-20) + 8 % microspheres +GDL	>167
Alginate +CaCO$_3$ (1 μm size) + GDL	40
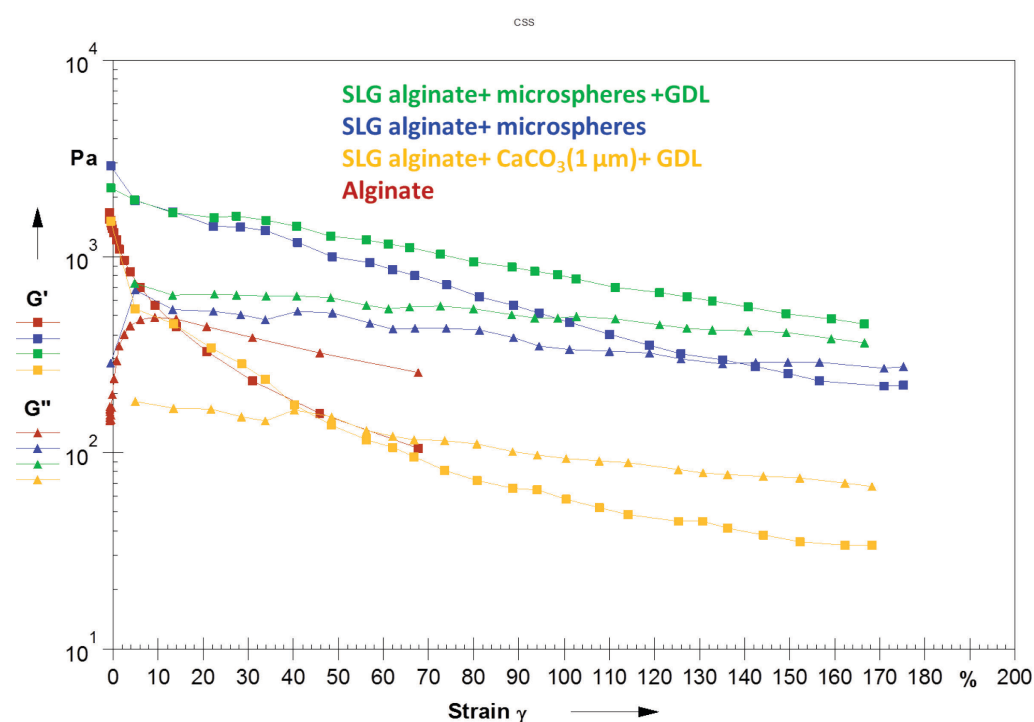
Supplementary Figure S3. Strain-dependent oscillatory rheology of in situ gelling alginate hydrogels (HG) and of the negative controls (references) consisting of an alginate hydrogel, crosslinked at higher calcium concentrations and an alginate hydrogel containing CaCO3 particles.
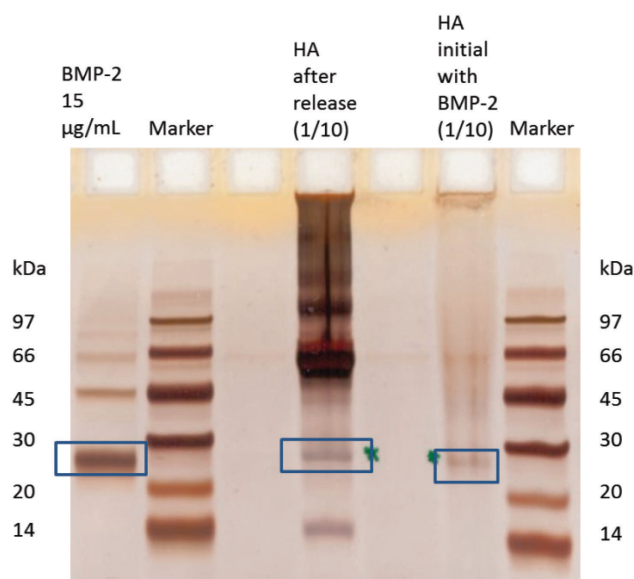
Supplementary Figure S4. SDS-PAGE of the BMP-2 bands (shown inside blue rectangles). Lanes from left to right are: control BMP-2 solution at 15 µg/mL; marker; empty lane; HA hydrogel after release diluted 10 times before loading; empty lane, HA hydrogel loaded with BMP-2 (before release) diluted 10 times before loading; marker. The density of BMP-2 band after release is more intense than before release. This might be related to the higher interaction between BMP-2 and HA initially.
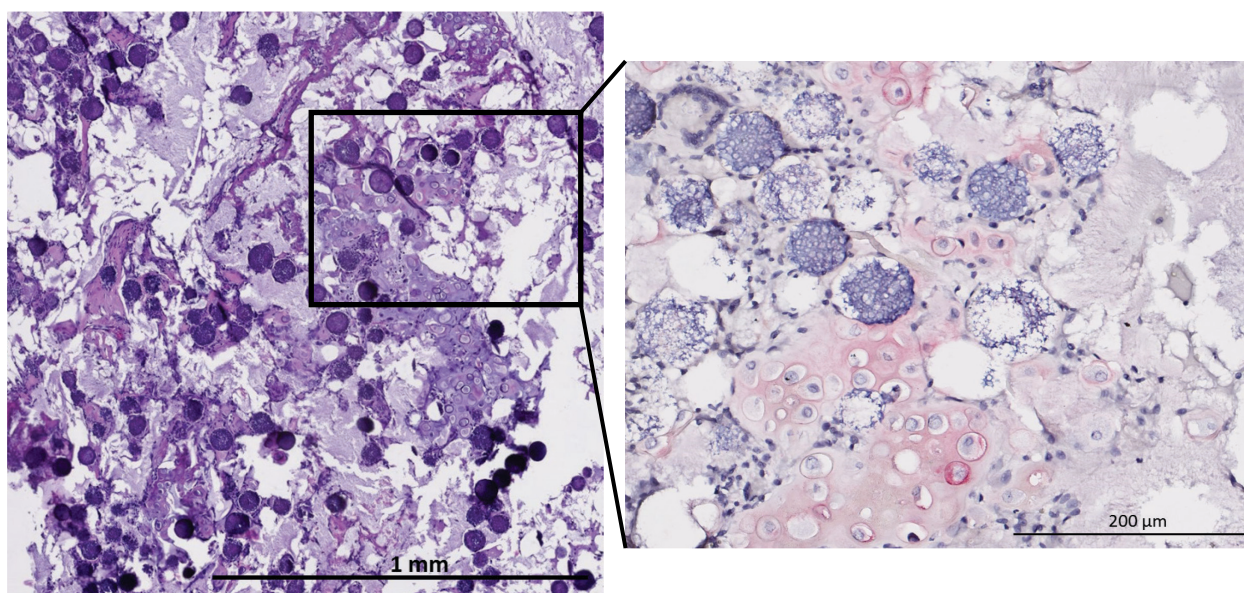
 Supplementary Figure S5. Endochondral ossification was observed within alginate composites since 4 week-period to the end of the experiment. Representative picture of alginate SLM formulation stained by H&E at 4 weeks after implantation. The magnification shows collagen II positive cells within the central region of the implant.

CHAPTER 5

INJECTABLE BMP-2 DELIVERY SYSTEM BASED ON COLLAGEN-DERIVED MICROSPHERES AND ALGINATE INDUCES BONE FORMATION IN A TIME AND DOSE DEPENDENT MANNER

D. Mumcuoglu [1,2§], S. Fahmy-Garcia[1,3§], Y. Ridwan [4,5], J. Nickel [6,7], E. Farrell [8], S.G.J.M. Kluijtmans[2]*, G.J.V.M van Osch [1,9]

1 Department of Orthopaedics, Erasmus MC, University Medical Centre, Rotterdam, The Netherlands
2 Fujifilm Manufacturing Europe B.V, Tilburg, The Netherlands
3 Department of Internal Medicine, Erasmus MC, University Medical Centre, Rotterdam, The Netherlands
4 Department of Genetics and Department of Radiotherapy, Erasmus MC, University Medical Centre, Rotterdam, The Netherlands
5 Department of Radiotherapy, Erasmus MC, University Medical Centre, Rotterdam, The Netherlands
6 Department for Tissue Engineering and Regenerative Medicine, University Hospital Wuerzburg, Germany
7 Fraunhofer IGB, Translational Centre Wuerzburg, Germany
8 Department of Oral and Maxillofacial Surgery, Special Dental Care and Orthodontics, Erasmus MC, University Medical Centre, Rotterdam, The Netherlands
9 Department of Otorhinolaryngology, Head and Neck Surgery, Erasmus MC, University Medical Centre Rotterdam, the Netherlands
§ D.Mumcuoglu and S. Fahmy-Garcia contributed equally to this work.

ABSTRACT

We aim to reduce the clinically used supra-physiological dose of BMP-2 (usually 1.5 mg/mL) that has a risk of adverse events, by using a more effective release system. We have previously developed a slow release system based on an injectable hydrogel composed of BMP-2 loaded recombinant collagen-based microspheres and alginate. In this current study, we investigate time and dose dependent subcutaneous ectopic bone formation for this system and the bone regeneration capacity in a calvarial defect model. Here, we report that BMP-2 doses 10 µg, 3 µg and 1 µg per implant (50 µg/mL, 15 µg/mL and 5 µg/mL concentration respectively) successfully induced ectopic bone formation subcutaneously in rats in a time and dose dependent manner as shown by micro CT and histology. In addition, we show the spatio-temporal control of BMP-2 retention for 4 weeks *in vivo* by imaging of fluorescently labelled BMP-2. In the subcritical calvarial defect model, micro-CT revealed a higher bone volume for the 2 µg BMP-2 per implant (50 µg/mL concentration) than the lower dose used (0.2 µg per implant, 5 µg/mL). With 50 µg/mL BMP-2 complete defect bridging was obtained after 8 weeks. The BMP-2 concentration of 5 µg/mL was not sufficient to heal a calvarial defect faster than the empty defect or biomaterial control without BMP-2. Overall, this injectable BMP-2 delivery system showed promising results at a 50 µg/mL BMP-2 concentration in both the ectopic and calvarial defect model in rats showing the potential of this composite hydrogel in bone regeneration therapies.

Key words: bone morphogenetic protein-2, slow release, injectable delivery system, ectopic bone formation model, calvarial bone defect model

INTRODUCTION

Autologous bone is widely used in bone grafting surgery. However, the limited availability of autologous bone and the discomfort related to the harvesting procedure, has diverted the field to seek for alternative methods involving biomaterials [231]. Bone morphogenetic proteins (BMP-2 and BMP-7), being successful in inducing bone formation, have been translated to clinics [194]. BMP-2 absorbed on collagen sponge has been approved by Food and Drug Administration for spinal fusion, tibial nonunions and oral-maxillofacial reconstructions [57, 58]. However, adverse events observed in clinics have limited the use of BMP-2 especially for off-label applications [63, 195, 196, 249]. These adverse events, mainly inflammation [233] and swelling [142], were associated to the supraphysiological dose of BMP-2 loaded in the collagen sponge [66] in combination with the strong burst release. Half of the loaded BMP-2 was released from the collagen sponge in the first two days *in vivo* [65]. Possibly these adverse events can be mitigated by using an appropriate release system comprising lower BMP-2 dose [234, 294]. Such a system might then broaden the potential use of BMP-2 in orthopaedic and maxillofacial surgery applications.

The dose or concentration of BMP-2 has been reported to be very important for bone formation [295-297]. Since no naturally bone-forming cells are present within the intradermal environment, subcutaneous ectopic bone can only be formed by injecting bone forming cells or by an osteoinductive protein such as BMP-2 that can recruit progenitor cells [298]. The concentration or dose of BMP-2 required to induce bone formation ectopically depends on the type of carrier material used. For example, using 5 µg BMP-2, 32% bone formation with 9 mm^3 β-tricalcium phosphate was achieved whereas hydroxyapatite with same amount of BMP-2 only formed 3 % bone in a rat ectopic model [235]. An amount of 5 µg rhBMP-2, implanted with 6 mm diameter collagen sponge, was required to induce a small intramuscular bone in mice with a maximum volume of 5 mm^3 [236]. Silk fibroin particles (10 mg) loaded with 5 µg BMP-2 induced a small volume (2 mm^3) of ectopic bone at 4 weeks in rats [237]. A low dose of BMP-2 (less than 1 µg) delivered on a collagen sponge or with brushite calcium-phosphate particles did not form bone at all in the palatal submucosa of rats [238], confirming the presence of a threshold dose. This threshold depends on the type of the material, application site and is associated with the release kinetics/ degradation time of the material and subsequent cellular infiltration rate [295].

We have previously developed an *in situ* gelling sustained BMP-2 release system that successfully induced ectopic bone formation. This hydrogel system is based on BMP-2 loaded microspheres from a recombinant protein based on collagen I (RCP) embedded in alginate. The major advantages of the developed system have been shown to be its thixotropic behaviour, resulting in easy handling and injectability, good BMP-2 release profile and good performance *in vivo* in terms of cellular infiltration, degradation and bone formation (Fahmy-Garcia *et al.*, manuscript submitted). The aim of the current study is to investigate time and dose dependent bone formation using this BMP-2 releasing hydrogel in

an ectopic bone formation model and, in addition, to test the bone regeneration capacity of two selected doses of BMP-2 in an orthotopic model. Hereto, we have subcutaneously injected formulations containing 4 different doses of BMP-2 (10 µg, 3 µg, 1 µg, 0.3 µg per implant; 50 µg/mL, 15 µg/mL, 5 µg/mL, 1.5 µg/mL concentration respectively) and an empty control subcutaneously on the dorsum of immune competent rats and followed ectopic bone formation over a time course of 10 weeks by micro-CT with histology at the end-point of 10 weeks. To study the spatio-temporal release of BMP-2 *in vivo*, formulations containing 3 different doses of fluorescently labelled BMP-2 were injected subcutaneously in rats and monitored over time course of 10 weeks by *in vivo* fluorescence imaging. Finally, two doses of BMP-2 (50 and 5 µg/mL) were further investigated in a calvarial defect model. For this purpose, 40 µL of the composite hydrogel formulation containing 2 µg BMP-2 or 0.2 µg BMP-2 was injected in 5 mm subcritical calvarial defects in immune competent rats and bone formation was studied by longitudinal imaging for 10 weeks by micro-CT.

MATERIALS AND METHODS

Materials

Recombinant protein based on human collagen I (RCP) is a product of Fujifilm, which is commercially available as Cellnest™. RCP is produced by genetically modified yeast *Pichia pastoris* in a fermentation process as described elsewhere [203, 204, 206]. RCP is a 571 amino acids protein, having an isoelectric point (pI) of 10.02 and a molecular weight of 51.2 kDa.

The recombinant human bone morphogenetic protein-2 (rhBMP-2, amino acids 283 to 396 plus an N-terminal Met-Ala) was expressed in E. coli, isolated from inclusion bodies, renatured and purified as previously described [209]. Lyophilised BMP-2 was dissolved in distilled water and the concentration was determined by UV/Vis spectrophotometry. Freshly dissolved BMP-2 was used for the experiments. For the fluorescence measurements, rhBMP-2 was fluorescently labeled using DyLight 800 (ThermoFisher Scientific, Waltham, MA, USA). For the labeling, dissolved BMP-2 solution was adjusted to pH 4.5 by addition of a 2M sodium acetate (pH 4.5) solution. Subsequently DyLight™ 800 NHS Ester, dissolved in dimethyl sulfoxide (DMSO), was added in a 5-fold molar excess and the mixture was incubated for 4 hours at 4°C while shaking. After incubation, the protein was separated from non-coupled dye by anionic exchange chromatography using a HiTrap SP HP column (GE Healthcare). Since the protein could not be eluted even at 2 M sodium chloride salt concentrations, it was recovered using an aqueous 6 M guanidinium hydrochloride solution. The protein was subsequently dialysed to 1 mM hydrochloric acid and finally to distilled water.

Pronova SLG 20 (sterile alginate where over 60% of the monomer units are guluronate) was ordered from Novamatrix (Sandvika, Norway). Hexamethylene diisocyanide (HMDIC), corn oil, sodium chloride, calcium carbonate ($CaCO_3$) and glucono delta lactone (GDL) were

purchased from Sigma-Aldrich (St. Louis, MO, USA). Ethanol, acetone and hydrochloric acid were purchased from Millipore (Billerica, MA, USA). The ELISA development kit and reagents for BMP-2 quantification were ordered from Peprotech (Rocky Hill, NJ, USA). Dulbecco's Modified Eagle's Medium (DMEM), fetal bovine serum (FBS), and penicillin-streptomycin (P/S) were ordered from Thermofisher Scientific (Waltham, MA, USA).

RCP microsphere preparation

RCP-calcium carbonate composite microspheres were produced by emulsification as described previously (Mumcuoglu *et al*., manuscript in press). Briefly, a 20% aqueous RCP solution was prepared and mixed with $CaCO_3$ fine powder (with a size of <1 µm) in a 1:1 (w/w) ratio of RCP to $CaCO_3$. This suspension was emulsified in corn oil at 50°C while stirring the emulsion at 800 rpm for 20 min. After cooling down the emulsion, the emulsified microspheres were washed three times with acetone. After overnight drying at 60°C, microspheres were sieved to 50-72 µm size using sieves (Retsch GmbH, Haan, Germany). Particles were subsequently crosslinked by hexamethylene diisocyanide (HMDIC) by mixing and stirring of 1 g of spheres, and 1mL of HMDIC in 100 ml ethanol for 1 day. Non-reacted crosslinker was removed by washing several times with ethanol. $CaCO_3$ was left in the particles since Ca^{2+} ions are used to crosslink alginate in the final hydrogel formulation. Particles were then gamma sterilised at 25 kG (Synergy Health, Etten Leur, The Netherlands).

Preparation of the RCP microsphere-alginate hydrogel formulations

SLG-20 alginate (NovaMatrix, Sandvika, Norway) was dissolved in 0.9 % sterile sodium chloride to create a 2% w/v solution. Sterile microspheres (68 mg) were incubated with 170 µL BMP-2 containing solution at 4 °C overnight. Initial BMP-2 concentrations used were 379.4 µg/mL, 113.8 µg/mL, 37.9 µg/mL, 11.4 µg/mL, to yield final BMP-2 concentrations in the hydrogel formulation of 50 µg/mL, 15 µg/mL, 5 µg/mL and 1.5 µg/mL respectively. Next day, when all BMP-2 containing liquid was absorbed, 1014 µL of the 2% w/v SLG solution was added and the swollen microspheres were resuspended. Then, 106 µL of 0.06 M fresh glucono delta lactone (GDL) solution was added and mixed immediately. GDL was used to dissolve minute amounts of $CaCO_3$ thereby crosslinking alginate and increasing the mechanical property of the formulation. The formulations were thoroughly mixed passing through 19 G needle immediately after addition of all components and stored overnight at 4 °C to equilibrate. Next day, the prepared formulations were mixed again prior to experiments.

In vitro *release of BMP-2 from hydrogel formulations*

Hydrogel formulations were prepared as described above containing either fluorescently labelled or wild-type BMP-2. Then 200 µL of each hydrogel was added to each well of 24 well plate inserts with 0.4 µm pore size. 1 mL DMEM with 10% FBS and 1 % P/S per well was

added to the reservoir plate. The plates were incubated at 37 °C under constant agitation at 300 rpm. At each time point, all medium (1 mL) was collected from the reservoir plate and changed with fresh medium (1 mL). Positive controls were 10 µg, 3 µg or 1 µg wild type or fluorescently labelled BMP-2 in 1 mL DMEM medium. At every time point, 100 µL of these positive controls was sampled. The collected release media and control samples were analysed by the rhBMP-2 ELISA development kit according to manufacturer's protocol. To calculate the fraction released at each time point, the concentrations detected in the release medium of the hydrogel samples were normalised to the concentrations of the positive controls to correct for loss by adsorbance to the tube and/or degradation of the protein.

Study design and ethics

All animal experiments were performed with prior approval of the Erasmus Medical Centre ethics committee for laboratory animal use (project number: AVD101002015114 and protocol numbers: EMC 15-114-03 and EMC 15-114-04). 10 week old male Sprague Dawley (SD) rats (Charles River) were used. The animals were randomly assigned and housed in pairs in specific pathogen free (SPF) conditions and allowed to adapt to the conditions of the animal house for 7 days before implantation. The animals were maintained at 22 ± 5°C on a 12 h dark/light cycle with *ad libitum* access to standard rat chow and water. At 10 weeks after implantation, animals were euthanised with CO_2 and the specimens were harvested for micro-CT analysis and histology.

Subcutaneous injection of *in situ* gelling formulations to study ectopic bone formation

To evaluate the effect of different doses of BMP-2 on ectopic bone formation, the hydrogel compositions were subcutaneously injected (total volume 200 µL per injection) in the dorsum of the rats (20 rats in total). Each animal received 4 or 5 randomly assigned injections. All injections were performed on animals under isoflurane inhalation. To study the BMP-2-dose effect on bone formation, four different BMP-2 concentration were used (50, 15, 5, 1.5 µg/mL) resulting in total doses of 10 µg, 3 µg, 1 µg and 0.3 µg BMP-2 per implant (n=8 per group), respectively. As a control, alginate with microspheres but without BMP-2 was injected (n=6). To investigate the spatio-temporal distribution of BMP-2 in the implanted material *in vivo*, 200 µL hydrogel containing fluorescently labelled BMP-2 was injected at different doses: 10 µg, 3 µg and 1 µg (n=6). Longitudinal imaging was performed by microCT and IVIS biweekly until the end of the experiment (10 weeks).

Calvarial defect model to study bone regeneration with *in situ* gelling formulations

To evaluate the effect of two hydrogel formulations with a selected dose of BMP-2 on orthotopic bone formation, two defects of 5 mm diameter were created in the rat calvaria (18 rats in total). Prior to the surgery, animals received intraperitoneal injections of 0.05 mg/kg of buprenorphine (Temgesic®, Indivior, UK) and 5 mL/kg sterile normal saline to

account for fluid loss. Surgeries were performed under 2.5% isoflurane anesthesia. The animal skulls were shaved and disinfected with ethanol swabs. Then, an incision was made through the skin of the calvarium and the periosteum, and full-thickness flaps were reflected. The defect was irrigated with 0.1 ml of 1% xylocaine with 1:200000 epinephrine (AstraZeneca, NL) along the sagittal midline of the skull. Under copious sterile saline irrigation, two 5-mm-diameter bone defects were prepared using a micro trephine drill with 5 mm diameter (Fine Science Tools, Germany) in each animal and any visible debris or bone chips were removed. Then, 40 μL of hydrogel formulation with BMP-2 or, as a control, without BMP-2 was injected into the defect. As sham control, empty defects were used (5 rats, 10 defects). As a biomaterial control alginate with microspheres were injected to the defects (5 rats, 10 defects). Alginate with microspheres loaded with 50 μg/mL BMP-2 (3 rats, 3 defects) was used to study healing with a high dose; alginate with microspheres loaded with 5 μg/mL (5 rats, 10 defects) was used to study healing with a low BMP-2 dose. The animal number of the 50 μg/mL BMP-2 cohort was kept small because it was expected to induce bone formation based on our results of ectopic bone formation study. After implantation, the periosteum and the skin above the defects were repositioned and sutured with polylactic acid sutures (Vycril 4.0, Ethicon, Johnson Prod., São José dos Campos, Brazil). All animals received three postoperative doses of buprenorphine for analgesia every 10 h during the next three days. Longitudinal imaging was performed biweekly by micro-CT until 10 weeks. At 10 weeks after implantation, animals were euthanised with CO_2 and the specimens were harvested for micro-CT analysis and histology. To reduce the number of experimental animals, this study was combined with another study and the biomaterial only and 50 μg/mL BMP-2 groups were used as controls for that other study (Fahmy-Garcia et al, in preparation).

Micro-CT imaging

Micro-CT (Quantum FX , Perkin Elmer, Waltham, MA, USA) was used to image animals after 1 week, 2 weeks, 4 weeks, 6 weeks, 8 weeks, 10 weeks after injection and also to image the implants retrieved at 10 weeks. To image the ectopic bone *in vivo* the following parameters were used: Field of view: 73mm, Voltage: 90kV, Current: 160 μA, Scan Time: 120 sec. To image the ectopic implants field of view of 20 mm, scan time of 120 sec. was used. To image the calvarial defects a 30 mm field of view, scan time of 3 min. was used. The trabecular and cortical bone mineral density (BMD) was determined on the basis of calibration scanning, using two phantoms with known density (0.25 g/cm^3 and 0.75 g/cm^3 ; Bruker MicroCT) measured under identical conditions. For image processing, Analyze software version 11.0 was used (Mayoclinic, Rochester, MN, USA). Threshold levels were set to 0.11 g/cm^3, 400 Hounsfield units.

Fluorescence imaging *in vivo*

An IVIS Imaging System 200 (Perkin Elmer, Waltham, MA, USA) was used to image fluorescent BMP in the animals immediately after the injection, at 3 days, 1 week, 2 weeks, 4 weeks, 6 weeks, 8 weeks and 10 weeks after injection. Imaging parameters were set to: exposure time 20 sec, excitation 745nm, emission 820nm and 840nm. For the image analysis, the region of interest was selected as circles of 3.0 ±0.1 cm^2 area for each implant and total the radiant efficiency [p/s] / [µW/cm²] was calculated by the Living image® software (PerkinElmer, Waltham, MA, USA). As a region of interest 3 cm^2 area was selected since this was the magnitude of area where signal was detected directly after injection.

Histology

For histological analysis of the subcutaneous ectopic bone formation, specimens were fixed in 4% formalin solution and decalcified with 10 % EDTA for 2-4 weeks. Implants were dehydrated and embedded in paraffin. Sections of 6 µm in thickness were prepared using a Leica microtome (Wetzlar, Germany) and mounted on subbed glass slides (Thermofisher Scientific, Waltham, MA, USA). Three cross sections of at least 200 µm apart from each other were collected from each implant. The sections were de-paraffinised and rinsed with distilled water to be stained with hematoxylin and eosin (H&E). The sections were imaged by NanoZoomer-XR (Hamamatsu, Japan).

Statistical analysis

The quantitative micro-CT data of *ex vivo* samples were analysed using one-way analysis of variance (ANOVA) and a Bonferroni post-hoc multiple comparison test. *In vivo* calvaria micro-CT data were analysed using two-way analysis of variance (ANOVA) and a Bonferroni post-hoc multiple comparison test. A value of *p < 0.05* was considered to be statistically relevant. Linear regression analysis of micro-CT data was done by Graph-pad to analyse the time dependent bone formation.

RESULTS

**BMP-2 was retained for at least four weeks *in vivo***

To monitor the retention of BMP-2 *in vivo*, composite hydrogels (alginate with RCP microspheres) with three different doses of fluorescently labelled BMP-2 were used. First, we confirmed *in vitro* that the release of fluorescently tagged (fluo) BMP-2 from the hydrogels was similar to wild type BMP-2 (Figure 1). The difference between the release of the two proteins was less than 10 % showing that labelled protein can be used to study retention of BMP-2 in vivo. Then, the fluorescence signal (shown as radiance efficiency) of the 3 doses injected subcutaneously was followed *in vivo* by fluorescence imaging. As shown in Figure 2, the fluorescence signal generated by the three different BMP-2 doses decreased until week 4. After 4 weeks, all fluorescence curves levelled off. Interestingly, the

fluorescence values did not drop to the background value indicating the presence of some remaining BMP-2 in the hydrogels. The curves corresponding to different doses were not significantly different due to high variation between animals.
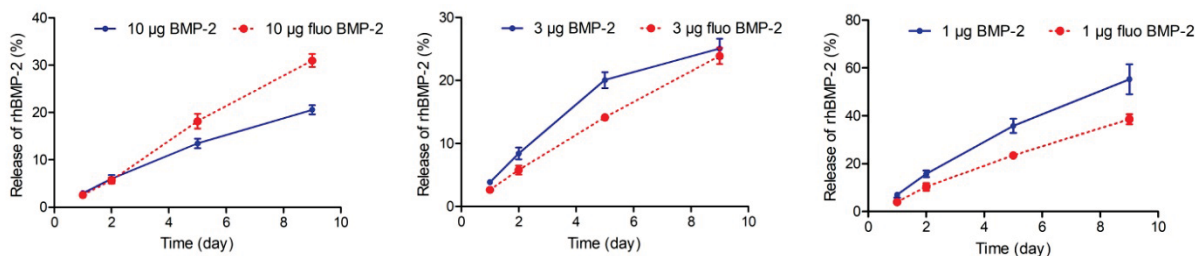
Figure 1. *In vitro* release of fluorescently labelled and non-labelled BMP-2 from the RCP microspheres with alginate hydrogel, showing no major difference between labelled and non-labelled BMP-2 release *in vitro* in DMEM with 10% FBS, 1%P/S.
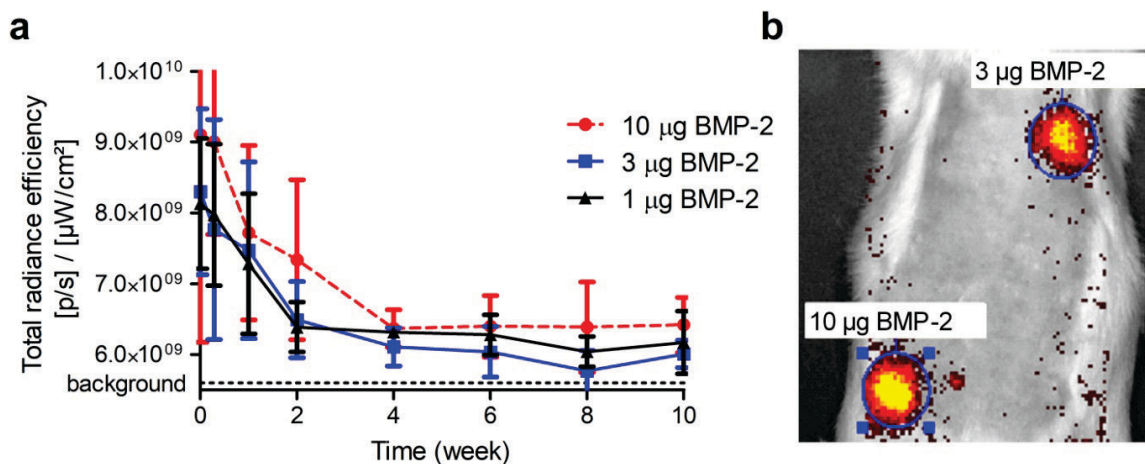

Figure 2. (**a**) BMP-2 is retained in RCP microspheres with alginate hydrogels *in vivo* for at least 4 weeks. The total radiance efficiency of the fluorescence signal is shown for three different doses of fluorescent BMP-2 (10µg, 3 µg and 1 µg) containing RCP microspheres with alginate that were injected subcutaneously in Sprague-dawley rats (n=6 injections). (**b**) Representative image of *in vivo* fluorescence imaging.

Microspheres with alginate hydrogel induced BMP-2 dose dependent ectopic bone formation

The effect of the BMP-2 dose on subcutaneous ectopic bone formation was investigated over a time period of 10 weeks using 4 different BMP-2 doses (representative micro CT images are shown in Figure 3a). At the end point of 10 weeks, the bone volume clearly was found to be dose dependent (Figure 3b). The highest dose of 10 µg (50 µg/mL concentration) induced the largest volume of ectopic bone, while the lowest doses of 0.3 µg

(1.5 µg/mL) and 0 µg BMP-2 failed to form bone. The composite hydrogel containing 1 µg BMP-2 (5 µg/mL), forming just a minute volume of bone, is the threshold to induce ectopic bone in rats. The bone mineral density, did not differ significantly (Figure 3c): 0.5 g/cm^3 density for 3 and 10 µg BMP-2 and 0.35 g/cm^3 for 1 µg BMP-2. For comparison tibia of animals were extracted and imaged using the same instrumental settings. The cortical bone of the tibia had a density between 1.2-2.0 g/cm^3 and the trabecular bone had a density between 0.15-0.5 g/cm^3 showing that ectopic bone formed subcutaneously had a density in the range of trabecular bone.
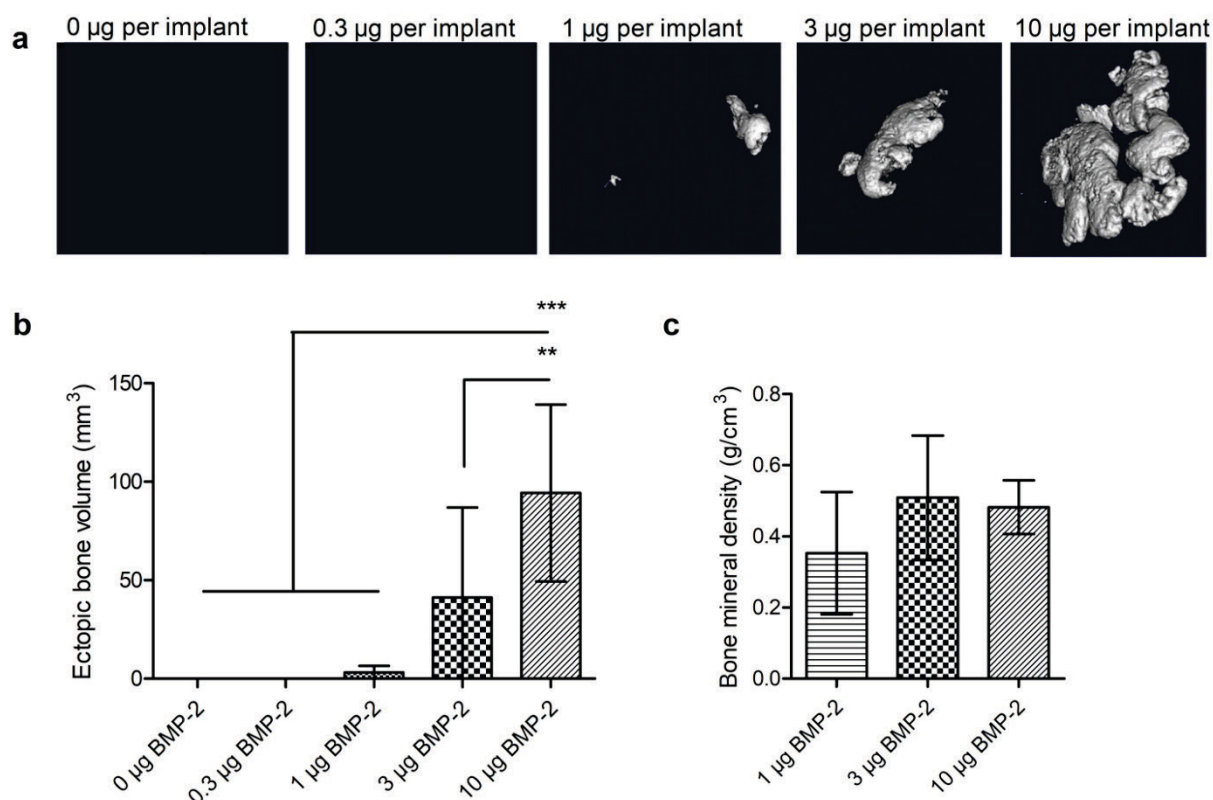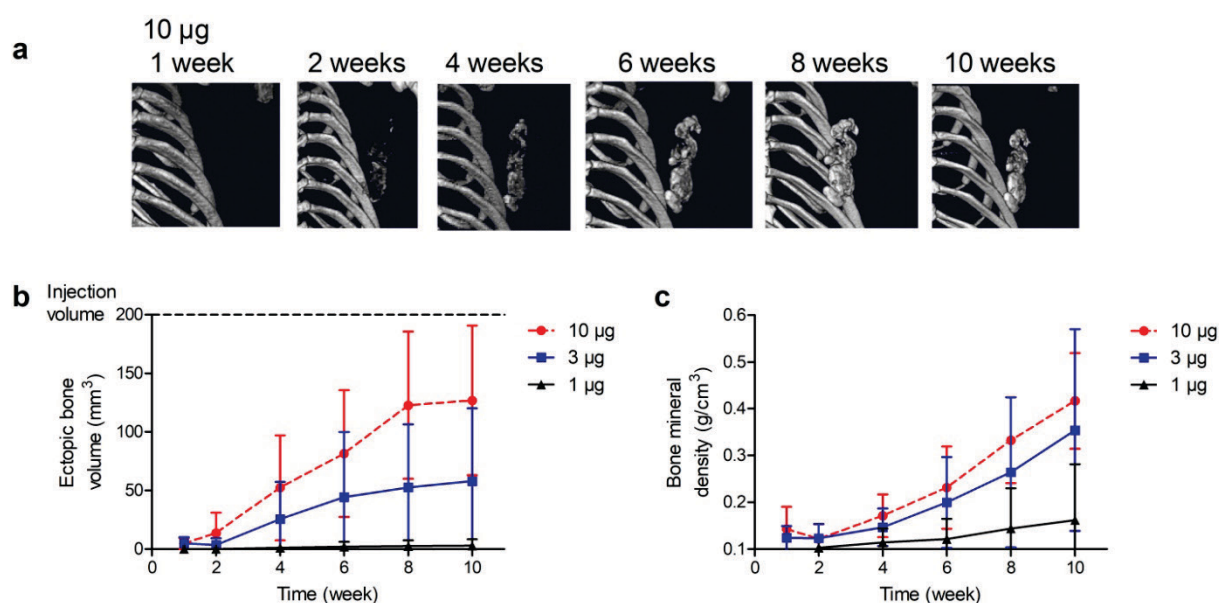

Figure 3. Ectopic bone formation at 10 weeks is BMP-2 dose dependent. (**a**) Representative images of microCT of implants retrieved at 10 weeks. (**b**) The volume of ectopic bone in mm^3. (**c**) Bone mineral density after thresholding to 0.11 g/cm^3, 400 Hounsfield units. Four different doses of BMP-2 (10µg, 3 µg, 1 µg, 0.3 µg, 0 µg) containing RCP microspheres with alginate (200 µL) were injected subcutaneously in Sprague-dawley rats (n=8 injections). Data is shown as mean ± SD, one-way ANOVA was performed to compare treatment groups, asterisk *** p<0.05, *** p<0.001* shows statistical significance.

Microspheres with alginate hydrogel containing different doses of BMP-2 showed different kinetics of bone formation

Longitudinal micro-CT imaging of rats for 10 weeks revealed a dose dependent rate of ectopic bone formation (Figure 4a and 4b). The volume of ectopic bone in the 10 µg BMP-2 group increased linearly between 1 week and 8 weeks with a rate of 16.9 ± 0.8 mm^3/week ($r^2=0.99$), after which a plateau was reached. In the 3 µg BMP-2 group, a two phase linear trend was observed. Between 2 and 6 weeks, a linear increase of bone volume with a rate of 10.2 ± 0.5 mm^3/week ($r^2=0.99$) was found, while a slower linear trend was observed between 6 and 10 weeks with a rate of 3.4 ± 0.4 mm^3/week ($r^2=0.99$). Although the amount of ectopic bone formed by 1 µg BMP-2 was very small with a volume of only 3.0 ± 5.5 mm^3 (mean $\pm$ SD) at week 10, the bone volume linearly increased between 1 week and 10 weeks (rate=0.36 ± 0.1 mm^3/week, $r^2=0.96$).

Significant mineralization could be observed after two weeks (Figure 4c). A linear increase in bone density was observed for 10 µg BMP-2 between 2 weeks and 10 weeks with a rate of 0.025 ± 0.002 g/cm^3 per week ($r^2=0.98$). In contrast to the bone volume, the mineral density did not reach a plateau at 10 weeks suggesting that mineralization can continue for longer than 10 weeks. Similar to 10 µg, 3 µg BMP-2 showed a linear increase between 2 and 10 weeks with a rate of 0.019 ± 0.002 ($r^2=0.96$). The 1 µg BMP-2 comprising hydrogel clearly mineralised slower than the other two doses with a rate of only 0.005 ± 0.001 ($r^2=0.97$).

Figure 4. Ectopic bone volume and density increase over time course of 10 weeks is BMP-2 dose dependent. (**a**) Representative micro-CT images of bone formed by 10 µg BMP-2 over 10 weeks. (**b**) The volume of ectopic bone in mm^3 after thresholding. (**c**) Mineral density of bone in g/cm^3 after thresholding. Threshold was set to 0.035 g/cm^3 to discriminate mineralised tissue from soft tissue. Five different doses of BMP-2 (10µg, 3 µg, 1 µg, 0.3 µg, 0

μg) containing RCP microspheres with alginate were injected subcutaneously in Sprague-dawley rats (n=8 injections). Data is shown as mean ± SD. Since 0.3 μg and 0 μg BMP-2 did not form any bone, they are not represented in this figure.

Ectopic bone formation confirmed by histology

The morphology of ectopic bone induced by five different doses of BMP-2 (10 μg, 3 μg, 1 μg, 0.3 μg, 0 μg) containing hydrogel was evaluated by histology at 10 weeks. As seen in Figure 5 bone tissue could be identified for the 10 μg, 3 μg, and 1 μg BMP-2 comprising hydrogels and no bone was found for the two lowest doses of 0.3 μg and 0 μg. The area of ectopic bone was the largest for the 10 μg samples (Figure 5), thereby confirming the CT data (Figure 3). Interestingly, for all BMP-2 doses, remnants of microspheres and gels could be observed indicating that the implants were not yet fully degraded at 10 weeks. This result is in line with the long term retention of BMP-2 as observed by fluorescence imaging. Bone formation was not only observed at the periphery of the hydrogel but also in some samples within the hydrogel construct. Microspheres were also observed within the hydrogel construct. Some of the microspheres were intact, some were infiltrated with cells. The microspheres which were infiltrated changed the spherical morphology probably as a sign of degradation. Small ossicles were detected around some microspheres. Around the implants, a layer of fibrous tissue was also observed which is a typical foreign body response upon implantation [299].

Microspheres with alginate hydrogel containing 50 μg/mL BMP-2 induced bone formation in a rat calvarial defect model

The regeneration capacity of the composite hydrogels with BMP-2 was tested in a subcritical-sized calvarial defect model. Hereto, biomaterial only, 5 μg/mL BMP-2 loaded biomaterial or 50 μg/mL BMP-2 loaded biomaterial were injected into a 5 mm calvarial defect and empty (sham) was used as a control (Figure 6a). The bone volume of 50 μg/mL BMP-2 was significantly higher than all other groups (Figure 6b), showing the regenerative capacity of this 50 μg/mL concentration of BMP-2 in the composite hydrogel formulation. The low concentration (5 μg/mL) did not form any additional bone compared to the biomaterial only or empty (sham) control. Interestingly, the bone volume of the empty defect was slightly higher at week 2 compared to the biomaterial only, albeit the difference was not statistically significant. At the end of the experiment, biomaterial and empty groups produced similar bone volumes. The bone mineral density gradually increased over time (Figure 6c). At week 2, 50 μg/mL BMP-2 group had a lower density compared to 5 μg/mL BMP-2 group. This effect reversed later at week 8 and 10, 50 μg/mL BMP-2 induced higher density compared to 5 μg/mL BMP-2 treated group.
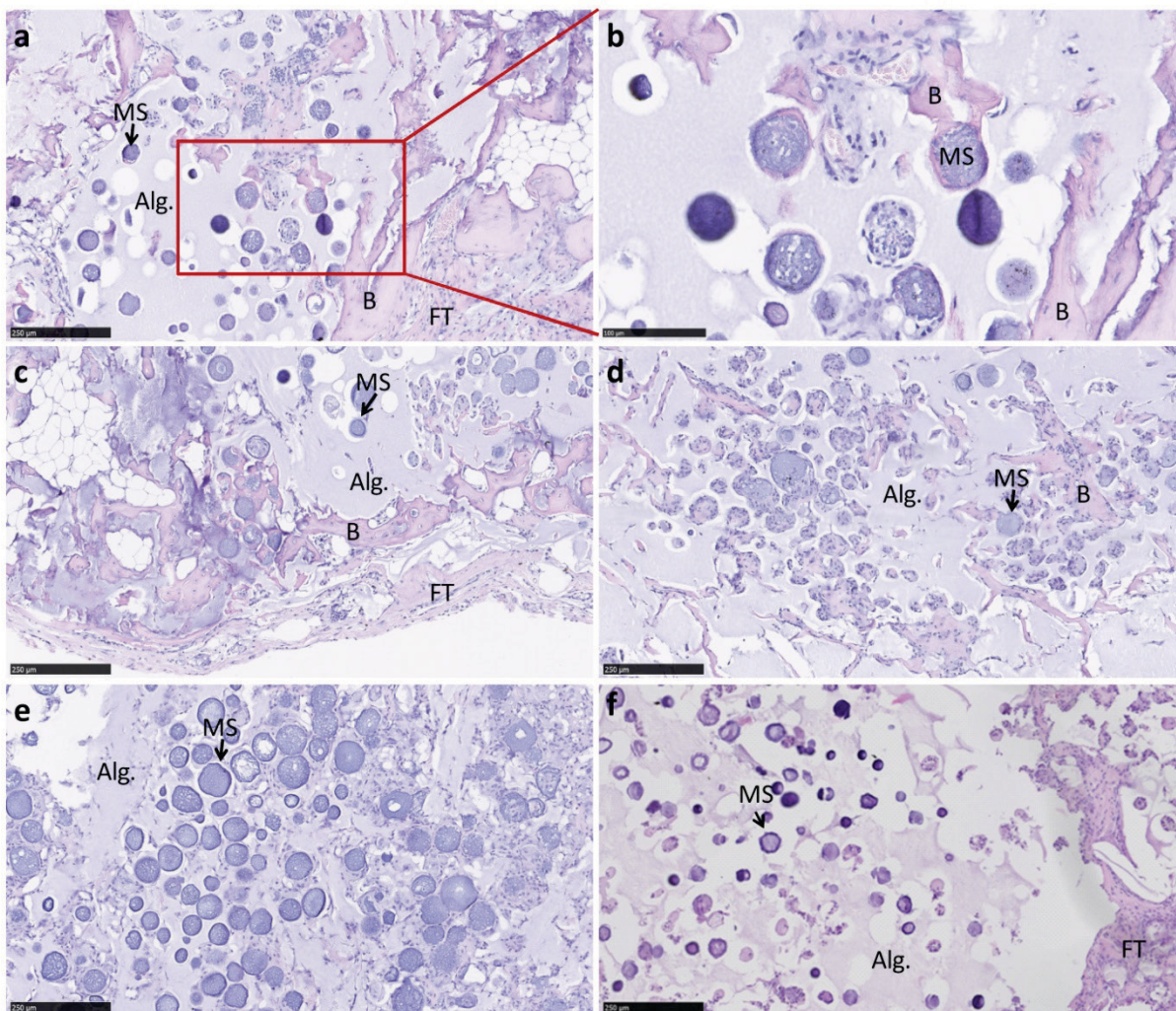
Figure 5. BMP-2 concentration dependent bone formation of alginate-RCP hydrogels was confirmed by histology. H&E staining revealed ossification for (**a**) 10 µg, (**c**) 3 µg, (**d**) 1 µg, while no bone was observed for (**e**) 0.3 µg, and (**f**) 0 µg BMP-2. (**b**) A closer representation of 10 µg BMP-2 sample showing bony tissue around microspheres. RCP microspheres (MS), alginate hydrogel (Alg.), bone formation (B), and fibrous tissue (FT) are indicated. Scale bar is 250 µm for a,c,d,e,f and 100 µm for f.

DISCUSSION

The aim of this study was to investigate whether a slow release system can be used to lower effective BMP-2 dose. In addition, we aimed to investigate the effect of the BMP-2 dose delivered by an *in situ* gelling hydrogel formulation on ectopic bone formation and, investigate the bone repair capacity of two selected doses of BMP-2 in a bone defect model. The composite hydrogel provided sustained release of BMP-2 for 4 weeks as shown *in vivo* by fluorescence imaging making use of fluorescently tagged BMP-2. Ectopic bone was formed for three different doses of BMP-2 (50, 15 and 5 µg/mL in a 200 µL implant) in a dose and time dependent manner, the highest BMP-2 dose showing the fastest bone

growth and highest bone volume at 10 weeks. The bone-forming dose of 50 µg/ml (2 µg per implant in a 5mm defect) in the ectopic model was confirmed to be also effective in a subcritical calvarial bone defect model.
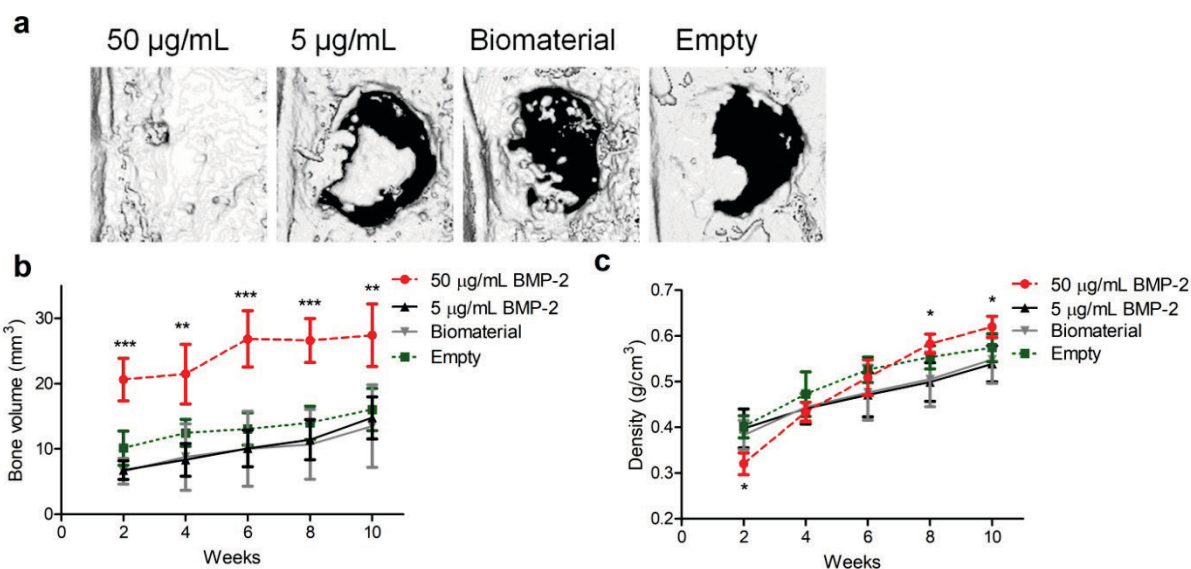
Figure 6. (**a**). Representative micro-CT images of calvaria (superior view) at week 10 after surgery and implantation. (**b**). Bone volume showing the regeneration of calvaria defects over 10 weeks. The bone volume of 50 µg/mL BMP-2 containing biomaterial was significantly higher at all time points compared to 5 µg/mL BMP-2, biomaterial and empty groups (*** p<0.01* or **** p<0.001*). (**c**). Bone density showing the regeneration of calvaria over 10 weeks. Bone density induced by 50 µg/mL BMP-2 was lower than that of 5 µg/mL BMP-2 group at week 2 (** p<0.05*). At week 8 and 10, density of induced bone tissue was higher in 50 µg/mL BMP-2 than 5 µg/mL BMP-2 group (** p<0.05*). Treatment groups were empty control (n=10), biomaterial only (n=10), 5 µg/mL BMP-2 containing biomaterial (n=10) and 50 µg/mL BMP-2 containing biomaterial (n=3). Data is shown as mean ± SD, two-way ANOVA was performed to compare treatment groups.

The BMP-2 delivery system used in this study was selected based on a previous study where a hydrogel composed of SLG alginate and BMP-2 loaded RCP-microspheres provided superior ectopic bone formation compared to other hydrogel formulations (Fahmy-Garcia *et al.*, manuscript submitted). The advantages of this delivery system are the easy handling due to its thixotropic behaviour, sustained BMP-2 release profile and the presence of cell attachment sites by the use of the RCP microspheres. In our current study, we show that *in situ* gelling hydrogel composite successfully regenerates bone with a concentration of 50 µg/mL BMP-2 (2 µg per implant in a 5 mm defect). In other preclinical studies with BMP-2 carriers, the BMP-2 dose needed to heal critical sized defect was generally higher; in a rat calvarial model similar to our model, complete healing of the defects was achieved with PLGA membranes adsorbed with 5 mg/mL of BMP-2 [300]. In another study using a 8 mm

rat calvarial model, 0.5 µg and 1 µg BMP-2 per implant delivered with gelatin particles did not result in complete bone bridging [301]. Partial healing of 8 mm rat calvarial defects of approximately 20% and 60% was observed with a composite comprising segmented polyurethane, poly[lactic-co-glycolic acid], and β-tricalcium phosphate loaded with 1.6 µg and 6.5 µg rhBMP-2, respectively [302]. Besides, other BMP-2 carriers in general induced lower ectopic bone volumes. For example, silk fibroin (2 mm^3) [237] and collagen sponge (5mm^3) [236] formed max 5 mm^3 ectopic bone using 5 µg BMP-2, which is lower than 41 mm^3 induced with 3 µg (15 µg/mL) BMP-2 in our ectopic model. Considering these earlier studies, our study shows that the *in situ* gelling formulation of RCP microspheres with alginate is a promising BMP-2 delivery system that might reduce the required effective dose of BMP-2 and thus potentially mitigate the adverse effects of BMP-2.

Besides the required threshold or effective dose of BMP-2 to induce bone formation, the hydrogel matrix also affects the bone formation process to which characteristics of the biomaterial, such as release, integrity, degradation and cell infiltration, should be aligned. Factors such as speed of bone formation, amount and location of the formed bone are important to be considered. The natural fracture healing process occurs around 4 weeks in rodents, [44] and it can take up to 3-4 months in humans [303]. In our ectopic model, the kinetics of bone formation was shown to be linear for the 10 µg BMP-2 group between week 1 and week 8, while the main release of BMP-2 was observed in the first 4 weeks, both processes matching the time frame of natural bone healing processes [41]. Interestingly, after 4 weeks, a small portion of BMP-2 was retained inside the hydrogel probably due to the strong interaction between BMP-2 and RCP microspheres as shown earlier (Chapter 3). This portion of BMP-2 will only be released upon further degradation of the material and could probably contribute to the bone volume increasing also after 4 weeks. With 10 µg BMP-2, ectopic bone volume reached a plateau at 8 weeks. This suggests that bone formation can be confined to the hydrogel area. Therefore this hydrogel formulation might eliminate the risk of excessive surrounding soft tissue calcification, which is a major concern in currently used BMP-2- based therapies [66].

Our ectopic model results indicated that hydrogels containing 3 µg and 10 µg BMP-2 are not only forming bone at the periphery of the implants but in the entire implant. Qualitative analysis of 3D micro-CT images revealed that the bone formation started at different locations throughout the implant around week 2. These results corroborate our previous findings (Chapter 4) that the hydrogel allows bone forming cells to infiltrate the gel at early time points.

Interestingly, hydrogels without or with a very low dose of BMP-2 seem to slightly, though not significantly, impede bone formation in the calvarial defect model at the early time points when compared to the empty control. After 10 weeks it was not different from the empty control. It is possible that empty defect induces higher initial inflammation and faster infiltration of inflammatory cells compared to RCP microspheres with alginate and therefore

the healing process starts earlier. Alginate is known for poor cell attachment [304, 305]. Possibly, alginate slightly delays cell infiltration compared to natural bone healing environment where there is fibrin clot hosting the infiltrated cells. These effects can be examined in a future study. However, as differences did not reach statistical significance and the endpoint healing for both groups was similar, we do not expect an inhibitory effect of the hydrogel matrix in overall bone healing. Overall, the benefit of having a slow release system outweighs this minor effect since the BMP condition healed much better than the control.

CONCLUSION

The injectable slow release BMP-2 delivery system resulted in a time and dose dependent bone formation in an ectopic and orthotopic model. This delivery system composed of alginate and RCP microspheres, provides sustained release of BMP-2, provides cell attachment and induces bone formation at a relatively low dose of BMP-2, making it promising for bone regeneration therapies.

ACKNOWLEDGEMENT

CHAPTER 6

DISCUSSION AND FUTURE PERSPECTIVES

In situations where self-healing of bone is insufficient, for example in non-unions or delayed unions, a surgical procedure using bone grafts is necessary. Due to the limited availability of autografts and the disease transmission risk associated to the use of allografts [306], the bone tissue engineering field has been seeking for alternatives. The choice of biomaterials and other components such as drugs or cells is important for the design of a successful bone tissue engineering construct [6]. Although each strategy has advantages and drawbacks, we have chosen a cell-free approach using only biomaterials and a growth factor. Cell-free systems are generally less costly and easier to be translated to the clinics [307]. Furthermore, we have chosen for bone morphogenetic protein-2 (BMP-2) as a growth factor because it is an FDA approved growth factor for bone regeneration and its effect on bone formation is well known[58]. As a BMP-2 carrier, we have used microspheres based on a recombinant protein derived from collagen I (RCP). Collagen I is the major organic extracellular matrix (ECM) component in bone. We aimed to design and compare different compositions of biomaterials in terms of BMP-2 release profile and bone regenerative capacity with a final goal to develop formulations that can induce or augment bone healing. In this design, we chose a simple approach to load the spheres by adsorption. As explained in chapter 2, adsorption is an easier process to be translated to the clinic compared to encapsulation or covalent linking in terms of handling and process control. This approach appeared to be successful in retaining BMP-2 due to a specific interaction between RCP and BMP-2 as described in Chapter 3. This interaction between RCP and BMP-2 has similar affinity constants as that of between BMP-2 and glycosaminoglycans [308]. In the study of Grunert *et al.* and in our study, both affinity constants were in the nanomolar range [104]. We then investigated the effectiveness of these BMP-2 loaded microspheres *in vivo* in a subcutaneous ectopic bone formation model. In this much more complex environment many other factors play a role as discussed later in this chapter. After the observation that the microsphere paste yielded only small amounts of bone, we designed a hydrogel scaffold to deliver the microspheres. The role of the hydrogel was to create a platform for the regenerating cells and also to confine the BMP-2 loaded microspheres *in situ*. In particular, alginate proved to be successful as a delivery hydrogel. We have shown that alginate further slowed down the release of BMP-2 and decreased the degradation rate of the RCP spheres to match the time frame of the bone formation process. In our study, a 5 mm calvarial defect completely healed using 50 µg/mL concentration of BMP-2 (2 µg per implant); thus, we reach the aimed bone volume (27 mm^3) with this concentration (chapter 5). The same concentration in the ectopic bone model induced around 100 mm^3 bone which was half of the injection volume. In a study where these models have both been employed, a composite implant of poly(lactic-co glycolic acid)/poly(propylene fumarate)/gelatin with 6.5 µg BMP-2 completely healed a 5 mm femoral defect [309]. However, it only induced 4 mm^3 ectopic bone volume of the 50 mm^3 implant in a subcutaneous ectopic model.

In order to further develop our formulations, we discuss **how the material properties can be adjusted for a better *in vivo* performance**. Several factors such as degradation rate,

interaction with the matrix, mechanism of drug release, host environment, carrier geometry contribute to the *in vivo* performance of a material, as indicated by Li *et al.* [65]. Here, some of these parameters are discussed in the light of our biomaterial.

Degradation rate

The material degradation rate has a huge effect on the regeneration of new tissue [310]. Non-degradable materials such as solid titanium implants do not allow tissue regeneration. If the scaffold degrades too slowly it might inhibit bone formation and delay the repair. Materials with insufficient interconnecting pores and a slow degradation rate possess a risk of encapsulation by a bony shell and as a result to become isolated from the remodelling process[65]. On the other hand, quickly degraded materials will not serve as a good scaffold for the regenerating tissue and will not support migrating cells.

Therefore, modulation of the timing of degradation is very crucial. This is also shown for our initial delivery system consisting of bare RCP microspheres carrying BMP-2 (Chapter 3b). The RCP microspheres that carried no BMP-2 or a low dose BMP-2 could not be retrieved at all at the end of the experiment (week 12) because they were fully degraded while no bone was formed. This confirms the results of Parvizi showing that non-loaded thermally crosslinked RCP microspheres were degraded mostly in the first month after subcutaneous injection [311]. Although we have not analyzed degradation by histology at early time points, our results point towards premature degradation of the microspheres. Due to this fast degradation, BMP-2 might have been released too rapidly and this resulted insufficient recruitment of progenitor cells. As a result, there was even a decline in the ectopic bone formation after 6 weeks, indicating that in the absence of a scaffold and a growth factor bone can start to resolve in a subcutaneous ectopic environment. Upon addition of an alginate hydrogel to the system (chapter 4 and 5), we detected some microspheres even at the end of the experiment at week 10, showing that alginate decreased the degradation time of the RCP microspheres compared to the bare microsphere formulation. Alginate apparently shielded the microspheres from quick invasion by cells and subsequent degradation. It is known that alginate hydrogels alone have variable degradation rates depending on the crosslinking degree, molecular weight and concentration [312]. In our system, the ionically crosslinked alginate matrix was only partially degraded at week 10. The higher ectopic bone volume obtained with the alginate hydrogel formulations in chapter 4, and the complete healing of the calvarial defect in chapter 5 suggests that the degradation rate of these formulations is matching well with the speed of the bone regeneration process.

Interaction with the matrix

Interactions of cells with the provided biomaterial matrix are extremely important because progenitor cells and inflammatory cells need to be recruited and reside at the regeneration site [313]. The recruited cells need a suitable microenvironment to be able to proliferate

and differentiate towards bone forming cells [314]. ECM proteins such as collagen can be suitable biomaterials for bone tissue engineering since collagen is the major component of bone organic matrix. Besides its function as cell attachment site, the biomaterial could serve as a matrix to bind secreted factors. This is important to maintain the activity of secreted factors in a regenerating tissue [315]. In our studies we used three types of biomaterials; recombinant peptide based on collagen I (RCP), alginate, and thermoresponsive, PNIPAAM modified hyaluronic acid.

In Chapter 4 and 5, it was clear that cells preferably attached to the RCP microspheres but not the alginate hydrogel. The presence of multiple RGD sequences in the collagen I derived protein most probably enhances the 'attractiveness' of the microspheres to adhere to. Interestingly, in the calvarial defect model the formulation with alginate and non-loaded microspheres (*i.e.* without BMP-2) even seemed to delay bone formation compared to an empty defect (Chapter 5). This can be a result of the lack of interaction between alginate and the cells. Cells in general can infiltrate into an alginate gel depending on the porosity of the gel [316], but cell attachment to the alginate gel is very poor [304, 305]. On the other hand, as we have seen in chapter 3b when only microspheres were injected, the paste was degraded too quickly as a result of the strong interaction between cells and the microspheres, which negatively affected the bone formation process. These results suggested that fine-tuning of the cellular infiltration rate is important for successful bone formation.

Interestingly, the hyaluronic acid formulation failed to induce bone formation (chapter 4). This result was further explored by investigating the infiltration of macrophages. Macrophages increased over time in the hyaluronic acid formulation, indicative for a progressing inflammatory reaction. On the other hand, in the SLG alginate formulation the number of infiltrated macrophages decreased over time. There might be two main reasons why hyaluronic acid failed to induce bone formation. Firstly, it retained most of BMP-2 as shown in the *in vitro* release experiments. Secondly, the timing of the inflammation did not match with the timing of bone formation process. It is known that inflammation is predominant typically in the first week of bone healing [44]. Therefore, this prolonged inflammation might have inhibited bone formation. However, the reason for the different inflammatory response to alginate and hyaluronic acid is yet to be elucidated.

Drug release profile

To obtain a sustained release profile and to control the initial burst release, the drug delivery material can be modulated [317]. In our case the BMP-2 release profile was altered by changing the particle characteristics (Chapter 3a). We have shown that the crosslinking method and the size of RCP particles influenced the release of BMP-2. Small-sized RCP microspheres had only 30 % release *in vitro* in the first two weeks and the rest of BMP-2 could only be released by degrading the particles. In addition, the interaction between the

drug and the matrix contributes to the resulting release profile. In our study, a specific interaction based on intermolecular forces occurs between BMP-2 and RCP (chapter 3). Due to this affinity of BMP-2 to the RCP matrix and its resulting *in vitro* release profile, we have hypothesized that microspheres can be a potential system to deliver BMP-2 and to induce bone formation. However, the *in vitro* release profile is not the only factor indicative for the effectiveness of the delivery system. The intrinsic degradation rate of the material and the host response are the two main contributors to the release profiles *in vivo*. Although we have not studied the *in vivo* release of BMP-2 from only microspheres, it is possible that rapid degradation of spheres influenced the resulting bone formation by changing the release kinetics.

The question, which release kinetic of BMP-2 is optimal, has been very controversial. In a study of Brown *et al.*, it is postulated that "the ideal pharmacokinetics for BMP-2 includes both a burst and sustained release is generally accepted"[227]. In their study, a burst release has been indicated as essential to enhance bone formation, while a sustained release without the burst did not form significantly more bone than the scaffold without rhBMP-2. However, only polyurethane (PUR) and PUR/microsphere [PUR/poly(lactic-co-glycolic acid)] composite scaffolds were tested in that study [227]. On the other hand, the clinical concerns of using BMP-2 which stem from the adverse events observed [318] are mainly associated to the burst release profile of BMP-2 [319]. Moreover, a sustained release profile of BMP-2 might be advantageous for bone healing since BMP-2 can retain longer term in the tissue, as shown by Jeon *et al*. [320] and as such continue to stimulate bone formation. In another study, reducing burst release has been shown to significantly increase the spinal fusion, when the initial burst release of BMP-2 from collagen sponge was reduced from 50% to 25% by addition of a cartilage oligomeric matrix protein (COMP) to the collagen sponge[321]. In the presence of COMP, the delivery of 2µg BMP-2 achieved a similar outcome to 10µg of BMP-2 alone when tested in spinal fusion model in rats.

In our study, the BMP-2 loaded RCP microspheres exhibit a small burst release of only up to 20 percent in the first 24 hours (Chapter 3). This burst release was reduced even further by using alginates (Chapter 4). The absence of a burst release and the prolonged retention of BMP-2 were confirmed *in vivo* by fluorescence imaging (Chapter 5). A gradual decrease of BMP-2 signal was observed for 4 weeks with a small amount of BMP-2 retained even at the end of the experiment (week 10). This clearly showed the long term retention of BMP-2 in the subcutaneous tissue when delivered with alginate and microspheres. Especially, obtaining a large volume of ectopic bone at the end of the experiment indicated that the drug release profile of BMP-2 from the composite hydrogel formulation matched the ectopic bone formation rate.

Materials better mimicking ECM composition and organization

In order to design better tissue engineering materials, we should understand how cells remodel (degrade and deposit) their own ECM [322, 323]. However natural ECM is much more complicated than the currently available biomaterials, in the sense that ECM contains many types of proteins, glycosaminoglycans and secreted factors. To mimic natural materials to a certain extent, smart materials that can selectively bind certain types of cells and certain types of secreted factors can be developed as a first step. In this way, we might be able to engineer the tissue by directing the type of cells and factors that will reside inside. In this thesis, we have used the well-known integrin binding peptide (arginine-glycine-lysine) or RGD to promote cell attachment. However, this peptide is not selective for a particular cell type [324]. In the future, recombinant proteins can be designed with a more selective binding peptide (based on the surface markers of cells) to recruit or host certain stem cells such as mesenchymal stem cells (MSCs) or osteoprogenitor cells.

ECM is organized in a specific way, meaning that the composition of ECM, its nano- and micro-scale architecture and the topography of the components are important elements in its organization. We have used collagen I based microspheres as a delivery system. To mimic the natural bone ECM composition and nanoscale architecture more closely, for example hydroxyapatite deposited collagen-like nanofibers can be designed and combined with a delivery system for BMP-2. As a first step towards such a system, RCP scaffolds were biomineralized with nanocrystalline hydroxyapatite and amorphous calcium phosphate [325]. Those biomimetic mineralized scaffolds enhanced MSC interaction and differentiation [326]. It is also known that the porosity and topography of the scaffold is very important for the cellular behaviour [327, 328] and nutrient support [231]. In a study where RCP scaffolds with linear pore structures were used, the pore size influenced the migration of ostoblast-like cells in this scaffold [329]. In the future, such scaffolds can be combined with the BMP-2 delivery system of this study to further enhance the functionality of the system.

Application area and mechanical loading

In our studies, the bone formation capacity of composite in situ gelling hydrogels was tested in a subcutaneous (ectopic) model and in a calvarial bone model, which are both non-load bearing. After obtaining successful bone formation in these models, we think that the applications of the hydrogels in non-load bearing bones such as calvarium or around the orbital cavity and in small defects in the mandibular or jaw bones in the maxillofacial surgery are possible [330]. There are several specific examples that application of tissue engineering products are suitable. For example, for maxillary reconstruction of flap after a large keratocyst, a tissue engineering material containing stem cells has been tested in a case study [331]. In another study, platelet gels have been tested in jaw bones with osteolytic lesions [332]. The reconstruction of critical size mandibular bone defects is a challenge in oral and maxillofacial surgery. For this application therefore cell-containing scaffolds have

been tested earlier [333, 334]. Another potential application is sinus augmentation, which is performed before the dental implant surgery in case of bone loss. For this sinus augmentation application, different sources of cells have been tested earlier [335, 336].

Mechanical loading is a very important parameter for the regeneration of load-bearing bones [337]. How the composite hydrogel loaded with BMP-2 will perform when mechanical forces are applied is difficult to predict. Since the mechanical properties of these hydrogels are far lower than that of bone and inorganic materials, they are not good candidates for treatment load bearing bones [338] unless used in combination with fixation techniques such as using plates and screws or used in combination with stiffer materials. In addition, the BMP-2 release may vary under mechanical loading as has been proposed in a nonhuman primate study on spinal arthrodesis, in which a BMP-2 loaded collagen sponge even prevented bone induction probably due to squeezing protein out of the sponge [339].

Large animal studies and clinical translation

Since the bone regeneration process is faster in rodents than in humans, the use of large animal tests before going to clinical trials is generally necessary. Besides, rodents could tolerate a quicker release rate due to their faster metabolic rate [65]. Therefore, a delivery system selected based on trials with rodents is not necessarily the best delivery system for humans. The selection of a suitable animal model depends on the application of the product. For example, for maxillofacial applications of this type of hydrogels, monkey [340], dog [341] or bovine bone [342] models can be used. For mandibular defects, canine [334] and rabbit models [333] have been used, while for segmented mandibular defects a mini-pig model has been applied [343]. Besides the animal, it is important to select the most relevant model for the intended application. For example, for long bone fractures there are single or segmental defect models for tibia. For long bone fracture applications, collagen sponge with BMP-2 was tested in a rabbit ulnar osteotomy model [344] and goat long bone fracture models[345]. For segmental fracture applications of this BMP-2 loaded collagen sponge, segmental defect models in rat femora [346], rabbit radii [347], rabbit ulnae [348], canine radii [349] have been used.

Clinical translation of a product in general is a long process not only because of regulations and legislations but also it is a process where the product is improved to perform best in humans [350-352]. There is always a trade-off between creating more complex designs for better therapies and easier and faster clinical translation of the therapies. For example, an acellular scaffold should face less regulatory inspection compared to cell-containing products according to Webber *et al.* [353], because of the risks associated with possible immunogenicity, teratoma formation, and cell culture adaptation/morphogenesis. Addition of growth factors increases the complexity of the product and increases the potential outcomes such as risk of adverse effects [318]. It is also important to note that during the regulatory approval process through the U.S. Food and Drug Administration (FDA), a tissue

engineering product can fall into four categories: tissues, biological products, drugs, or medical devices. For example, a simple scaffold material can be classified as a medical device; however, when additional components such as cells or biologicals are added, product falls into more than one category which complicates the approval process. It is also important to know that BMP-2 adsorbed collagen sponge (INFUSE® Bone Graft, Medtronic) has been approved as a Class III medical device by FDA. Although the regulatory approval pathway depends on the exact application, it is expected that our formulation of alginate, RCP microspheres and BMP-2 as a combination product can be translated to the clinic.

Conclusion

The main research question of this thesis was: Which of the four designs of BMP-2 delivery system with which composition and release profile will induce bone healing? It turned out that SLG alginate with BMP-2 loaded RCP microspheres was effective to deliver BMP-2 and induces ectopic bone formation. In addition, this formulation was effective to stimulate calvarial defect healing. In a more general sense, this thesis contributed to the deeper understanding of the importance of the design of a delivery system and a scaffold for bone regeneration. We have developed a potential material that can be used as a basis for bone regeneration therapies and can be further tuned for specific applications.

CHAPTER 7

SUMMARY

NEDERLANDSE SAMENVATTING

SUMMARY

The research described in this thesis aimed to develop a bone regeneration therapy using biomaterials and growth factors. First, the current literature and current therapies involving growth factor delivery for bone regeneration was reviewed (chapter 2). We mainly focused on bone morphogenetic protein-2 as a growth factor due to its potential and its widespread use in bone regeneration therapies. The protein delivery therapies were divided in non-covalent delivery and covalent coupling strategies mentioning advantages and drawbacks of each system. We have indicated that the release profile of the delivered protein via non-covalent linking is important for the performance of the medicinal product. Based on the literature, in order to eliminate the adverse effects of clinical BMP-2 product, the release profile of BMP-2 should be improved.

In chapter 3a RCP microspheres were developed for BMP-2 delivery. Collagen I based recombinant protein was (RCP) chosen for this purpose, because collagen I is the main component of the organic extracellular matrix in bone. A small library of different RCP microspheres was created to study the effect of several physicochemical characteristics on the BMP-2 release profile. Among several parameters investigated, size and crosslinking affected the BMP-2 release. We have selected small sized, densely chemically crosslinked particles for further studies because this type of particle demonstrated the lowest initial burst release. Typical release curves for this particle type had a small initial burst release in the first two days and a subsequent slower release up to around 30% release of BMP-2 within two weeks. When the particles were degraded after two weeks of release, the remaining BMP-2 was liberated suggesting that the degradation will contribute significantly to the *in vivo* release profile of BMP-2. Based on the release curves, we hypothesized that there is an interaction between BMP-2 and RCP. Therefore, surface plasmon resonance (SPR) was used to study the interaction of these proteins. This SPR technique indeed confirmed the affinity between BMP-2 and RCP with binding constants in the nanomolar range. Using BMP-2 variants to study the interacting domain of BMP-2 with RCP, we found that the N-terminal domain of BMP-2 is involved in this binding.

The BMP-2 adsorbed microspheres were tested in a rat ectopic bone formation model in chapter 3b. The microspheres in a form of paste containing 83 µg/mL, 8.3 µg/mL or 0.83 µg/mL BMP-2 were injected subcutaneously to rats. At the end of the experiment, only the high dose BMP-2 containing group could be retrieved and only this group induced a small amount of ectopic bone (2.5 mm^3). The other doses failed to induce bone formation and microspheres were degraded completely in the end of the experiment indicating that only microspheres is not optimal for bone therapy.

To improve bone formation, we have combined microspheres with in-situ gelling hydrogels in chapter 4. Two types of alginate, SLM and SLG, and one type of thermosensitive hyaluronic acid were developed for this study. These hydrogels were designed not only to

deliver and keep the microspheres at the site but also to act as a scaffold for the regenerating tissue and to fill a defect. The alginate formulations with microspheres interestingly showed a thixotropic behaviour which has allowed the handling of the material to be much easier compared to non-reversible in-situ gelling hydrogels. In addition, the alginate hydrogels contributed to the retention of BMP-2 and eliminated its burst release. Interestingly, thermosensitive hyaluronic acid retained most of the BMP-2. When the alginate and hyaluronic acid formulations were compared in an ectopic model in rats, clear differences in bone formation and inflammation were observed. SLG-alginate with microspheres induced the most bone volume at week 10. In contrast, the hyaluronic acid formulation gave no bone and an interesting inflammatory profile, in which the inflammation markers increased over weeks until the end of the experiment. This was different from the alginates for which there was a higher inflammation initially which decreased over-time. Overall, SLG alginate with microspheres formulation was selected as the best formulation for a potential bone regenerative product due to the highest ectopic bone volume induced and favourable inflammatory profile.

The SLG alginate-RCP microspheres formulation was selected for further studies in ectopic and orthotopic bone formation models in rats as described in chapter 5. First, the effect of BMP-2 dose delivered was tested in the ectopic bone model using 10, 3, 1, 0.3 and 0 µg BMP-2 per implant. The bone volume at 10 weeks was the highest with 10 µg (50 µg/mL) which was approximately 100 mm^3, half the volume of the injected hydrogel. The second highest dose of 3 µg (15 µg/mL) BMP-2 induced moderate bone formation. The density of bone formed by 10 µg and 3 µg were similar at 10 weeks. A lower dose, 1 µg (5 µg/mL) BMP-2, induced a small volume of bone, less than 5 mm^3, in some of the implants. Negative control (0 µg) and 0.3 µg did not induce bone formation. This study showed the existence of a threshold of BMP-2 dose for ectopic bone formation. In a subsequent calvarial defect experiment, 50 µg/mL and 5 µg/mL BMP-2 containing hydrogels were tested. The high concentration (50 µg/mL) regenerated the calvaria completely in 10 weeks and induced significantly more bone volume compared to empty or biomaterial controls. The lowest concentration (5 µg/mL) did not induce more bone than the controls with biomaterial only or the empty controls. This study showed that the effective concentration of BMP-2 to induce both ectopic and orthotopic bone is higher than 5 µg/mL, and optimally between 15-50 µg/mL.

Finally, the *in vivo* retention profile was studied using a fluorescently labelled BMP-2 and *in vivo* imaging for 10 weeks as described in chapter 5. Studying the retention of BMP-2 *in vivo* was important in the understanding of temporal availability of BMP-2 in the tissue and of the *in vivo* release profile of BMP-2. Fluorescent imaging showed that BMP-2 was gradually decreased over a period of at least 4 weeks, a time frame that matches well with typical bone regeneration processes. This *in vivo* retention profile is more favourable compared to the commercial BMP-2 carrier (collagen sponge) which releases half of the BMP-2 within 2 days and the rest within first week.

Overall, we have developed a potential product for bone regeneration based on BMP-2 loaded RCP microspheres and alginate. This material might find a broad application area for bone regeneration due to the slow release profile of BMP-2 and its injectability. After selecting a suitable application, for example in maxillofacial surgery, the material should be tested in a relevant large animal model. If successful in a large animal model, the developed injectable slow release system would be ready for further testing in clinical studies.

NEDERLANDSE SAMENVATTING

Het doel van het onderzoek beschreven in dit proefschrift is om een therapie voor botregeneratie te ontwikkelen met behulp van biomaterialen en groeifactoren. Als eerste is een overzicht gemaakt van de stand van de literatuur en bestaande therapieën voor botgeneratie die gebruik maken van afgiftesystemen voor groeifactoren (hoofdstuk 2). Hierbij lag de nadruk op de groeifactor bone morphogenetic protein-2 (BMP-2) vanwege het wijdverspreide gebruik er van in therapieën voor botregeneratie. De therapieën die gebruik maken van afgiftesystemen werden hierbij opgedeeld in niet-covalente en covalente koppelingstrategieën waarbij voor- en nadelen van de betreffende systemen werden behandeld. Het afgifteprofiel van het niet-covalent gebonden eiwit blijkt erg belangrijk voor de medicinale werkzaamheid van het product. Gebaseerd op deze literatuur is onze conclusie dat het afgifte-profiel van BMP-2 verbeterd moet worden om de negatieve bijeffecten ervan te elimineren.

In hoofdstuk 3a werden microscopisch kleine bollen van RCP ontwikkeld voor gecontroleerde BMP-2 afgifte. RCP is een recombinant eiwit gebaseerd op collageen I en is gekozen omdat collageen I het hoofdbestanddeel is van de organische extracellulaire matrix in bot. Een kleine set van verschillende RCP bolletjes werd gemaakt om het effect van diverse fysisch-chemische eigenschappen op het BMP-2 afgifteprofiel te bestuderen. Vooral de bolgrootte en manier van crosslinking bleken de BMP-2 afgifte sterk te beïnvloeden. Vanwege de relatief kleine initiële afgifte (de zogeheten 'burst-release') werden kleine, chemisch gecrosslinkte RCP-deeltjes geselecteerd voor de vervolgstudies. Het afgifteprofiel voor dit type deeltjes bestond uit een kleine initiële afgifte in de eerste twee dagen gevolgd door een langzame afgifte gedurende twee weken tot circa 30% van de BMP-2. De rest van de BMP-2 werd pas afgegeven door de deeltjes af te breken met enzym. Dit geeft aan dat degradatie een belangrijke rol zal spelen bij afgifte in het lichaam. De afgifte profielen suggereerden een duidelijke interactie tussen BMP-2 en RCP. Om dit verder te onderzoeken werd gebruik gemaakt van Surface Plasmon Resonance (SPR). Deze techniek bevestigde inderdaad het bestaan van een affiniteit tussen BMP-2 en RCP met bindingsconstanten in de nanomolair range. Door gebruik te maken van verschillende BMP-2 varianten om de interactie te bestuderen, werd duidelijk dat het N-terminal domein van BMP-2 betrokken is bij deze binding.

Zoals beschreven in hoofdstuk 3b, werden de door adsorptie van BMP-2 geladen RCP deeltjes getest in een ectopisch botvormingsmodel in ratten. In de vorm van een pasta werden de deeltjes, geladen met 83 µg/mL, 8.3 µg/mL of 0.83 µg/mL BMP-2, subcutaan geïnjecteerd. Aan het einde van het experiment, bleek alleen de hoogste dosis BMP-2 een kleine hoeveelheid ectopisch bot te geven (2.5 mm^3). De andere doses gaven geen enkele botvorming te zien en de deeltjes waren volledig gedegradeerd. Dit geeft aan dat BMP-2 geladen RCP deeltjes alleen niet optimaal zijn voor botvorming

Om de botvorming te verbeteren zijn in hoofdstuk 4 de deeltjes gecombineerd met *in situ* gelerende hydrogelen. Hiertoe werden twee typen alginate gebruikt, SLM and SLG, en een thermosensitief hyaluronzuur. Deze hydrogelen dienen als afgiftesysteem voor de RCP-deeltjes en om de deeltjes bij elkaar te houden op de plek van injectie maar ook als basis voor het regenererende weefsel en om het defect te vullen. De alginaat-formuleringen waren goed hanteerbaar en injecteerbaar vanwege hun thixotropische eigenschappen. Daarnaast droegen de alginaat gelen bij aan het vasthouden van de BMP-2 en het verder verlagen van de initiële afgifte. De thermosensitieve hyaluronzuur gelen hielden vrijwel alle BMP-2 vast. Vergelijking van deze alginaat en hyaluronzuur formuleringen in een ectopisch botmodel in ratten gaf grote verschillen te zien in botvorming en ontstekingsverschijnselen. Vooral de SLG-alginaat formulering met de BMP-2 geladen RCP-deeltjes gaf het meeste botvolume na 10 weken. De hyaluronzuur formulering gaf daarentegen geen bot en een interessant ontstekingspatroon te zien waarin de ontstekingsindicatoren toenamen gedurende het experiment. Voor de alginaten zagen we juist een sterkere ontsteking in het begin die af nam in de loop van het experiment. Op basis van deze resultaten, werd de formulering met SLG-alginaat gekozen als beste basis voor een botregeneratieproduct

Deze SLG-alginaat formulering werd vervolgens gebruikt voor vervolgstudies naar ectopische en orthotopische botvorming in ratten zoals beschreven in hoofdstuk 5. Als eerste werd het effect van de BMP-2 dosis getest in het ectopisch botmodel met beladingen van 10, 3, 1, 0.3 en 0 μg BMP-2. Na 10 weken was het botvolume het grootst voor de hoogste dosis van 10 μg (50 μg/mL). Deze BMP-2 hoeveelheid gaf ongeveer 100mm^3 bot, wat de helft van het volume is van de geïnjecteerde hydrogel. De op één na hoogste dosis van 3 μg (15 μg/mL) BMP-2 gaf duidelijk minder bot. De dichtheid van het gevormde bot na 10 weken was vergelijkbaar voor de 10 μg en 3 μg BMP-2 formuleringen. De formulering met 1 μg (5 μg/mL) BMP-2 gaf maar heel weinig botvorming, met minder dan 5 mm^3 bot in sommige implantaten. De negatieve controle (0μg) en 0.3 μg BMP-2 vormden geen ectopisch bot. Deze studie laat duidelijk zien dat er een minimum grenswaarde van de BMP-2 dosis bestaat om ectopische botvorming te induceren. Vervolgens werden hydrogel-formuleringen met 50 μg/mL and 5 μg/mL BMP-2 getest in een calvarium defect model. De hoogste concentratie (50 μg/mL) gaf volledige regeneratie van het calvarium defect in 10 weken en significant meer botvolume dan de lege controle en de controle met formulering zonder BMP-2, dus alleen het biomateriaal. De laagste BMP-2 concentratie (5 μg/mL) gaf niet meer bot dan deze controles. Deze *in vivo* studie laat zien dat de effectieve BMP-2 concentratie om ectopisch en orthotopisch bot te vormen groter is dan 5 μg/mL, en waarschijnlijk optimaal is tussen 15 en 50 μg/mL.

Tot slot werd het *in vivo* afgifteprofiel bestudeerd met behulp van fluorescent gelabelde BMP-2 en *in vivo* beeldvorming gedurende 10 weken zoals beschreven in hoofdstuk 5. Deze studie was belangrijk om inzicht te krijgen in de lokale beschikbaarheid van BMP-2 in het weefsel en het *in vivo* afgifteprofiel van BMP-2. Fluorescentiemetingen lieten een geleidelijke afname van BMP-2 zien gedurende 4 weken. Deze tijdsduur komt goed overeen

met de typische tijdsduur van botregeneratieprocessen. Daarnaast is dit geleidelijke *in vivo* afgifteprofiel veel beter dan dat van de commerciële BMP-2 carrier (collageen spons) die de helft van de BMP-2 af geeft binnen 2 dagen en de rest binnen een week.

Concluderend, is in dit onderzoek een potentieel product ontwikkeld voor botregeneratie gebaseerd op een hydrogel formulering van BMP-2 geladen RCP-deeltjes en alginaat. Dit materiaal is mogelijk inzetbaar in een breed toepassingsgebied binnen de botregeneratie vanwege het geleidelijke BMP-2 afgifteprofiel en goede injecteerbaarheid. Na selectie van een geschikte toepassing, bijvoorbeeld voor op het gebied van aangezichtschirurgie, moet het materiaal getest worden in een relevant groot proefdiermodel. Bij goede resultaten is het ontwikkelde injecteerbare afgiftesysteem klaar om verder getest te worden in klinische studies.

Chapter 7

CHAPTER 8

REFERENCES

1. Ratner, B.D., et al., *Biomaterials science: an introduction to materials in medicine*. 2004: Academic press.
2. Bergmann, C.P. and A. Stumpf, *Biomaterials*, in *Dental Ceramics: Microstructure, Properties and Degradation*. 2013, Springer Berlin Heidelberg: Berlin, Heidelberg. p. 9-13.
3. Keane, T.J. and S.F. Badylak. *Biomaterials for tissue engineering applications*. in *Seminars in pediatric surgery*. 2014. Elsevier.
4. Lanza, R., R. Langer, and J.P. Vacanti, *Principles of tissue engineering*. 2011: Academic press.
5. Vats, A., et al., *Scaffolds and biomaterials for tissue engineering: a review of clinical applications.* Clin Otolaryngol Allied Sci, 2003. **28**(3): p. 165-72.
6. Castells-Sala, C., et al., *Current applications of tissue engineering in biomedicine.* Journal of Biochips & Tissue Chips, 2013(S2): p. 1.
7. Tabata, Y., *Biomaterial technology for tissue engineering applications.* Journal of the Royal Society Interface, 2009. **6**(Suppl 3): p. S311-S324.
8. Drury, J.L. and D.J. Mooney, *Hydrogels for tissue engineering: scaffold design variables and applications.* Biomaterials, 2003. **24**(24): p. 4337-4351.
9. O'brien, F.J., *Biomaterials & scaffolds for tissue engineering.* Materials today, 2011. **14**(3): p. 88-95.
10. Keane, T.J. and S.F. Badylak, *Biomaterials for tissue engineering applications.* Semin Pediatr Surg, 2014. **23**(3): p. 112-8.
11. Burg, K.J., S. Porter, and J.F. Kellam, *Biomaterial developments for bone tissue engineering.* Biomaterials, 2000. **21**(23): p. 2347-59.
12. Gunatillake, P.A. and R. Adhikari, *Biodegradable synthetic polymers for tissue engineering.* Eur Cell Mater, 2003. **5**: p. 1-16; discussion 16.
13. Liu, H., E.B. Slamovich, and T.J. Webster, *Less harmful acidic degradation of poly (lactic-co-glycolic acid) bone tissue engineering scaffolds through titania nanoparticle addition.* International journal of nanomedicine, 2006. **1**(4): p. 541.
14. Sung, H.J., et al., *The effect of scaffold degradation rate on three-dimensional cell growth and angiogenesis.* Biomaterials, 2004. **25**(26): p. 5735-42.
15. Vasita, R., I.K. Shanmugam, and D.S. Katt, *Improved biomaterials for tissue engineering applications: surface modification of polymers.* Curr Top Med Chem, 2008. **8**(4): p. 341-53.
16. Mano, J.F., et al., *Natural origin biodegradable systems in tissue engineering and regenerative medicine: present status and some moving trends.* J R Soc Interface, 2007. **4**(17): p. 999-1030.
17. Cen, L., et al., *Collagen tissue engineering: development of novel biomaterials and applications.* Pediatr Res, 2008. **63**(5): p. 492-6.
18. Vamvakaki, M., et al., *Smart Materials for Tissue Engineering*. 2017: Royal Society of Chemistry.
19. D'Este, M., M. Alini, and D. Eglin, *Single step synthesis and characterization of thermoresponsive hyaluronan hydrogels.* Carbohydrate polymers, 2012. **90**(3): p. 1378-1385.
20. Gutowska, A., B. Jeong, and M. Jasionowski, *Injectable gels for tissue engineering.* The Anatomical Record, 2001. **263**(4): p. 342-349.
21. Guvendiren, M., H.D. Lu, and J.A. Burdick, *Shear-thinning hydrogels for biomedical applications.* Soft matter, 2012. **8**(2): p. 260-272.
22. Wang, Q., et al., *Injectable PLGA based colloidal gels for zero-order dexamethasone release in cranial defects.* Biomaterials, 2010. **31**(18): p. 4980-4986.
23. Wang, Y., et al., *Self-Healing and Injectable Shear Thinning Hydrogels Based on Dynamic Oxaborole-Diol Covalent Cross-Linking.* ACS Biomaterials Science & Engineering, 2016. **2**(12): p. 2315-2323.

24.   Loebel, C., et al., *Shear-thinning and self-healing hydrogels as injectable therapeutics and for 3D-printing.* Nature protocols, 2017. **12**(8): p. 1521.

25.   Hori, Y., A.M. Winans, and D.J. Irvine, *Modular injectable matrices based on alginate solution/microsphere mixtures that gel in situ and co-deliver immunomodulatory factors.* Acta biomaterialia, 2009. **5**(4): p. 969-982.

26.   Khademhosseini, A. and R. Langer, *Drug delivery and tissue engineering.* Chem Eng Prog, 2006. **102**(2): p. 38-42.

27.   Alley, S.C., N.M. Okeley, and P.D. Senter, *Antibody–drug conjugates: targeted drug delivery for cancer.* Current opinion in chemical biology, 2010. **14**(4): p. 529-537.

28.   Cho, K., et al., *Therapeutic nanoparticles for drug delivery in cancer.* Clinical cancer research, 2008. **14**(5): p. 1310-1316.

29.   Hickok, N.J. and I.M. Shapiro, *Immobilized antibiotics to prevent orthopaedic implant infections.* Advanced drug delivery reviews, 2012. **64**(12): p. 1165-1176.

30.   Sokolsky-Papkov, M., et al., *Polymer carriers for drug delivery in tissue engineering.* Advanced drug delivery reviews, 2007. **59**(4): p. 187-206.

31.   Bilati, U., E. Allémann, and E. Doelker, *Strategic approaches for overcoming peptide and protein instability within biodegradable nano-and microparticles.* European Journal of Pharmaceutics and Biopharmaceutics, 2005. **59**(3): p. 375-388.

32.   Biswas, S. and C.S. Kumar, *Nanotechnology-Based Spatiotemporal Controlled Drug Delivery Strategies*, in *Nanomedicine-Basic and Clinical Applications in Diagnostics and Therapy*. 2011, Karger Publishers. p. 53-70.

33.   Mourino, V. and A.R. Boccaccini, *Bone tissue engineering therapeutics: controlled drug delivery in three-dimensional scaffolds.* J R Soc Interface, 2010. **7**(43): p. 209-27.

34.   Giannoudis, P.V., H. Dinopoulos, and E. Tsiridis, *Bone substitutes: an update.* Injury, 2005. **36 Suppl 3**: p. S20-7.

35.   Dimitriou, R., et al., *Bone regeneration: current concepts and future directions.* BMC medicine, 2011. **9**(1): p. 66.

36.   Kini, U. and B. Nandeesh, *Physiology of bone formation, remodeling, and metabolism*, in *Radionuclide and hybrid bone imaging*. 2012, Springer. p. 29-57.

37.   Barnes, G.L., et al., *Growth factor regulation of fracture repair.* J Bone Miner Res, 1999. **14**(11): p. 1805-15.

38.   Gerstenfeld, L.C., et al., *Fracture healing as a post-natal developmental process: molecular, spatial, and temporal aspects of its regulation.* J Cell Biochem, 2003. **88**(5): p. 873-84.

39.   Giannoudis, P.V., et al., *Inflammation, Bone Healing, and Anti-Inflammatory Drugs: An Update.* J Orthop Trauma, 2015. **29 Suppl 12**: p. S6-9.

40.   Charbord, P., *Bone marrow mesenchymal stem cells: historical overview and concepts.* Hum Gene Ther, 2010. **21**(9): p. 1045-56.

41.   Marsell, R. and T.A. Einhorn, *The biology of fracture healing.* Injury, 2011. **42**(6): p. 551-5.

42.   Dimitriou, R., E. Tsiridis, and P.V. Giannoudis, *Current concepts of molecular aspects of bone healing.* Injury, 2005. **36**(12): p. 1392-404.

43.   Kalfas, I.H., *Principles of bone healing.* Neurosurg Focus, 2001. **10**(4): p. E1.

44.   Einhorn, T.A. and L.C. Gerstenfeld, *Fracture healing: mechanisms and interventions.* Nat Rev Rheumatol, 2015. **11**(1): p. 45-54.

45.   Dimitriou, R., et al., *Complications following autologous bone graft harvesting from the iliac crest and using the RIA: a systematic review.* Injury, 2011. **42 Suppl 2**: p. S3-15.

46.   van der Stok, J., *Bone Graft Substitutes*. 2015, Erasmus University Rotterdam.

47.   Campana, V., et al., *Bone substitutes in orthopaedic surgery: from basic science to clinical practice.* J Mater Sci Mater Med, 2014. **25**(10): p. 2445-61.

48.   Pryor, L.S., et al., *Review of bone substitutes.* Craniomaxillofac Trauma Reconstr, 2009. **2**(3): p. 151-60.

49. Greenwald, A.S., et al., *Bone-graft substitutes: facts, fictions, and applications.* J Bone Joint Surg Am, 2001. **83-A Suppl 2 Pt 2**: p. 98-103.

50. Langer, R. and J.P. Vacanti, *Tissue engineering.* Science, 1993. **260**(5110): p. 920-6.

51. Lee, S.H. and H. Shin, *Matrices and scaffolds for delivery of bioactive molecules in bone and cartilage tissue engineering.* Adv Drug Deliv Rev, 2007. **59**(4-5): p. 339-59.

52. Urist, M.R., *Bone: formation by autoinduction.* Science, 1965. **150**(3698): p. 893-9.

53. Schlange, T., et al., *BMP2 is required for early heart development during a distinct time period.* Mech Dev, 2000. **91**(1-2): p. 259-70.

54. Shimasaki, S., et al., *A functional bone morphogenetic protein system in the ovary.* Proc Natl Acad Sci U S A, 1999. **96**(13): p. 7282-7.

55. Guo, X. and X.F. Wang, *Signaling cross-talk between TGF-beta/BMP and other pathways.* Cell Res, 2009. **19**(1): p. 71-88.

56. Rahman, M.S., et al., *TGF-beta/BMP signaling and other molecular events: regulation of osteoblastogenesis and bone formation.* Bone Res, 2015. **3**: p. 15005.

57. Burkus, J.K., et al., *Clinical and radiographic outcomes of anterior lumbar interbody fusion using recombinant human bone morphogenetic protein-2.* Spine (Phila Pa 1976), 2002. **27**(21): p. 2396-408.

58. Rengachary, S.S., *Bone morphogenetic proteins: basic concepts.* Neurosurg Focus, 2002. **13**(6): p. e2.

59. *Summary of safety and effectiveness data*. 2002, FDA: https://www.accessdata.fda.gov/cdrh_docs/pdf/P000058b.pdf.

60. Simmonds, M.C., et al., *Safety and effectiveness of recombinant human bone morphogenetic protein-2 for spinal fusion: a meta-analysis of individual-participant data.* Ann Intern Med, 2013. **158**(12): p. 877-89.

61. Fu, R., et al., *Effectiveness and harms of recombinant human bone morphogenetic protein-2 in spine fusion: a systematic review and meta-analysis.* Ann Intern Med, 2013. **158**(12): p. 890-902.

62. Carragee, E.J., E.L. Hurwitz, and B.K. Weiner, *A critical review of recombinant human bone morphogenetic protein-2 trials in spinal surgery: emerging safety concerns and lessons learned.* Spine J, 2011. **11**(6): p. 471-91.

63. Epstein, N.E., *Complications due to the use of BMP/INFUSE in spine surgery: The evidence continues to mount.* Surg Neurol Int, 2013. **4**(Suppl 5): p. S343-52.

64. Agrawal, V. and M. Sinha, *A review on carrier systems for bone morphogenetic protein-2.* J Biomed Mater Res B Appl Biomater, 2017. **105**(4): p. 904-925.

65. Li, R.H. and J.M. Wozney, *Delivering on the promise of bone morphogenetic proteins.* Trends Biotechnol, 2001. **19**(7): p. 255-65.

66. James, A.W., et al., *A Review of the Clinical Side Effects of Bone Morphogenetic Protein-2.* Tissue Eng Part B Rev, 2016. **22**(4): p. 284-97.

67. Sfeir, C., et al., *Fracture Repair*, in *Bone regeneration and repair, biology and clinical applications*, G.E.F. Jay R. Lieberman, Editor. 2005, Springer. p. 21-44.

68. Meling, T., K. Harboe, and K. Soreide, *Incidence of traumatic long-bone fractures requiring in-hospital management: a prospective age- and gender-specific analysis of 4890 fractures.* Injury, 2009. **40**(11): p. 1212-9.

69. Tosounidis, T., et al., *Fracture healing and bone repair: an update.* Trauma, 2009. **11**: p. 145–156.

70. Littenberg, B., et al., *Closed fractures of the tibial shaft - A meta-analysis of three methods of treatment.* Journal of Bone and Joint Surgery-American Volume, 1998. **80A**(2): p. 174-183.

71. Dimitriou, R., E. Tsiridis, and P.V. Giannoudis, *Current concepts of molecular aspects of bone healing.* Injury-International Journal of the Care of the Injured, 2005. **36**(12): p. 1392-1404.

72. Friedlaender, G.E., et al., *Osteogenic protein-1 (bone morphogenetic protein-7) in the treatment of tibial nonunions - A prospective, randomized clinical trial comparing rhOP-1*

with fresh bone autograft. Journal of Bone and Joint Surgery-American Volume, 2001. **83A**: p. S151-S158.

73.   Logeart-Avramoglou, D., et al., *Engineering bone: challenges and obstacles.* Journal of Cellular and Molecular Medicine, 2005. **9**(1): p. 72-84.

74.   Argintar, E., S. Edwards, and J. Delahay, *Bone morphogenetic proteins in orthopaedic trauma surgery.* Injury-International Journal of the Care of the Injured, 2011. **42**(8): p. 730-734.

75.   Axelrad, T.W. and T.A. Einhorn, *Bone morphogenetic proteins in orthopaedic surgery.* Cytokine & Growth Factor Reviews, 2009. **20**(5-6): p. 481-488.

76.   Sasso, R.C., J.C. LeHuec, and C. Shaffrey, *Iliac crest bone graft donor site pain after anterior lumbar interbody fusion: a prospective patient satisfaction outcome assessment.* J Spinal Disord Tech, 2005. **18 Suppl**: p. S77-81.

77.   Arrington, E.D., et al., *Complications of iliac crest bone graft harvesting.* Clin Orthop Relat Res, 1996(329): p. 300-9.

78.   Schneppendahl, J., et al., *Synergistic effects of HBO and PRP improve bone regeneration with autologous bone grafting.* Injury, 2016.

79.   Rodriguez, I.A., et al., *Platelet-rich plasma in bone regeneration: engineering the delivery for improved clinical efficacy.* Biomed Res Int, 2014. **2014**: p. 392398.

80.   Komatsu, D.E. and S.J. Warden, *The control of fracture healing and its therapeutic targeting: improving upon nature.* J Cell Biochem, 2010. **109**(2): p. 302-11.

81.   Reddi, A.H., *Bone morphogenetic proteins: from basic science to clinical applications.* J Bone Joint Surg Am, 2001. **83-A Suppl 1**(Pt 1): p. S1-6.

82.   Wozney, J.M., et al., *Novel regulators of bone formation: molecular clones and activities.* Science, 1988. **242**(4885): p. 1528-34.

83.   Hogan, B.L., *Bone morphogenetic proteins: multifunctional regulators of vertebrate development.* Genes Dev, 1996. **10**(13): p. 1580-94.

84.   Massague, J., *TGF-beta signal transduction.* Annu Rev Biochem, 1998. **67**: p. 753-91.

85.   Reddi, A.H., *Role of morphogenetic proteins in skeletal tissue engineering and regeneration.* Nature Biotechnology, 1998. **16**(3): p. 247-52.

86.   Reddi, A.H., *BMPs: from bone morphogenetic proteins to body morphogenetic proteins.* Cytokine Growth Factor Rev, 2005. **16**(3): p. 249-50.

87.   Li, J.Z., et al., *Osteogenic potential of five different recombinant human bone morphogenetic protein adenoviral vectors in the rat.* Gene Ther, 2003. **10**(20): p. 1735-43.

88.   Miyazono, K., Y. Kamiya, and M. Morikawa, *Bone morphogenetic protein receptors and signal transduction.* J Biochem, 2010. **147**(1): p. 35-51.

89.   Hartigan, N., L. Garrigue-Antar, and K.E. Kadler, *Bone morphogenetic protein-1 (BMP-1). Identification of the minimal domain structure for procollagen C-proteinase activity.* J Biol Chem, 2003. **278**(20): p. 18045-9.

90.   Daluiski, A., et al., *Bone morphogenetic protein-3 is a negative regulator of bone density.* Nature Genetics, 2001. **27**(1): p. 84-8.

91.   Shen, B., et al., *BMP-13 emerges as a potential inhibitor of bone formation.* Int J Biol Sci, 2009. **5**(2): p. 192-200.

92.   Klammert, U., et al., *GDF-5 can act as a context-dependent BMP-2 antagonist.* BMC Biol, 2015. **13**: p. 77.

93.   Massague, J., S.W. Blain, and R.S. Lo, *TGFbeta signaling in growth control, cancer, and heritable disorders.* Cell, 2000. **103**(2): p. 295-309.

94.   Carcamo, J., et al., *Type I receptors specify growth-inhibitory and transcriptional responses to transforming growth factor beta and activin.* Mol Cell Biol, 1994. **14**(6): p. 3810-21.

95.   ten Dijke, P., K. Miyazono, and C.H. Heldin, *Signaling via hetero-oligomeric complexes of type I and type II serine/threonine kinase receptors.* Curr Opin Cell Biol, 1996. **8**(2): p. 139-45.

96.   Heldin, C.H., K. Miyazono, and P. ten Dijke, *TGF-beta signalling from cell membrane to nucleus through SMAD proteins.* Nature, 1997. **390**(6659): p. 465-71.

97.   Massague, J., J. Seoane, and D. Wotton, *Smad transcription factors.* Genes Dev, 2005. **19**(23): p. 2783-810.

98.   Nickel, J., et al., *Intricacies of BMP receptor assembly.* Cytokine Growth Factor Rev, 2009. **20**(5-6): p. 367-77.

99.   Katagiri, T. and T. Watabe, *Bone Morphogenetic Proteins.* Cold Spring Harb Perspect Biol, 2016. **8**(6).

100.   Luo, J., et al., *TGFbeta/BMP type I receptors ALK1 and ALK2 are essential for BMP9-induced osteogenic signaling in mesenchymal stem cells.* J Biol Chem, 2010. **285**(38): p. 29588-98.

101.   Groppe, J., et al., *Structural basis of BMP signalling inhibition by the cystine knot protein Noggin.* Nature, 2002. **420**(6916): p. 636-42.

102.   Harrington, A.E., et al., *Structural basis for the inhibition of activin signalling by follistatin.* EMBO J, 2006. **25**(5): p. 1035-45.

103.   Albers, C.E., et al., *L51P - A BMP2 variant with osteoinductive activity via inhibition of Noggin.* Bone, 2012. **51**(3): p. 401-6.

104.   Ruppert, R., E. Hoffmann, and W. Sebald, *Human bone morphogenetic protein 2 contains a heparin-binding site which modifies its biological activity.* Eur J Biochem, 1996. **237**(1): p. 295-302.

105.   Irie, A., et al., *Heparan sulfate is required for bone morphogenetic protein-7 signaling.* Biochem Biophys Res Commun, 2003. **308**(4): p. 858-65.

106.   Wurzler, K.K., et al., *[Evaluation of the osteoinductive potential of genetically modified BMP-2 variants].* Mund Kiefer Gesichtschir, 2004. **8**(2): p. 83-92.

107.   Ginn, S.L., et al., *Gene therapy clinical trials worldwide to 2012 - an update.* J Gene Med, 2013. **15**(2): p. 65-77.

108.   Luo, T., et al., *Enhanced bone regeneration around dental implant with bone morphogenetic protein 2 gene and vascular endothelial growth factor protein delivery.* Clin Oral Implants Res, 2012. **23**(4): p. 467-73.

109.   Lee, S.J., et al., *Enhancement of bone regeneration by gene delivery of BMP2/Runx2 bicistronic vector into adipose-derived stromal cells.* Biomaterials, 2010. **31**(21): p. 5652-9.

110.   Dalle Carbonare, L., G. Innamorati, and M.T. Valenti, *Transcription factor Runx2 and its application to bone tissue engineering.* Stem Cell Rev, 2012. **8**(3): p. 891-7.

111.   Gafni, Y., et al., *Gene therapy platform for bone regeneration using an exogenously regulated, AAV-2-based gene expression system.* Mol Ther, 2004. **9**(4): p. 587-95.

112.   Evans, C.H., *Gene delivery to bone.* Adv Drug Deliv Rev, 2012. **64**(12): p. 1331-40.

113.   Baltzer, A.W. and J.R. Lieberman, *Regional gene therapy to enhance bone repair.* Gene Ther, 2004. **11**(4): p. 344-50.

114.   Pelled, G., et al., *Direct gene therapy for bone regeneration: gene delivery, animal models, and outcome measures.* Tissue Eng Part B Rev, 2010. **16**(1): p. 13-20.

115.   Engelhardt, J.F., et al., *Ablation of E2A in recombinant adenoviruses improves transgene persistence and decreases inflammatory response in mouse liver.* Proc Natl Acad Sci U S A, 1994. **91**(13): p. 6196-200.

116.   Buning, H., et al., *Recent developments in adeno-associated virus vector technology.* J Gene Med, 2008. **10**(7): p. 717-33.

117.   Park, J., et al., *Bone regeneration in critical size defects by cell-mediated BMP-2 gene transfer: a comparison of adenoviral vectors and liposomes.* Gene Ther, 2003. **10**(13): p. 1089-98.

118.   Betz, O.B., et al., *Direct percutaneous gene delivery to enhance healing of segmental bone defects.* J Bone Joint Surg Am, 2006. **88**(2): p. 355-65.

119.   Egermann, M., et al., *Effect of BMP-2 gene transfer on bone healing in sheep.* Gene Ther, 2006. **13**(17): p. 1290-9.

120.   Thompson, D.D., et al., *FDA Guidelines and animal models for osteoporosis.* Bone, 1995. **17**(4 Suppl): p. 125S-133S.

121. Alhakamy, N.A., et al., *Noncovalently associated cell-penetrating peptides for gene delivery applications.* Ther Deliv, 2013. **4**(6): p. 741-57.

122. Sullivan, M., *Histone targeted non-viral gene delivery to enhance bone repair.* GrantomeHistone targeted non-viral gene delivery to enhance bone repair, 2014.

123. Jang, J.H., D.V. Schaffer, and L.D. Shea, *Engineering biomaterial systems to enhance viral vector gene delivery.* Mol Ther, 2011. **19**(8): p. 1407-15.

124. Wehrhan, F., et al., *PEG matrix enables cell-mediated local BMP-2 gene delivery and increased bone formation in a porcine critical size defect model of craniofacial bone regeneration.* Clin Oral Implants Res, 2012. **23**(7): p. 805-13.

125. Kolk, A., et al., *A strategy to establish a gene-activated matrix on titanium using gene vectors protected in a polylactide coating.* Biomaterials, 2011. **32**(28): p. 6850-9.

126. Wegman, F., et al., *Osteogenic differentiation as a result of BMP-2 plasmid DNA based gene therapy in vitro and in vivo.* Eur Cell Mater, 2011. **21**: p. 230-242.

127. Chen, J., et al., *Simultaneous regeneration of articular cartilage and subchondral bone in vivo using MSCs induced by a spatially controlled gene delivery system in bilayered integrated scaffolds.* Biomaterials, 2011. **32**(21): p. 4793-805.

128. Song, J.J. and H.C. Ott, *Organ engineering based on decellularized matrix scaffolds.* Trends Mol Med, 2011. **17**(8): p. 424-32.

129. Zachos, T., et al., *Mesenchymal stem cell-mediated gene delivery of bone morphogenetic protein-2 in an articular fracture model.* Mol Ther, 2007. **15**(8): p. 1543-50.

130. Meijer, G.J., et al., *Cell-based bone tissue engineering.* PLoS Med, 2007. **4**(2): p. e9.

131. Banwart, J.C., M.A. Asher, and R.S. Hassanein, *Iliac crest bone graft harvest donor site morbidity. A statistical evaluation.* Spine (Phila Pa 1976), 1995. **20**(9): p. 1055-60.

132. Owen, M. and A.J. Friedenstein, *Stromal stem cells: marrow-derived osteogenic precursors.* Ciba Found Symp, 1988. **136**: p. 42-60.

133. Wu, S.M. and K. Hochedlinger, *Harnessing the potential of induced pluripotent stem cells for regenerative medicine.* Nat Cell Biol, 2011. **13**(5): p. 497-505.

134. Cyranoski, D., *Next-generation stem cells cleared for human trial.* Nature, 2014.

135. Horwitz, E.M., et al., *Isolated allogeneic bone marrow-derived mesenchymal cells engraft and stimulate growth in children with osteogenesis imperfecta: Implications for cell therapy of bone.* Proc Natl Acad Sci U S A, 2002. **99**(13): p. 8932-7.

136. Kaigler, D., et al., *Stem cell therapy for craniofacial bone regeneration: a randomized, controlled feasibility trial.* Cell Transplant, 2013. **22**(5): p. 767-77.

137. Xiao, C., et al., *Bone marrow stromal cells with a combined expression of BMP-2 and VEGF-165 enhanced bone regeneration.* Biomed Mater, 2011. **6**(1): p. 015013.

138. Webber, M.J., et al., *A Perspective on the Clinical Translation of Scaffolds for Tissue Engineering.* Ann Biomed Eng, 2014.

139. Lin, Y., et al., *Bone regeneration by BMP-2 enhanced adipose stem cells loading on alginate gel.* Histochem Cell Biol, 2008. **129**(2): p. 203-10.

140. Gao, J., et al., *The dynamic in vivo distribution of bone marrow-derived mesenchymal stem cells after infusion.* Cells Tissues Organs, 2001. **169**(1): p. 12-20.

141. Sahin, A.O. and M. Buitenhuis, *Molecular mechanisms underlying adhesion and migration of hematopoietic stem cells.* Cell Adh Migr, 2012. **6**(1): p. 39-48.

142. Perri, B., et al., *Adverse swelling associated with use of rh-BMP-2 in anterior cervical discectomy and fusion: a case study.* Spine J, 2007. **7**(2): p. 235-9.

143. Woo, E.J., et al., *Extensive limb swelling after immunization: reports to the Vaccine Adverse Event Reporting System.* Clinical Infectious Diseases, 2003. **37**(3): p. 351-8.

144. King, W.J. and P.H. Krebsbach, *Growth factor delivery: how surface interactions modulate release in vitro and in vivo.* Adv Drug Deliv Rev, 2012. **64**(12): p. 1239-56.

145. Patel, Z.S., et al., *Biodegradable gelatin microparticles as delivery systems for the controlled release of bone morphogenetic protein-2.* Acta Biomater, 2008. **4**(5): p. 1126-38.

146. Lutolf, M.P., et al., *Repair of bone defects using synthetic mimetics of collagenous extracellular matrices.* Nat Biotechnol, 2003. **21**(5): p. 513-8.

147. Shekaran, A., et al., *Bone regeneration using an alpha 2 beta 1 integrin-specific hydrogel as a BMP-2 delivery vehicle.* Biomaterials, 2014. **35**(21): p. 5453-61.

148. Boerckel, J.D., et al., *Effects of protein dose and delivery system on BMP-mediated bone regeneration.* Biomaterials, 2011. **32**(22): p. 5241-51.

149. Lee, J.W., et al., *Bone regeneration using a microstereolithography-produced customized poly(propylene fumarate)/diethyl fumarate photopolymer 3D scaffold incorporating BMP-2 loaded PLGA microspheres.* Biomaterials, 2011. **32**(3): p. 744-52.

150. Hernandez, A., et al., *Material-related effects of BMP-2 delivery systems on bone regeneration.* Acta Biomater, 2012. **8**(2): p. 781-91.

151. Young, C.L., Z.T. Britton, and A.S. Robinson, *Recombinant protein expression and purification: a comprehensive review of affinity tags and microbial applications.* Biotechnology Journal, 2012. **7**(5): p. 620-34.

152. Terpe, K., *Overview of tag protein fusions: from molecular and biochemical fundamentals to commercial systems.* Appl Microbiol Biotechnol, 2003. **60**(5): p. 523-33.

153. Magdeldin, S., *Affinity Chromatography.* InTech, 2012.

154. Steen Redeker, E., et al., *Protein engineering for directed immobilization.* Bioconjug Chem, 2013. **24**(11): p. 1761-77.

155. Bessa, P.C., et al., *Expression, purification and osteogenic bioactivity of recombinant human BMP-4, -9, -10, -11 and -14.* Protein Expr Purif, 2009. **63**(2): p. 89-94.

156. Grunder, T., et al., *Bone morphogenetic protein (BMP)-2 enhances the expression of type II collagen and aggrecan in chondrocytes embedded in alginate beads.* Osteoarthritis Cartilage, 2004. **12**(7): p. 559-67.

157. Yuvaraj, S., et al., *E. coli-produced BMP-2 as a chemopreventive strategy for colon cancer: a proof-of-concept study.* Gastroenterol Res Pract, 2012. **2012**: p. 895462.

158. Wehrhan, F., et al., *Critical size defect regeneration using PEG-mediated BMP-2 gene delivery and the use of cell occlusive barrier membranes - the osteopromotive principle revisited.* Clin Oral Implants Res, 2013. **24**(8): p. 910-20.

159. Zhao, Y., et al., *The osteogenic effect of bone morphogenetic protein-2 on the collagen scaffold conjugated with antibodies.* Journal of Controlled Release, 2010. **141**(1): p. 30-7.

160. Hamilton, P.T., et al., *Improved bone morphogenetic protein-2 retention in an injectable collagen matrix using bifunctional peptides.* Plos One, 2013. **8**(8): p. e70715.

161. Gron, H., et al., *Methods and compositions for promoting localization of pharmaceutically active agents to bone*. 2008: U.S.

162. Sasisekharan, R., S. Ernst, and G. Venkataraman, *On the regulation of fibroblast growth factor activity by heparin-like glycosaminoglycans.* Angiogenesis, 1997. **1**(1): p. 45-54.

163. Kim, S.E., et al., *The effect of immobilization of heparin and bone morphogenic protein-2 (BMP-2) to titanium surfaces on inflammation and osteoblast function.* Biomaterials, 2011. **32**(2): p. 366-73.

164. Lee, D.W., et al., *Gentamicin and bone morphogenic protein-2 (BMP-2)-delivering heparinized-titanium implant with enhanced antibacterial activity and osteointegration.* Bone, 2012. **50**(4): p. 974-82.

165. Kim, S.E., et al., *Osteogenesis induction of periodontal ligament cells onto bone morphogenic protein-2 immobilized PCL fibers.* Carbohydr Polym, 2014. **99**: p. 700-9.

166. Kim, T.H., et al., *In vitro and in vivo evaluation of bone formation using solid freeform fabrication-based bone morphogenic protein-2 releasing PCL/PLGA scaffolds.* Biomedical Materials, 2014. **9**(2): p. 025008.

167. Guzman, R., et al., *Chitosan scaffolds containing calcium phosphate salts and rhBMP-2: in vitro and in vivo testing for bone tissue regeneration.* Plos One, 2014. **9**(2): p. e87149.

168. Chilkoti, A., P.H. Tan, and P.S. Stayton, *Site-directed mutagenesis studies of the high-affinity streptavidin-biotin complex: contributions of tryptophan residues 79, 108, and 120.* Proc Natl Acad Sci U S A, 1995. **92**(5): p. 1754-8.

169. Uludag, H., et al., *Biotinated bone morphogenetic protein-2: In vivo and in vitro activity.* Biotechnol Bioeng, 1999. **65**(6): p. 668-72.

170. Wiemann, M., et al., *A reporter-cell assay for the detection of BMP-2 immobilized on porous and nonporous materials.* J Biomed Mater Res, 2002. **62**(1): p. 119-27.

171. Lagunas, A., et al., *Continuous bone morphogenetic protein-2 gradients for concentration effect studies on C2C12 osteogenic fate.* Nanomedicine, 2013. **9**(5): p. 694-701.

172. Schliephake, H., et al., *Effect of oligonucleotide mediated immobilization of bone morphogenic proteins on titanium surfaces.* Biomaterials, 2012. **33**(5): p. 1315-22.

173. Chatzinikolaidou, M., et al., *Peri-implant reactivity and osteoinductive potential of immobilized rhBMP-2 on titanium carriers.* Acta biomaterialia, 2010. **6**(11): p. 4405-21.

174. Bauer, S., et al., *Covalent functionalization of TiO2 nanotube arrays with EGF and BMP-2 for modified behavior towards mesenchymal stem cells.* Integr Biol (Camb), 2011. **3**(9): p. 927-36.

175. Kashiwagi, K., T. Tsuji, and K. Shiba, *Directional BMP-2 for functionalization of titanium surfaces.* Biomaterials, 2009. **30**(6): p. 1166-75.

176. Tabisz, B., et al., *Site-Directed Immobilization of BMP-2: Two Approaches for the Production of Innovative Osteoinductive Scaffolds.* Biomacromolecules, 2017. **18**(3): p. 695-708.

177. Wang, L., et al., *A new functional suppressor tRNA/aminoacyl-tRNA synthetase pair for the in vivo incorporation of unnatural amino acids into proteins.* Journal of the American Chemical Society, 2000. **122**(20): p. 5010-5011.

178. Pohl, T.L., et al., *Surface immobilization of bone morphogenetic protein 2 via a self-assembled monolayer formation induces cell differentiation.* Acta biomaterialia, 2012. **8**(2): p. 772-80.

179. Suzuki, Y., et al., *Alginate hydrogel linked with synthetic oligopeptide derived from BMP-2 allows ectopic osteoinduction in vivo.* J Biomed Mater Res, 2000. **50**(3): p. 405-9.

180. Heinecke, K., et al., *Receptor oligomerization and beyond: a case study in bone morphogenetic proteins.* BMC Biol, 2009. **7**: p. 59.

181. Saito, A., et al., *Prolonged ectopic calcification induced by BMP-2-derived synthetic peptide.* J Biomed Mater Res A, 2004. **70**(1): p. 115-21.

182. Madl, C.M., et al., *Presentation of BMP-2 mimicking peptides in 3D hydrogels directs cell fate commitment in osteoblasts and mesenchymal stem cells.* Biomacromolecules, 2014. **15**(2): p. 445-55.

183. Seol, Y.J., et al., *Enhanced osteogenic promotion around dental implants with synthetic binding motif mimicking bone morphogenetic protein (BMP)-2.* J Biomed Mater Res A, 2006. **77**(3): p. 599-607.

184. Poh, C.K., et al., *Cobalt chromium alloy with immobilized BMP peptide for enhanced bone growth.* J Orthop Res, 2011. **29**(9): p. 1424-30.

185. Balasundaram, G., C. Yao, and T.J. Webster, *TiO2 nanotubes functionalized with regions of bone morphogenetic protein-2 increases osteoblast adhesion.* J Biomed Mater Res A, 2008. **84**(2): p. 447-53.

186. Kim, M.J., et al., *BMP-2 peptide-functionalized nanopatterned substrates for enhanced osteogenic differentiation of human mesenchymal stem cells.* Biomaterials, 2013. **34**(30): p. 7236-46.

187. Meinel, L., et al., *Osteogenesis by human mesenchymal stem cells cultured on silk biomaterials: comparison of adenovirus mediated gene transfer and protein delivery of BMP-2.* Biomaterials, 2006. **27**(28): p. 4993-5002.

188. Place, E.S., N.D. Evans, and M.M. Stevens, *Complexity in biomaterials for tissue engineering.* Nat Mater, 2009. **8**(6): p. 457-70.

189. Dimitriou, R., et al., *Bone regeneration: current concepts and future directions.* BMC Med, 2011. **9**: p. 66.

190. Finkemeier, C.G., *Bone-grafting and bone-graft substitutes.* J Bone Joint Surg Am, 2002. **84-A**(3): p. 454-64.

191. Moore, W.R., S.E. Graves, and G.I. Bain, *Synthetic bone graft substitutes.* ANZ J Surg, 2001. **71**(6): p. 354-61.

192. Lee, D.H., et al., *Chemotactic migration of human mesenchymal stem cells and MC3T3-E1 osteoblast-like cells induced by COS-7 cell line expressing rhBMP-7.* Tissue Eng, 2006. **12**(6): p. 1577-86.

193. Seeherman, H. and J.M. Wozney, *Delivery of bone morphogenetic proteins for orthopedic tissue regeneration.* Cytokine Growth Factor Rev, 2005. **16**(3): p. 329-45.

194. McKay, W.F., S.M. Peckham, and J.M. Badura, *A comprehensive clinical review of recombinant human bone morphogenetic protein-2 (INFUSE Bone Graft).* Int Orthop, 2007. **31**(6): p. 729-34.

195. Woo, E.J., *Adverse events reported after the use of recombinant human bone morphogenetic protein 2.* J Oral Maxillofac Surg, 2012. **70**(4): p. 765-7.

196. Shields, L.B., et al., *Adverse effects associated with high-dose recombinant human bone morphogenetic protein-2 use in anterior cervical spine fusion.* Spine (Phila Pa 1976), 2006. **31**(5): p. 542-7.

197. Issa, J.P., et al., *Sustained release carriers used to delivery bone morphogenetic proteins in the bone healing process.* Anat Histol Embryol, 2008. **37**(3): p. 181-7.

198. Ma, D., et al., *A composited PEG-silk hydrogel combining with polymeric particles delivering rhBMP-2 for bone regeneration.* Mater Sci Eng C Mater Biol Appl, 2016. **65**: p. 221-31.

199. Lee, E.J. and H.E. Kim, *Accelerated bony defect healing by chitosan/silica hybrid membrane with localized bone morphogenetic protein-2 delivery.* Mater Sci Eng C Mater Biol Appl, 2016. **59**: p. 339-45.

200. Boskey, A.L., *Bone composition: relationship to bone fragility and antiosteoporotic drug effects.* Bonekey Rep, 2013. **2**: p. 447.

201. Solorio, L., et al., *Gelatin microspheres crosslinked with genipin for local delivery of growth factors.* J Tissue Eng Regen Med, 2010. **4**(7): p. 514-23.

202. Browne, S., D.I. Zeugolis, and A. Pandit, *Collagen: finding a solution for the source.* Tissue Eng Part A, 2013. **19**(13-14): p. 1491-4.

203. De Boer, A.L., et al., *RGD containing recombinant gelatin*. 2012, Google Patents.

204. Parvizi, M., et al., *Development of recombinant collagen-peptide-based vehicles for delivery of adipose-derived stromal cells.* J Biomed Mater Res A, 2016. **104**(2): p. 503-16.

205. Gorgieva, S. and V. Kokol, *Collagen-vs. gelatine-based biomaterials and their biocompatibility: review and perspectives*. 2011: INTECH open access publisher.

206. Tuin, A., et al., *Recombinant gelatin microspheres: novel formulations for tissue repair?* Tissue Eng Part A, 2010. **16**(6): p. 1811-21.

207. Weiner, A.A., et al., *Modulation of protein release from photocrosslinked networks by gelatin microparticles.* Int J Pharm, 2008. **360**(1-2): p. 107-14.

208. Kim, H.K., H.J. Chung, and T.G. Park, *Biodegradable polymeric microspheres with "open/closed" pores for sustained release of human growth hormone.* J Control Release, 2006. **112**(2): p. 167-74.

209. Kirsch, T., J. Nickel, and W. Sebald, *Isolation of recombinant BMP receptor IA ectodomain and its 2:1 complex with BMP-2.* FEBS Lett, 2000. **468**(2-3): p. 215-9.

210. Depprich, R., et al., *[Comparison of the osteogenic activity of bone morphogenetic protein (BMP) mutants].* Mund Kiefer Gesichtschir, 2005. **9**(6): p. 363-8.

211. Nilsson, K., F. Buzsaky, and K. Mosbach, *Growth of anchorage–dependent cells on macroporous microcarriers.* Nature Biotechnology, 1986. **4**(11): p. 989-990.

212. Satake, K., et al., *The spectrophotometric determination of amine, amino acid and peptide with 2, 4, 6-trinitrobenzene 1-sulfonic acid.* The Journal of Biochemistry, 1960. **47**(5): p. 654-660.

213. Poldervaart, M.T., et al., *Sustained release of BMP-2 in bioprinted alginate for osteogenicity in mice and rats.* PLoS One, 2013. **8**(8): p. e72610.

214. Herrera, B. and G.J. Inman, *A rapid and sensitive bioassay for the simultaneous measurement of multiple bone morphogenetic proteins. Identification and quantification of BMP4, BMP6 and BMP9 in bovine and human serum.* BMC Cell Biol, 2009. **10**: p. 20.

215. Brum, A.M., et al., *Connectivity Map-based discovery of parbendazole reveals targetable human osteogenic pathway.* Proc Natl Acad Sci U S A, 2015. **112**(41): p. 12711-6.

216. Dash, S., et al., *Kinetic modeling on drug release from controlled drug delivery systems.* Acta Pol Pharm, 2010. **67**(3): p. 217-23.

217. Korsmeyer, R.W., et al., *Mechanisms of solute release from porous hydrophilic polymers.* International journal of pharmaceutics, 1983. **15**(1): p. 25-35.

218. Sanger, T., M. Laub, and H.P. Jennissen, *Release of 125I-RhBMP-2 from Foamed Poly-(D,L)-Lactide.* Biomed Tech (Berl), 2013.

219. Knaus, P. and W. Sebald, *Cooperativity of binding epitopes and receptor chains in the BMP/TGFbeta superfamily.* Biol Chem, 2001. **382**(8): p. 1189-95.

220. Vogel, F., *Klonierung, Expression und Charakterisierung von Mutanten des Bone Morphogenetic Protein-2*, in *Department of Physiological Chemistry II*. 2002, Julius-Maximilians-Universität Würzburg: Universität Würzburg. p. 127.

221. Kirsch, T., J. Nickel, and W. Sebald, *BMP-2 antagonists emerge from alterations in the low-affinity binding epitope for receptor BMPR-II.* EMBO J, 2000. **19**(13): p. 3314-24.

222. Fu, Y. and W.J. Kao, *Drug release kinetics and transport mechanisms from semi-interpenetrating networks of gelatin and poly(ethylene glycol) diacrylate.* Pharm Res, 2009. **26**(9): p. 2115-24.

223. Siepmann, J. and F. Siepmann, *Mathematical modeling of drug delivery.* Int J Pharm, 2008. **364**(2): p. 328-43.

224. Koppolu, B.P., et al., *Controlling chitosan-based encapsulation for protein and vaccine delivery.* Biomaterials, 2014. **35**(14): p. 4382-9.

225. Bhakta, G., et al., *Hyaluronic acid-based hydrogels functionalized with heparin that support controlled release of bioactive BMP-2.* Biomaterials, 2012. **33**(26): p. 6113-22.

226. Scarfi, S., *Use of bone morphogenetic proteins in mesenchymal stem cell stimulation of cartilage and bone repair.* World J Stem Cells, 2016. **8**(1): p. 1-12.

227. Brown, K.V., et al., *Improving bone formation in a rat femur segmental defect by controlling bone morphogenetic protein-2 release.* Tissue Eng Part A, 2011. **17**(13-14): p. 1735-46.

228. Yang, H.S., et al., *Comparison between heparin-conjugated fibrin and collagen sponge as bone morphogenetic protein-2 carriers for bone regeneration.* Exp Mol Med, 2012. **44**(5): p. 350-5.

229. Fujioka-Kobayashi, M., et al., *Absorbable collagen sponges loaded with recombinant bone morphogenetic protein 9 induces greater osteoblast differentiation when compared to bone morphogenetic protein 2.* Clinical and Experimental Dental Research, 2017. **3**(1): p. 32-40.

230. Matassi, F., et al., *New biomaterials for bone regeneration.* Clin Cases Miner Bone Metab, 2011. **8**(1): p. 21-4.

231. Polo-Corrales, L., M. Latorre-Esteves, and J.E. Ramirez-Vick, *Scaffold design for bone regeneration.* J Nanosci Nanotechnol, 2014. **14**(1): p. 15-56.

232. El Bialy, I., W. Jiskoot, and M. Reza Nejadnik, *Formulation, Delivery and Stability of Bone Morphogenetic Proteins for Effective Bone Regeneration.* Pharm Res, 2017. **34**(6): p. 1152-1170.

233. Zara, J.N., et al., *High doses of bone morphogenetic protein 2 induce structurally abnormal bone and inflammation in vivo.* Tissue Eng Part A, 2011. **17**(9-10): p. 1389-99.

234. Agrawal, V. and M. Sinha, *A review on carrier systems for bone morphogenetic protein-2.* J Biomed Mater Res B Appl Biomater, 2016.

235. Tazaki, J., et al., *BMP-2 release and dose-response studies in hydroxyapatite and beta-tricalcium phosphate.* Biomed Mater Eng, 2009. **19**(2-3): p. 141-6.

236. Kim, I.S., et al., *Promising efficacy of Escherichia coli recombinant human bone morphogenetic protein-2 in collagen sponge for ectopic and orthotopic bone formation and comparison with mammalian cell recombinant human bone morphogenetic protein-2.* Tissue Eng Part A, 2011. **17**(3-4): p. 337-48.

237. Bessa, P.C., et al., *Silk fibroin microparticles as carriers for delivery of human recombinant bone morphogenetic protein-2: in vitro and in vivo bioactivity.* Tissue Eng Part C Methods, 2010. **16**(5): p. 937-45.

238. Martinez-Sanz, E., et al., *Osteoinduction in the palatal submucosa by injecting BMP-2 on 2 different carriers.* J Craniofac Surg, 2012. **23**(2): p. 594-8.

239. Kokubo, T., H.M. Kim, and M. Kawashita, *Novel bioactive materials with different mechanical properties.* Biomaterials, 2003. **24**(13): p. 2161-75.

240. Murphy, C.M., et al., *A collagen-hydroxyapatite scaffold allows for binding and co-delivery of recombinant bone morphogenetic proteins and bisphosphonates.* Acta Biomater, 2014. **10**(5): p. 2250-8.

241. Hannink, G., et al., *Evaluation of collagen/heparin coated TCP/HA granules for long-term delivery of BMP-2.* J Mater Sci Mater Med, 2013. **24**(2): p. 325-32.

242. Fischer, A.H., et al., *Hematoxylin and eosin staining of tissue and cell sections.* CSH Protoc, 2008. **2008**: p. pdb prot4986.

243. Parvizi, M., *Cardiovascular Tissue Engineering and Regeneration Based on Adipose Tissue-derived Stem/stromal Cells*. 2016: University of Groningen.

244. Van Vlierberghe, S., P. Dubruel, and E. Schacht, *Biopolymer-based hydrogels as scaffolds for tissue engineering applications: a review.* Biomacromolecules, 2011. **12**(5): p. 1387-408.

245. Kretlow, J.D., et al., *Injectable biomaterials for regenerating complex craniofacial tissues.* Adv Mater, 2009. **21**(32-33): p. 3368-93.

246. Amini, A.A. and L.S. Nair, *Injectable hydrogels for bone and cartilage repair.* Biomed Mater, 2012. **7**(2): p. 024105.

247. Hustedt, J.W. and D.J. Blizzard, *The controversy surrounding bone morphogenetic proteins in the spine: a review of current research.* Yale J Biol Med, 2014. **87**(4): p. 549-61.

248. Valentin-Opran, A., et al., *Clinical evaluation of recombinant human bone morphogenetic protein-2.* Clin Orthop Relat Res, 2002(395): p. 110-20.

249. Poon, B., et al., *Bone morphogenetic protein-2 and bone therapy: successes and pitfalls.* J Pharm Pharmacol, 2016. **68**(2): p. 139-47.

250. Mumcuoglu, D., et al., *BMP-2 release from synthetic collagen peptide particles*, in *Front. Bioeng. Biotechnol. Conference Abstract: 10th World Biomaterials Congress*. 2016.

251. Venkatesan, J., et al., *Alginate composites for bone tissue engineering: a review.* Int J Biol Macromol, 2015. **72**: p. 269-81.

252. Zhang, J., Q. Wang, and A. Wang, *In situ generation of sodium alginate/hydroxyapatite nanocomposite beads as drug-controlled release matrices.* Acta Biomater, 2010. **6**(2): p. 445-54.

253. Sun, J. and H. Tan, *Alginate-based biomaterials for regenerative medicine applications.* Materials, 2013. **6**(4): p. 1285-1309.

254. Zhao, N., et al., *Effect of hyaluronic acid in bone formation and its applications in dentistry.* J Biomed Mater Res A, 2016. **104**(6): p. 1560-9.

255. Martinez-Sanz, E., et al., *Bone reservoir: Injectable hyaluronic acid hydrogel for minimal invasive bone augmentation.* J Control Release, 2011. **152**(2): p. 232-40.

256. Kisiel, M., et al., *Improving the osteogenic potential of BMP-2 with hyaluronic acid hydrogel modified with integrin-specific fibronectin fragment.* Biomaterials, 2013. **34**(3): p. 704-12.

257. Maus, U., et al., *Lack of effect on bone healing of injectable BMP-2 augmented hyaluronic acid.* Arch Orthop Trauma Surg, 2008. **128**(12): p. 1461-6.

258. D'Este, M., M. Alini, and D. Eglin, *Single step synthesis and characterization of thermoresponsive hyaluronan hydrogels.* Carbohydr Polym, 2012. **90**(3): p. 1378-85.

259. Utomo, L., et al., *Preparation and characterization of a decellularized cartilage scaffold for ear cartilage reconstruction.* Biomed Mater, 2015. **10**(1): p. 015010.

260. Van Tomme, S.R., G. Storm, and W.E. Hennink, *In situ gelling hydrogels for pharmaceutical and biomedical applications.* Int J Pharm, 2008. **355**(1-2): p. 1-18.

261. Lee, J.H., et al., *Fabrication of an rhBMP-2 loaded porous beta-TCP microsphere-hyaluronic acid-based powder gel composite and evaluation of implant osseointegration.* J Mater Sci Mater Med, 2014. **25**(9): p. 2141-51.

262. Cox, T.R. and J.T. Erler, *Remodeling and homeostasis of the extracellular matrix: implications for fibrotic diseases and cancer.* Dis Model Mech, 2011. **4**(2): p. 165-78.

263. West, E.R., et al., *Physical properties of alginate hydrogels and their effects on in vitro follicle development.* Biomaterials, 2007. **28**(30): p. 4439-4448.

264. Banerjee, A., et al., *The influence of hydrogel modulus on the proliferation and differentiation of encapsulated neural stem cells.* Biomaterials, 2009. **30**(27): p. 4695-9.

265. Barbucci, R., et al., *Hyaluronic acid hydrogel in the treatment of osteoarthritis.* Biomaterials, 2002. **23**(23): p. 4503-13.

266. Leong, P.L. and E.F. Morgan, *Measurement of fracture callus material properties via nanoindentation.* Acta Biomater, 2008. **4**(5): p. 1569-75.

267. Donnelly, H., et al., *Bone and cartilage differentiation of a single stem cell population driven by material interface.* J Tissue Eng, 2017. **8**: p. 2041731417705615.

268. D'Este, M., et al., *Evaluation of an injectable thermoresponsive hyaluronan hydrogel in a rabbit osteochondral defect model.* J Biomed Mater Res A, 2016. **104**(6): p. 1469-78.

269. Kaneko, K., et al., *Hyaluronan inhibits BMP-induced osteoblast differentiation.* FEBS Lett, 2015. **589**(4): p. 447-54.

270. Bhakta, G., et al., *The influence of collagen and hyaluronan matrices on the delivery and bioactivity of bone morphogenetic protein-2 and ectopic bone formation.* Acta Biomater, 2013. **9**(11): p. 9098-106.

271. Mountziaris, P.M., et al., *Harnessing and modulating inflammation in strategies for bone regeneration.* Tissue Eng Part B Rev, 2011. **17**(6): p. 393-402.

272. Subramanian, S., et al., *Salicylic Acid-Based Polymers for Guided Bone Regeneration Using Bone Morphogenetic Protein-2.* Tissue Engineering Part A, 2015. **21**(13-14): p. 2013-2024.

273. Yuasa, M., et al., *Dexamethasone enhances osteogenic differentiation of bone marrow- and muscle-derived stromal cells and augments ectopic bone formation induced by bone morphogenetic protein-2.* PLoS One, 2015. **10**(2): p. e0116462.

274. Maciel, J., et al., *Adsorbed fibrinogen enhances production of bone- and angiogenic-related factors by monocytes/macrophages.* Tissue Eng Part A, 2014. **20**(1-2): p. 250-63.

275. Grotenhuis, N., et al., *Biomaterials Influence Macrophage-Mesenchymal Stem Cell Interaction In Vitro.* Tissue Eng Part A, 2016. **22**(17-18): p. 1098-107.

276. Chen, Z., et al., *Osteogenic differentiation of bone marrow MSCs by beta-tricalcium phosphate stimulating macrophages via BMP2 signalling pathway.* Biomaterials, 2014. **35**(5): p. 1507-18.

277. Grotenhuis, N., et al., *A culture model to analyze the acute biomaterial-dependent reaction of human primary macrophages.* Biochem Biophys Res Commun, 2013. **433**(1): p. 115-20.

278. He, H., et al., *Immobilized heavy chain-hyaluronic acid polarizes lipopolysaccharide-activated macrophages toward M2 phenotype.* J Biol Chem, 2013. **288**(36): p. 25792-803.

279. Lin, C.C., A.T. Metters, and K.S. Anseth, *Functional PEG-peptide hydrogels to modulate local inflammation induced by the pro-inflammatory cytokine TNFalpha.* Biomaterials, 2009. **30**(28): p. 4907-14.

280. Lee, K.B., et al., *Inflammatory characteristics of rhBMP-2 in vitro and in an in vivo rodent model.* Spine (Phila Pa 1976), 2011. **36**(3): p. E149-54.

281. Tannoury, C.A. and H.S. An, *Complications with the use of bone morphogenetic protein 2 (BMP-2) in spine surgery.* Spine J, 2014. **14**(3): p. 552-9.

282. Xu, L., et al., *Sox11-modified mesenchymal stem cells (MSCs) accelerate bone fracture healing: Sox11 regulates differentiation and migration of MSCs.* FASEB J, 2014.

283. Zhang, X.C., et al., *Enhanced osteogenic activity and anti-inflammatory properties of Lenti-BMP-2-loaded TiO2 nanotube layers fabricated by lyophilization following trehalose addition.* International Journal of Nanomedicine, 2016. **11**.

284. Fernandes Stefanello, T., et al., *Thermoresponsive hyaluronic acid nanogels as hydrophobic drug carrier to macrophages.* Acta Biomater, 2014. **10**(11): p. 4750-8.

285. Chen, W.Y. and G. Abatangelo, *Functions of hyaluronan in wound repair.* Wound Repair Regen, 1999. **7**(2): p. 79-89.

286. Thomas, A., K.G. Harding, and K. Moore, *Alginates from wound dressings activate human macrophages to secrete tumour necrosis factor-alpha.* Biomaterials, 2000. **21**(17): p. 1797-802.

287. Ayala, P., et al., *Engineered composite fascia for stem cell therapy in tissue repair applications.* Acta Biomater, 2015. **26**: p. 1-12.

288. Hemshekhar, M., et al., *Emerging roles of hyaluronic acid bioscaffolds in tissue engineering and regenerative medicine.* Int J Biol Macromol, 2016. **86**: p. 917-28.

289. Deng, Y., et al., *Injectable in situ cross-linking chitosan-hyaluronic acid based hydrogels for abdominal tissue regeneration.* Sci Rep, 2017. **7**(1): p. 2699.

290. Abdalla, S., et al., *Hyaluronic acid-based hydrogel induces neovascularization and improves cardiac function in a rat model of myocardial infarction.* Interact Cardiovasc Thorac Surg, 2013. **17**(5): p. 767-72.

291. Cui, F.Z., et al., *Hyaluronic acid hydrogel immobilized with RGD peptides for brain tissue engineering.* J Mater Sci Mater Med, 2006. **17**(12): p. 1393-401.

292. Agarwal, T., et al., *Alginate Bead Based Hexagonal Close Packed 3D Implant for Bone Tissue Engineering.* ACS Appl Mater Interfaces, 2016. **8**(47): p. 32132-32145.

293. Yu, J., et al., *The effect of injected RGD modified alginate on angiogenesis and left ventricular function in a chronic rat infarct model.* Biomaterials, 2009. **30**(5): p. 751-6.

294. Mumcuoglu, D., et al., *How to use BMP-2 for clinical applications? A review on pros and cons of existing delivery strategies.* J Transl Sci, 2017. **3**(5).

295. Bessa, P.C., M. Casal, and R.L. Reis, *Bone morphogenetic proteins in tissue engineering: the road from laboratory to clinic, part II (BMP delivery).* J Tissue Eng Regen Med, 2008. **2**(2-3): p. 81-96.

296. Choi, J.W., et al., *Appropriate and Effective Dosage of BMP-2 for the Ideal Regeneration of Calvarial Bone Defects in Beagles.* Plast Reconstr Surg, 2016. **138**(1): p. 64e-72e.

297. Yamaji, K., et al., *Effects of dose of recombinant human BMP-2 on bone formation at palatal sites in young and old rats.* Dent Mater J, 2007. **26**(4): p. 481-6.

298. Scott, M.A., et al., *Brief review of models of ectopic bone formation.* Stem Cells Dev, 2012. **21**(5): p. 655-67.

299. Morais, J.M., F. Papadimitrakopoulos, and D.J. Burgess, *Biomaterials/tissue interactions: possible solutions to overcome foreign body response.* AAPS J, 2010. **12**(2): p. 188-96.

300. Ono, M., et al., *Regeneration of calvarial defects with Escherichia coli -derived rhBMP-2 adsorbed in PLGA membrane.* Cells Tissues Organs, 2013. **198**(5): p. 367-76.

301. Young, S., et al., *Dose effect of dual delivery of vascular endothelial growth factor and bone morphogenetic protein-2 on bone regeneration in a rat critical-size defect model.* Tissue Eng Part A, 2009. **15**(9): p. 2347-62.

302. Rodriguez-Evora, M., et al., *Osteogenic effect of local, long versus short term BMP-2 delivery from a novel SPU-PLGA-betaTCP concentric system in a critical size defect in rats.* Eur J Pharm Sci, 2013. **49**(5): p. 873-84.

303. Garcia, P., et al., *Rodent animal models of delayed bone healing and non-union formation: a comprehensive review.* Eur Cell Mater, 2013. **26**: p. 1-12; discussion 12-4.

304. Rowley, J.A., G. Madlambayan, and D.J. Mooney, *Alginate hydrogels as synthetic extracellular matrix materials.* Biomaterials, 1999. **20**(1): p. 45-53.

305. Sarker, B., et al., *Evaluation of fibroblasts adhesion and proliferation on alginate-gelatin crosslinked hydrogel.* PLoS One, 2014. **9**(9): p. e107952.

306. Buck, B., T.I. Malinin, and M.D. Brown, *Bone Transplantation and Human Immunodeficiency Virus: An Estimate of Risk of Acquired Immunodeficiency Syndrome (AIDS).* Clinical orthopaedics and related research, 1989. **240**: p. 129-136.

307. Taraballi, F., et al., *Concise Review: Biomimetic Functionalization of Biomaterials to Stimulate the Endogenous Healing Process of Cartilage and Bone Tissue.* Stem Cells Transl Med, 2017.

308. Grunert, M., et al., *Isolation of a native osteoblast matrix with a specific affinity for BMP2.* J Mol Histol, 2007. **38**(5): p. 393-404.

309. Kempen, D.H., et al., *Enhanced bone morphogenetic protein-2-induced ectopic and orthotopic bone formation by intermittent parathyroid hormone (1-34) administration.* Tissue Eng Part A, 2010. **16**(12): p. 3769-77.

310. Velasco, M.A., C.A. Narvaez-Tovar, and D.A. Garzon-Alvarado, *Design, materials, and mechanobiology of biodegradable scaffolds for bone tissue engineering.* Biomed Res Int, 2015. **2015**: p. 729076.

311. Parvizi, M., *Cardiovascular tissue engineering and regeneration based on adipose tissue-derived stem/stromal cells* in 2016, University of Groningen

312. Lee, K.Y. and D.J. Mooney, *Alginate: properties and biomedical applications.* Prog Polym Sci, 2012. **37**(1): p. 106-126.

313. Murphy, C.M., et al., *Cell-scaffold interactions in the bone tissue engineering triad.* Eur Cell Mater, 2013. **26**: p. 120-32.

314. Zohar, R., *Signals between cells and matrix mediate bone regeneration*, in *Bone Regeneration*. 2012, InTech.

315. Hudalla, G.A. and W.L. Murphy, *Biomaterials that regulate growth factor activity via bioinspired interactions.* Adv Funct Mater, 2011. **21**(10): p. 1754-1768.

316. Bajpai, A., et al., *Smart Biomaterial Devices: Polymers in Biomedical Sciences*. 2016: CRC Press.

317. Lauzon, M.A., et al., *Bone repair: new developments in growth factor delivery systems and their mathematical modeling.* J Control Release, 2012. **162**(3): p. 502-20.

318. Woo, E.J., *Adverse events reported after the use of recombinant human bone morphogenetic protein 2.* Journal of Oral and Maxillofacial Surgery, 2012. **70**(4): p. 765-767.

319. Haidar, Z.S., R.C. Hamdy, and M. Tabrizian, *Delivery of recombinant bone morphogenetic proteins for bone regeneration and repair. Part A: Current challenges in BMP delivery.* Biotechnol Lett, 2009. **31**(12): p. 1817-24.

320. Jeon, O., et al., *Long-term delivery enhances in vivo osteogenic efficacy of bone morphogenetic protein-2 compared to short-term delivery.* Biochem Biophys Res Commun, 2008. **369**(2): p. 774-80.

321. Refaat, M., et al., *Binding to COMP Reduces the BMP2 Dose for Spinal Fusion in a Rat Model.* Spine (Phila Pa 1976), 2016. **41**(14): p. E829-36.

322. Tibbitt, M.W. and K.S. Anseth, *Hydrogels as extracellular matrix mimics for 3D cell culture.* Biotechnol Bioeng, 2009. **103**(4): p. 655-63.

323. Hinderer, S., S.L. Layland, and K. Schenke-Layland, *ECM and ECM-like materials - Biomaterials for applications in regenerative medicine and cancer therapy.* Adv Drug Deliv Rev, 2016. **97**: p. 260-9.

324. Bellis, S.L., *Advantages of RGD peptides for directing cell association with biomaterials.* Biomaterials, 2011. **32**(18): p. 4205-10.

325. Ramirez-Rodriguez, G.B., et al., *Biomimetic mineralization of recombinant collagen type I derived protein to obtain hybrid matrices for bone regeneration.* J Struct Biol, 2016. **196**(2): p. 138-146.

326. Ramirez-Rodriguez, G.B., et al., *Biomineralized Recombinant Collagen-Based Scaffold Mimicking Native Bone Enhances Mesenchymal Stem Cell Interaction and Differentiation.* Tissue Eng Part A, 2017.

327. Suarez-Gonzalez, D., et al., *Controlled nucleation of hydroxyapatite on alginate scaffolds for stem cell-based bone tissue engineering.* J Biomed Mater Res A, 2010. **95**(1): p. 222-34.

328. Stevens, M.M. and J.H. George, *Exploring and engineering the cell surface interface.* Science, 2005. **310**(5751): p. 1135-8.

329. Pawelec, K.M., H.A. van Boxtel, and S. Kluijtmans, *Ice-templating of anisotropic structures with high permeability.* Mater Sci Eng C Mater Biol Appl, 2017. **76**: p. 628-636.

330. Jayaram, M., et al., *Hydrogels in maxillofacial prosthesis.* Indian Journal of Multidisciplinary Dentistry, 2017. **7**(1): p. 29-33.

331. Mesimaki, K., et al., *Novel maxillary reconstruction with ectopic bone formation by GMP adipose stem cells.* Int J Oral Maxillofac Surg, 2009. **38**(3): p. 201-9.

332. Dominijanni, A., et al., *Platelet gel in oral and maxillofacial surgery: a single-centre experience.* Blood Transfus, 2012. **10**(2): p. 200-4.

333. Ren, T., et al., *The bone formation in vitro and mandibular defect repair using PLGA porous scaffolds.* J Biomed Mater Res A, 2005. **74**(4): p. 562-9.

334. Yuan, J., et al., *Repair of canine mandibular bone defects with bone marrow stromal cells and porous beta-tricalcium phosphate.* Biomaterials, 2007. **28**(6): p. 1005-13.

335. Springer, I.N., et al., *Two techniques for the preparation of cell-scaffold constructs suitable for sinus augmentation: steps into clinical application.* Tissue Eng, 2006. **12**(9): p. 2649-56.

336. Schimming, R. and R. Schmelzeisen, *Tissue-engineered bone for maxillary sinus augmentation.* J Oral Maxillofac Surg, 2004. **62**(6): p. 724-9.

337. Tobias, J.H., *Editorial: Mechanical Loading and Bone.* Front Endocrinol (Lausanne), 2015. **6**: p. 184.

338. Gibbs, D.M., et al., *A review of hydrogel use in fracture healing and bone regeneration.* J Tissue Eng Regen Med, 2016. **10**(3): p. 187-98.

339. Martin, G.J., Jr., et al., *Posterolateral intertransverse process spinal arthrodesis with rhBMP-2 in a nonhuman primate: important lessons learned regarding dose, carrier, and safety.* J Spinal Disord, 1999. **12**(3): p. 179-86.

340. Boyne, P.J., *Animal studies of application of rhBMP-2 in maxillofacial reconstruction.* Bone, 1996. **19**(1 Suppl): p. 83S-92S.

341. Park, J.B., et al., *Periodontal regeneration in class III furcation defects of beagle dogs using guided tissue regenerative therapy with platelet-derived growth factor.* J Periodontol, 1995. **66**(6): p. 462-77.

342. Schliephake, H., et al., *The use of basic fibroblast growth factor (bFGF) for enhancement of bone ingrowth into pyrolized bovine bone.* Int J Oral Maxillofac Surg, 1995. **24**(2): p. 181-6.

343. Schliephake, H., et al., *Use of cultivated osteoprogenitor cells to increase bone formation in segmental mandibular defects: an experimental pilot study in sheep.* International journal of oral and maxillofacial surgery, 2001. **30**(6): p. 531-537.

344. Bouxsein, M.L., et al., *Recombinant human bone morphogenetic protein-2 accelerates healing in a rabbit ulnar osteotomy model.* J Bone Joint Surg Am, 2001. **83-A**(8): p. 1219-30.

345.   Welch, R.D., et al., *Effect of recombinant human bone morphogenetic protein-2 on fracture healing in a goat tibial fracture model.* J Bone Miner Res, 1998. **13**(9): p. 1483-90.

346.   Yasko, A.W., et al., *The healing of segmental bone defects, induced by recombinant human bone morphogenetic protein (rhBMP-2). A radiographic, histological, and biomechanical study in rats.* J Bone Joint Surg Am, 1992. **74**(5): p. 659-70.

347.   Hollinger, J.O., et al., *Recombinant human bone morphogenetic protein-2 and collagen for bone regeneration.* J Biomed Mater Res, 1998. **43**(4): p. 356-64.

348.   Bostrom, M., et al., *Use of bone morphogenetic protein-2 in the rabbit ulnar nonunion model.* Clin Orthop Relat Res, 1996(327): p. 272-82.

349.   Zabka, A.G., et al., *Histomorphometric description of allograft bone remodeling and union in a canine segmental femoral defect model: a comparison of rhBMP-2, cancellous bone graft, and absorbable collagen sponge.* J Orthop Res, 2001. **19**(2): p. 318-27.

350.   Webber, M.J., et al., *A perspective on the clinical translation of scaffolds for tissue engineering.* Annals of biomedical engineering, 2015. **43**(3): p. 641-656.

351.   Madry, H., et al., *Barriers and strategies for the clinical translation of advanced orthopaedic tissue engineering protocols.* Eur Cell Mater, 2014. **27**: p. 17-21; discussion 21.

352.   Vranckx, J.J. and M. Den Hondt, *Tissue engineering and surgery: from translational studies to human trials.* Innovative Surgical Sciences, 2017.

353.   Webber, M.J., et al., *A perspective on the clinical translation of scaffolds for tissue engineering.* Ann Biomed Eng, 2015. **43**(3): p. 641-56.

CHAPTER 9

APPENDICES

PhD portfolio

Summary of PhD training and teaching

Name PhD student: Zahide Didem Mumcuoglu Guvenc	PhD period: 2014-2017
Erasmus MC Department: Orthopaedics	Promotor: Prof. Dr. Gerjo van Osch
Research School: Molecular Medicine	Co-promoter: Dr. Sebastiaan Kluijtmans

1. PhD training		
	Year	**Workload (ECTS)**
General courses		
- Basic Introduction Course on SPSS	2014	1
- Biomedical English Writing and Communication	2015	3
- Research Integrity	2015	
- Laboratory animal science, Leiden	2015	4
- Clinical trials monitoring, Utrecht Summer School	2016	4
- GMP meets development, ECA Academy, Prague, Czech Republic	2017	1
Specific courses (e.g. Research school, Medical Training)		
- Translational Imaging Workshop by AMIE	2014	1
- Intellectual property course, Fujifilm, Tilburg	2014-2015	2
- Microscopic Image Analysis: From Theory to Practice	2015	1
- Introduction in Graphpad Prism	2015	
- Protein structure course	2015	2
Seminars and workshops		2
- Workshop on Microsoft Excel	2015	
- Minisymposium "From Biomaterials Design to Clinical Applications", Eindhoven	2015	
- Symposium on Career Perspectives for Young Biomedical Scientists	2015	
- Masterclass Cell-Based Bone Regeneration, Nijmegen	2015	
- PhD day	2016-2017	
- Molecular Medicine Day, Rotterdam	2017	
Presentations		5
- Bioinspire progress meetings, Fujifilm, Tilburg (x8)	2014-2016	
- Bio-inspire EU project consortium meetings, Europe (x6)	2014-2017	
- Skeleton research discussions, Erasmus MC (x3)	2015-2017	
(Inter)national conferences		
- 4th Joint Meeting of European Calcified Tissue Society and International Bone and Mineral Society, Rotterdam "Synthetic collagen peptide (SCP) microspheres for tuned BMP-2 release in bone regeneration"	2015	1
- European Society of Biomaterials, Krakow, Poland "BMP-2 Release from Collagenous Particles"	2015	1
- World Biomaterials Congress, Montreal, Canada "BMP-2 release from synthetic collagen peptide particles"	2016	1
- Netherlands Society for Biomaterials and Tissue Engineering, Lunteren	2016	1

	Year	Workload
"Development of Injectable BMP-2 Delivery Materials Using Collagen-I Based Recombinant Peptide Microspheres"		
- Tissue Engineering and Regenerative Medicine International Society, Davos, Switzerland "Development of Injectable BMP-2 Delivery Materials Using Collagen-I Based Recombinant Peptide Microspheres"	2017	1
Other		
- Patent application, Fujifilm, Tilburg	2016	1
2. Teaching		
	Year	**Workload (ECTS)**
Supervising Master's theses		
- BMP-2 Release From Gelatine Microspheres And Hydrogels, Miranda Jekhmane, Department of Physical Chemistry and Soft Matter, Wageningen University	2015	5
- Protein release from microspheres, Coby van den Elzen, Life Sciences, Fontys University of Applied Sciences	2016	5

Curriculum Vitae

Didem Mumcuoglu was born in Izmir, Turkey in 1989. She finished high school in 2007 and entered university entrance exam in Turkey in which she succeeded to be at the top one percent of the applicants guaranteed her admission to Molecular Biology and Genetics at Middle East Technical University in Ankara, Turkey and granted scholarship for Bachelor's and Master's studies. She did an internship for 3 months in Barcelona, Spain in the group of Dr. Montserrat Cespedes where she practiced basic molecular biology techniques for the project screening of genetic mutations in cancer cells. In the last year of her studies, she was involved in a project for development of superparamagnetic iron oxide nanoparticles for cancer therapy in group of Prof. Dr. Ufuk Gunduz. After finishing her bachelor's degree in 2012, she decided to continue her career in biomaterials and regenerative medicine field, thus, decided to learn materials by doing a master's in Materials Science and Nanotechnology in Bilkent University, Ankara, Turkey. During her master's she performed two years of research in National Nanotechnology Center, Ankara in the group of Dr. Ayse Begum Tekinay and Dr. Mustafa Guler. During her studies she investigated self-assembled nanomaterials and their applications as a carrier for oligonucleotide drugs. She defended her master's thesis in June 2014 and moved to Netherlands for her PhD studies in July 2014. Her PhD study was funded by Marie Curie ITN, named as Bio-inspire involving Fujifilm Manufacturing, Tilburg and Erasmus MC, University Medical Center, Rotterdam as project partners. Her role in the consortium was to develop a growth factor delivery system for bone regeneration under supervision of Dr. Sebastiaan Kluijtmans and Prof. dr. Gerjo van Osch. She is currently working as a post-doctoral researcher in the group of Prof. dr. Patricia Dankers for the application of supramolecular polymers in pancreatic islet cell therapy.

My loving parents Servet Mumcuoglu and Feryat Mumcuoglu thanks for your moral support and thanks for encouraging me for this biggest adventure in my life. Thanks for your endless love and believing in me. Knowing that you are always proud of me means a lot to me. My loving husband and life partner, Ugur Ali Guvenc, you carried a lot in the last years when I was frustrated, disappointed. You comforted me with your love and support. Thanks for advices to keep me strong and motivated till the end. I could not stand alone in this adventure.